

**IMPROVEMENT OF COMPATIBILITY AND
TOUGHNESS OF SAWDUST/POLY(LACTIC ACID)
COMPOSITES**

Jiraporn Nomai



**A Thesis Submitted in Partial Fulfillment of the Requirements for the
Degree of Master of Engineering in Polymer Engineering**

Suranaree University of Technology

Academic Year 2013

การปรับปรุงความเข้ากันได้และความเหนียวของพอลิเมอร์คอมโพสิต
ระหว่างผงซีดีเดียวกับพอลิแล็กติกแอซิด



นางสาวจิราพร โนใหม่

วิทยานิพนธ์นี้เป็นส่วนหนึ่งของการศึกษาตามหลักสูตรปริญญาวิศวกรรมศาสตรมหาบัณฑิต
สาขาวิชาวิศวกรรมพอลิเมอร์
มหาวิทยาลัยเทคโนโลยีสุรนารี
ปีการศึกษา 2556

**IMPROVEMENT OF COMPATIBILITY AND
TOUGHNESS OF SAWDUST/POLY(LACTIC ACID)
COMPOSITES**

Jiraporn Nomai



**A Thesis Submitted in Partial Fulfillment of the Requirements for the
Degree of Master of Engineering in Polymer Engineering**

Suranaree University of Technology

Academic Year 2013

**IMPROVEMENT OF COMPATIBILITY AND TOUGHNESS OF
SAWDUST/POLY(LACTIC ACID) COMPOSITES**

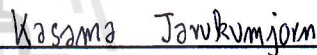
Suranaree University of Technology has approved this thesis submitted in partial fulfillments of the requirements for a Master's Degree.

Thesis Examining Committee



(Assoc. Prof. Dr. Yupaporn Ruksakulpiwat)

Chairperson



(Asst. Prof. Dr. Kasama Jarukumjorn)

Member (Thesis Advisor)



(Asst. Prof. Dr. Nitinat Suppakarn)

Member



(Prof. Dr. Sukit Limpijumnong)

Vice Rector for Academic Affairs
and Innovation



(Assoc. Prof. Ft. Lt. Dr. Kontorn Chamniprasart)

Dean of Institute of Engineering

จิราพร โนใหม่ : การปรับปรุงความเข้ากันได้และความเหนียวของพอลิเมอร์คอมโพสิตระหว่างผงซีลี้อยู่กับพอลิแลคติกแอซิด (IMPROVEMENT OF COMPATIBILITY AND TOUGHNESS OF SAWDUST/POLY(LACTIC ACID) COMPOSITES)

อาจารย์ที่ปรึกษา : ผู้ช่วยศาสตราจารย์ ดร.กษมา จารุกัจฉา, 152 หน้า.

ในการศึกษานี้ ผงซีลี้อยู่ถูกเตรียมให้อยู่ในรูปของผงซีลี้อยู่ที่ไม่ผ่านการตัดแปรและผ่านการตัดแปรด้วยการทำอัลคาไลน์เซชัน สำหรับผงซีลี้อยู่ที่ผ่านการตัดแปรด้วยการทำอัลคาไลน์เซชัน ผงซีลี้อยู่ถูกตัดแปรด้วยสารละลายโซเดียมไฮดรอกไซด์ความเข้มข้น 2.5 และ 10 เปอร์เซ็นต์ โดยน้ำหนักต่อปริมาตร เป็นเวลา 30 และ 60 นาที ผลจากการวิเคราะห์ห้องปฏิบัติการทางเคมี การวิเคราะห์หมู่ฟังก์ชัน และการวิเคราะห์น้ำหนักภายใต้ความร้อน แสดงให้เห็นว่าหลังจากการตัดแปรด้วยการทำอัลคาไลน์เซชัน ปริมาณเอมิเซลลูโลสและลิกนินของผงซีลี้อยู่ที่ผ่านการตัดแปรด้วยการทำอัลคาไลน์เซชันลดลงอย่างมีนัยสำคัญ ภาพถ่ายจากกล้องจุลทรรศน์อิเล็กตรอนแบบส่องกราดแสดงให้เห็นว่าพื้นผิวของผงซีลี้อยู่ที่ผ่านการตัดแปรด้วยการทำอัลคาไลน์เซชันสะอาด และมีความขรุขระมากกว่าผงซีลี้อยู่ที่ไม่ผ่านการตัดแปรด้วยการทำอัลคาไลน์เซชัน โดยสภาวะการตัดแปรด้วยการทำอัลคาไลน์เซชันที่เหมาะสม คือ ความเข้มข้นสารละลายโซเดียมไฮดรอกไซด์ 2 เปอร์เซ็นต์ โดยน้ำหนักต่อปริมาตร เป็นเวลา 30 นาที

พอลิเมอร์คอมโพสิตระหว่างพอลิแลคติกแอซิดและผงซีลี้อยู่ที่อัตราส่วนต่างๆ คือ 80/20 70/30 และ 60/40 เปอร์เซ็นต์โดยน้ำหนัก ถูกเตรียมด้วยเครื่องอัดรีดแบบสกรูคู่และชิ้นงานทดสอบถูกเตรียมด้วยเครื่องฉีดขึ้นรูป เมื่อปริมาณผงซีลี้อยู่ที่ไม่ผ่านการตัดแปรด้วยการทำอัลคาไลน์เซชันเพิ่มขึ้น ค่ามอดุลัสแรงดึง และค่ามอดุลัสแรงดัดโค้งของพอลิแลคติกแอซิดคอมโพสิตมีค่าเพิ่มขึ้น แต่ค่าความต้านแรงดึง ค่าความต้านแรงดัดโค้ง ค่าความต้านทานต่อแรงกระแทก และค่าความยืดหยุ่นสูงสุด ณ จุดขาดลดลง ความเสถียรต่อความร้อนของพอลิแลคติกแอซิดคอมโพสิตลดลงอย่างต่อเนื่องเมื่อปริมาณของผงซีลี้อยู่ที่ไม่ผ่านการตัดแปรด้วยการทำอัลคาไลน์เซชันเพิ่มขึ้น อุณหภูมิเปลี่ยนสภาพแก้ว และอุณหภูมิการหลอมเหลวของพอลิแลคติกแอซิดไม่มีการเปลี่ยนแปลงอย่างมีนัยสำคัญตามปริมาณผงซีลี้อยู่ที่ไม่ผ่านการตัดแปรด้วยการทำอัลคาไลน์เซชันที่เพิ่มขึ้น ในขณะที่อุณหภูมิการตกผลึกเพิ่มขึ้น ปริมาณผลึกของพอลิแลคติกแอซิดลดลงเมื่อปริมาณของผงซีลี้อยู่ที่ไม่ผ่านการตัดแปรด้วยการทำอัลคาไลน์เซชันเพิ่มขึ้น การตัดแปรพื้นผิวของผงซีลี้อยู่ด้วยการทำอัลคาไลน์เซชันส่งผลต่อการปรับปรุงสมบัติทางกล และความเสถียรต่อความร้อนของพอลิแลคติกแอซิดคอมโพสิต นอกจากนี้พอลิเมอร์คอมโพสิตระหว่างพอลิแลคติกแอซิดและผงซีลี้อยู่ที่ผ่านการตัดแปรด้วยการทำอัลคาไลน์เซชันแสดงปริมาณผลึกของพอลิแลคติกแอซิดที่สูงกว่าพอลิเมอร์

คอมโพสิทระหว่างพอลิแลกติกแอซิดและผงซีลี้อยู่ที่ไม่ผ่านการตัดแปรด้วยการทำอัลคาไลน์เซชัน ภายถ่ายจากกล้องจุลทรรศน์อิเล็กตรอนแบบส่องกราดแสดงให้เห็นว่าการตัดแปรผงซีลี้อยู่ด้วยการ ทำอัลคาไลน์เซชันปรับปรุงการยึดติดที่บริเวณอินเทอร์เฟสระหว่างผงซีลี้อยู่และพอลิแลกติกแอซิด และการแตกตัวของผงซีลี้อยู่ในพอลิแลกติกแอซิดเมทริกซ์

พอลิวิวิธินอะดิเปตโคเทอเรพทาเรต ถูกใช้เพื่อปรับปรุงความเหนียวของพอลิแลกติก- แอซิดคอมโพสิท เมื่อปริมาณพอลิวิวิธินอะดิเปตโคเทอเรพทาเรตเพิ่มขึ้น ค่าความยืดสูงสุด ฅ จุดขาด และค่าความต้านทานต่อแรงกระแทกของพอลิแลกติกแอซิดคอมโพสิทเพิ่มขึ้น ในขณะที่ค่า ความต้านแรงดึง ค่ามอดูลัสแรงดึง ค่าความต้านแรงดัดโค้ง และค่ามอดูลัสแรงดัดโค้งลดลง ความ- เสถียรต่อความร้อนของพอลิแลกติกแอซิดคอมโพสิทเพิ่มขึ้นตามปริมาณของพอลิวิวิธินอะดิเปต- โคเทอเรพทาเรตที่เพิ่มขึ้น อุณหภูมิเปลี่ยนสภาพแก้วและอุณหภูมิการหลอมเหลวของพอลิแลกติก แอซิดในพอลิเมอร์คอมโพสิทเปลี่ยนแปลงอย่างไม่มีนัยสำคัญเมื่อปริมาณพอลิวิวิธินอะดิเปตโค- เทอเรพทาเรตเพิ่มขึ้น อุณหภูมิการตกผลึกของพอลิแลกติกแอซิดในพอลิเมอร์คอมโพสิทลดลง ในขณะที่ปริมาณผลึกของพอลิแลกติกแอซิดในพอลิเมอร์คอมโพสิทเพิ่มขึ้นเมื่อปริมาณพอลิวิวิ- ธินอะดิเปตโคเทอเรพทาเรตเพิ่มขึ้น ภายถ่ายจากกล้องจุลทรรศน์อิเล็กตรอนแบบส่องกราดแสดง ลักษณะของการแตกหักแบบเหนียวในพอลิแลกติกแอซิดคอมโพสิทที่มีการปรับปรุงความเหนียว ด้วยพอลิวิวิธินอะดิเปตโคเทอเรพทาเรต

พอลิแลกติกแอซิดกราฟท์มาลิกแอนไฮไดรด์ถูกใช้เป็นสารปรับปรุงความเข้ากันได้ และ ปริมาณของพอลิแลกติกแอซิดกราฟท์มาลิกแอนไฮไดรด์ คือ 3 5 และ 10 เปอร์เซ็นต์โดยน้ำหนัก พอลิเมอร์คอมโพสิทที่มีการปรับปรุงความเข้ากันได้มีสมบัติทางกล และความเสถียรต่อความร้อนที่ สูงกว่าพอลิเมอร์คอมโพสิทที่ไม่มีการปรับปรุงความเข้ากันได้ ปริมาณพอลิแลกติกแอซิดกราฟท์- มาลิกแอนไฮไดรด์ที่เหมาะสมสำหรับการปรับปรุงความเข้ากันได้ของพอลิเมอร์คอมโพสิทระหว่าง พอลิแลกติกแอซิดและผงซีลี้อยู่ที่ปรับปรุงความเหนียวด้วยพอลิวิวิธินอะดิเปตโคเทอเรพทาเรต คือ 5 เปอร์เซ็นต์โดยน้ำหนัก เมื่อปริมาณพอลิแลกติกแอซิดกราฟท์มาลิกแอนไฮไดรด์เพิ่มขึ้น อุณหภูมิเปลี่ยนสภาพแก้ว อุณหภูมิการหลอมเหลว และอุณหภูมิการตกผลึกของพอลิแลกติกแอซิด ในพอลิเมอร์คอมโพสิทลดลง ในขณะที่ปริมาณผลึกของพอลิแลกติกแอซิดในพอลิเมอร์คอมโพสิท เพิ่มขึ้น ภายถ่ายจากกล้องจุลทรรศน์อิเล็กตรอนแบบส่องกราดยืนยันว่าพอลิแลกติกแอซิดกราฟท์- มาลิกแอนไฮไดรด์ปรับปรุงความเข้ากันได้ของคอมโพสิท

สาขาวิชา วิศวกรรมพอลิเมอร์

ปีการศึกษา 2556

ลายมือชื่อนักศึกษา จิราพร ไนใหม่

ลายมือชื่ออาจารย์ที่ปรึกษา ณงนา จรุงไชย

JIRAPORN NOMAI : IMPROVEMENT OF COMPATIBILITY AND
TOUGHNESS OF SAWDUST/POLY(LACTIC ACID) COMPOSITES.

THESIS ADVISOR : ASST. PROF. KASAMA JARUKUMJORN, Ph.D.,
152 PP.

POLY(LACTIC ACID)/SAWDUST/COMPOSITE/ALKALI TREATMENT/
POLY(BUTYLENE ADIPATE-CO-TEREPHTHALATE)/POLY(LACTIC ACID)
GRAFTED WITH MALEIC ANHYDRIDE

In this study, sawdust was prepared as untreated sawdust (UT) and alkali treated sawdust (AT). For AT, sawdust was treated with 2, 5, and 10% w/v sodium hydroxide (NaOH) solution for 30 and 60 min. Filler composition, functional group analysis, and thermogravimetric analysis results showed that after alkali treatment, hemicellulose and lignin contents of AT significantly decreased. SEM micrographs revealed that surface of AT was cleaner and rougher than UT. The optimum alkali treatment condition was 2% w/v NaOH for 30 min.

The composites of PLA/sawdust at various ratios of 80/20, 70/30, and 60/40 w/w were prepared using a twin screw extruder and test specimens were molded using an injection molding machine. With increasing UT content, tensile modulus and flexural modulus of PLA composites increased whereas tensile strength, flexural strength, impact strength, and elongation at break decreased. Thermal stability of PLA composites was continuously decreased when UT content was increased. With increasing UT content, glass transition temperature and melting temperature of PLA insignificantly changed while cold crystallization temperature was increased. Degree of crystallinity of PLA was decreased when UT content was increased. Alkali treatment

improved mechanical properties and thermal stability of PLA composites. Additionally, AT/PLA composites exhibited higher degree of crystallinity of PLA than those of UT/PLA composites. SEM micrographs showed that alkali treatment improved sawdust-PLA interfacial adhesion and dispersion of sawdust in PLA matrix.

Poly(butylene adipate-co-terephthalate) (PBAT) was used to improve toughness of PLA composites. With increasing PBAT content, elongation at break and impact strength of PLA composites were increased whereas tensile strength, tensile modulus, flexural strength, and flexural modulus were decreased. Thermal stability of PLA composites was improved with increasing PBAT content. As PBAT content was increased glass transition temperature and melting temperature of PLA in the composites insignificantly changed. Cold crystallization temperature of PLA in the composites was decreased whereas degree of crystallinity of PLA in the composites was increased when PBAT content was increased. SEM micrographs exhibited some features of ductile fracture in the PLA composites toughened with PBAT.

PLA grafted with maleic anhydride (PLA-g-MA) was used as a compatibilizer and its contents were 3, 5, and 10 wt%. The compatibilized composites had higher mechanical properties and thermal stability than the uncompatibilized composite. The optimum content of PLA-g-MA for sawdust/PLA/PBAT composite was 5 wt%. With increasing PLA-g-MA content, glass transition temperature, melting temperature, and cold crystallization temperature of PLA in the composites were decreased. However, degree of crystallinity of PLA in the composites was increased. SEM micrographs confirmed that PLA-g-MA improved the compatibility of the composites.

School of Polymer Engineering

Academic Year 2013

Student's Signature Jiraporn Nomai

Advisor's Signature Kasama Jankumjorn

ACKNOWLEDGEMENTS

I gratefully acknowledge the financial supports from Suranaree University of Technology and Center of Excellence on Petrochemical and Material Technology.

First and foremost, I would like to express my sincere gratitude to my thesis advisor, Asst. Prof. Dr. Kasama Jarukumjorn, for her excellent supervision, inspiring guidance, and encouragement throughout the period of the study. My appreciation goes to Assoc. Prof. Dr. Yupaporn Raksakulpiwat and Asst. Prof. Dr. Nitinat Suppakarn, for their valuable suggestions and guidance as committee members. The author is also grateful to all the faculty and staff members of the School of Polymer Engineering and the Center for Scientific and Technological Equipment of Suranaree University of Technology for their help and assistance throughout the period of this study.

In addition, I am sincerely grateful to Piyarat sawmill for supplying iron wood sawdust.

Finally, my graduation would not be achieved without best wish from my parents, Mr. Phol and Mrs. Longma Nomai, and my brothers, Mr. Wissanu and Mr. Winai Nomai, who give me a valuable life with their endless love, support, and encouragement throughout my life.

Jiraporn Nomai

TABLE OF CONTENTS

	Page
ABSTRACT (THAI)	I
ABSTRACT (ENGLISH)	III
ACKNOWLEDGEMENTS	V
TABLE OF CONTENTS	VI
LIST OF TABLES	XI
LIST OF FIGURES	XIII
SYMBOLS AND ABBREVIATIONS.....	XIX
CHAPTER	
I INTRODUCTION	1
1.1 Background	1
1.2 Research objectives	4
1.3 Scope and limitation of the study	5
II LITERATURE REVIEW	6
2.1 Interfacial modification of lignocellulosic filler/ polymer composites	6
2.1.1 Filler surface treatment.....	7
2.1.1.1 Chemical treatment	7
2.1.1.1.1 Alkali treatment.....	7

TABLE OF CONTENTS (Continued)

	Page
2.1.1.1.2 Silane treatment.....	15
2.1.1.1.3 Acrylic acid treatment	19
2.1.1.2 Physical treatment	20
2.1.1.2.1 Heat treatment	20
2.1.1.2.2 Corona treatment	23
2.1.1.2.3 Plasma treatment	25
2.1.2 Matrix modification	26
2.1.3 Addition of compatibilizer	29
2.2 Toughness improvement of lignocellulosic filler/ polymer composites	31
2.2.1 Toughness improvement of lignocellulosic filler/polymer composites by adding plasticizer	31
2.2.2 Toughness improvement of lignocellulosic filler/polymer composites by adding flexible polymer component	32
III EXPERIMENTAL.....	38
3.1 Materials	38
3.2 Experimental	38
3.2.1 Preparation of sawdust.....	38
3.2.2 Characterization of sawdust.....	39

TABLE OF CONTENTS (Continued)

	Page
3.2.2.1 Filler composition determination.....	39
3.2.2.2 Functional group analysis	40
3.2.2.3 Thermal properties	40
3.2.2.4 Morphological properties.....	41
3.2.3 Preparation of poly(lactic acid) grafted with maleic anhydride.....	41
3.2.4 Characterization of poly(lactic acid) grafted with maleic anhydride.....	41
3.2.4.1 Determination of maleic anhydride content.....	41
3.2.4.2 Fourier transform infrared spectroscopy.....	42
3.2.5 Preparation of sawdust/PLA composites	42
3.2.6 Preparation of sawdust/PLA/PBAT composites and compatibilized sawdust/PLA/PBAT composites.....	43
3.2.7 Characterization of PLA, sawdust/PLA, sawdust/PLA/PBAT, and compatibilized sawdust/PLA/PBAT composites.....	44
3.2.7.1 Mechanical properties	44
3.2.7.2 Thermal properties	44

TABLE OF CONTENTS (Continued)

	Page
3.2.7.3 Morphological properties.....	45
IV RESULTS AND DISCUSSION	46
4.1 Effect of alkali treatment on properties of sawdust	46
4.1.1 Filler composition	46
4.1.2 Functional group analysis	47
4.1.3 Thermal properties	52
4.1.4 Morphological properties	59
4.2 Characterization of PLA-g-MA	63
4.3 Effects of alkali treatment and sawdust content on properties of sawdust/PLA composites.....	65
4.3.1 Mechanical properties	65
4.3.1.1 Tensile properties	65
4.3.1.2 Flexural properties.....	69
4.3.1.3 Impact properties.....	71
4.3.2 Thermal properties	74
4.3.3 Morphological properties.....	81
4.4 Effect of poly(butylene adipate- <i>co</i> -terephthalate) (PBAT) content on properties of sawdust/PLA composites.....	85
4.4.1 Mechanical properties	85
4.4.1.1 Tensile properties	85

TABLE OF CONTENTS (Continued)

	Page
4.4.1.2 Flexural properties.....	89
4.4.1.3 Impact properties.....	91
4.4.2 Thermal properties	94
4.4.3 Morphological properties.....	98
4.5 Effect of poly(lactic acid) grafted with maleic anhydride (PLA-g-MA) content on properties of sawdust/PLA/PBAT composites.....	103
4.5.1 Mechanical properties	103
4.5.1.1 Tensile properties.....	103
4.5.1.2 Flexural properties.....	106
4.5.1.3 Impact properties.....	108
4.5.2 Thermal properties	111
4.5.3 Morphological properties.....	116
V CONCLUSIONS.....	119
REFERENCES	121
APPENDIX A PUBLICATIONS	138
BIOGRAPHY	152

LIST OF TABLES

Table	Page
4.1 Filler composition of untreated sawdust and alkali treated sawdust.....	47
4.2 Infrared main transitions for untreated sawdust.....	49
4.3 Thermal decomposition temperatures of untreated sawdust and alkali treated sawdust with different NaOH concentrations and treatment times.....	58
4.4 Mechanical properties of PLA, untreated sawdust/PLA composites, and alkali treated sawdust/PLA composites with different sawdust contents.	73
4.5 Thermal decomposition temperatures of PLA, untreated sawdust/ PLA composites, and alkali treated sawdust/PLA composites with different sawdust contents.....	76
4.6 Thermal characteristics of PLA, untreated sawdust/PLA composites, and alkali treated sawdust/PLA composites with different sawdust contents.	80
4.7 Mechanical properties of sawdust/PLA composite and sawdust/ PLA/PBAT composites with different PBAT contents.	93

LIST OF TABLES (Continued)

Table		Page
4.8	Thermal decomposition temperatures of PBAT, sawdust/PLA composite, and sawdust/PLA/PBAT composites with different PBAT contents.	95
4.9	Thermal characteristics of PBAT, sawdust/PLA composite and sawdust/PLA/PBAT composites with different PBAT contents	97
4.10	Mechanical properties of uncompatibilized sawdust/PLA/PBAT composite and compatibilized sawdust/PLA/PBAT composites with different PLA-g-MA contents.....	110
4.11	Thermal decomposition temperatures of uncompatibilized sawdust/PLA/PBAT composite and compatibilized sawdust/PLA/PBAT composites with different PLA-g-MA contents.	113
4.12	Thermal characteristics of uncompatibilized sawdust/PLA/PBAT composite and compatibilized sawdust/PLA/PBAT composites with different PLA-g-MA contents.....	115

LIST OF FIGURES

Figure	Page
4.1	ATR-FTIR spectrum of untreated sawdust.....50
4.2	ATR-FTIR spectra of (a) UT, (b) AT2%_30min, (c) AT5%_30min, (d) AT10%_30min, (e) AT2%_60min, (f) AT5%_60min, and (g) AT10%_60min.52
4.3	TGA and DTA curve of untreated sawdust.54
4.4	TGA curves of untreated sawdust and alkali treated sawdust with different NaOH concentrations and treatment times.57
4.5	DTA curves of untreated sawdust and alkali treated sawdust with different NaOH concentrations and treatment times.57
4.6	SEM micrographs at 200x magnification of (a) UT, (b) AT2%_30min, (c) AT5%_30min, (d) AT10%_30min, (e) AT2%_60min, (f) AT5%_60min, and (g) AT10%_60min.61
4.7	SEM micrographs at 500x magnification of (a) UT, (b) AT2%_30min, (c) AT5%_30min, (d) AT10%_30min, (e) AT2%_60min, (f) AT5%_60min, and (g) AT10%_60min.62
4.8	FTIR spectra of PLA, PLA-g-MA, and MA.....64
4.9	FTIR second derivative spectra of PLA, PLA-g-MA, and MA.....64

LIST OF FIGURES (Continued)

Figure	Page
4.10 Tensile strength of PLA, untreated sawdust/PLA composites, and alkali treated sawdust/PLA composites with different sawdust contents.	67
4.11 Tensile modulus of PLA, untreated sawdust/PLA composites, and alkali treated sawdust/PLA composites with different sawdust contents.	68
4.12 Elongation at break of PLA, untreated sawdust/PLA composites, and alkali treated sawdust/PLA composites with different sawdust contents.	68
4.13 Flexural strength of PLA, untreated sawdust/PLA composites, and alkali treated sawdust/PLA composites with different sawdust contents.	70
4.14 Flexural modulus of PLA, untreated sawdust/PLA composites, and alkali treated sawdust/PLA composites with different sawdust contents.	71
4.15 Impact strength of PLA, untreated sawdust/PLA composites, and alkali treated sawdust/PLA composites with different sawdust contents.	72
4.16 TGA curves of PLA, untreated sawdust/PLA composites, and alkali treated sawdust/PLA composites with different sawdust contents.	77

LIST OF FIGURES (Continued)

Figure	Page
4.17	DTA curves of PLA, untreated sawdust/PLA composites, and alkali treated sawdust/PLA composites with different sawdust contents.77
4.18	DSC thermograms of PLA, untreated sawdust/PLA composites, and alkali treated sawdust/PLA composites with different sawdust contents (the second heating, heating rate 5°C/min).81
4.19	SEM micrographs at 100x magnification of (a) PLA/UT20, (b) PLA/UT30, (c) PLA/UT40, (d) PLA/AT20, (e) PLA/AT30, and (f) PLA/AT40 composites.....83
4.20	SEM micrographs at 300x magnification of (a) PLA/UT20, (b) PLA/UT30, (c) PLA/UT40, (d) PLA/AT20, (e) PLA/AT30, and (f) PLA/AT40 composites.....84
4.21	Tensile strength of sawdust/PLA composite and sawdust/PLA/PBAT composites with different PBAT contents.....88
4.22	Tensile modulus of sawdust/PLA composite and sawdust/PLA/PBAT composites with different PBAT contents.....88
4.23	Elongation at break of sawdust/PLA composite and sawdust/PLA/PBAT composites with different PBAT contents.....89
4.24	Flexural strength of sawdust/PLA composite and sawdust/PLA/PBAT composites with different PBAT contents.....90

LIST OF FIGURES (Continued)

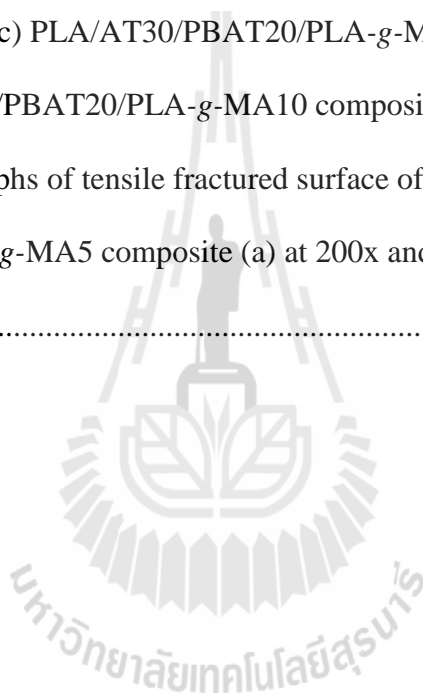
Figure	Page
4.25	Flexural modulus of sawdust/PLA composite and sawdust/PLA/ PBAT composites with different PBAT contents.....91
4.26	Impact strength of sawdust/PLA composite and sawdust/PLA/PBAT composites with different PBAT contents.92
4.27	TGA curves of PBAT, sawdust/PLA composite, and sawdust/PLA/ PBAT composites with different PBAT contents.....95
4.28	DTA curves of PBAT, sawdust/PLA composite, and sawdust/PLA/ PBAT composites with different PBAT contents.....96
4.29	DSC thermograms of PBAT, sawdust/PLA composite and sawdust/PLA/PBAT composites with different PBAT contents (the second heating, heating rate 5°C/min).....98
4.30	SEM micrographs of impact fractured surface at 1500x magnification of (a) PLA/AT30, (b) PLA/AT30/PBAT10, (c) PLA/AT30/PBAT20, and (d) PLA/AT30/PBAT30 composites..... 100
4.31	SEM micrographs of tensile fractured surface at 200x magnification of (a) PLA/AT30, (b) PLA/AT30/PBAT10, (c) PLA/AT30/PBAT20, and (d) PLA/AT30/PBAT30 composites..... 101
4.32	SEM micrographs of tensile fractured surface at 1500x magnification of (a) PLA/AT30, (b) PLA/AT30/PBAT10, (c) PLA/AT30/PBAT20, and (d) PLA/AT30/PBAT30 composites..... 102

LIST OF FIGURES (Continued)

Figure	Page
4.33 Tensile strength of sawdust/PLA/PBAT composites with different PLA-g-MA contents.....	105
4.34 Tensile modulus of sawdust/PLA/PBAT composites with different PLA-g-MA contents.....	105
4.35 Elongation at break of sawdust/PLA/PBAT composites with different PLA-g-MA contents.....	106
4.36 Flexural strength of sawdust/PLA/PBAT composites with different PLA-g-MA contents.....	107
4.37 Flexural modulus of sawdust/PLA/PBAT composites with different PLA-g-MA contents.....	108
4.38 Impact strength of sawdust/PLA/PBAT composites with different PLA-g-MA contents.....	109
4.39 TGA curves of sawdust/PLA/PBAT composites with different PLA-g-MA contents.....	112
4.40 DTA curves of sawdust/PLA/PBAT composites with different PLA-g-MA contents.....	112
4.41 DSC thermograms of uncompatibilized sawdust/PLA/PBAT composite and compatibilized sawdust/PLA/PBAT composites with different PLA-g-MA contents (the second heating, heating rate 5°C/min).....	115

LIST OF FIGURES (Continued)

Figure	Page
4.42 SEM micrographs of impact fractured surface at 1500x magnification of (a) PLA/AT30/PBAT20, (b) PLA/AT30/PBAT20/PLA-g-MA3, (c) PLA/AT30/PBAT20/PLA-g-MA5, and (d) PLA/AT30/PBAT20/PLA-g-MA10 composites.....	117
4.43 SEM micrographs of tensile fractured surface of PLA/AT30/PBAT20/PLA-g-MA5 composite (a) at 200x and (b) at 1500x magnification.	118



SYMBOLS AND ABBREVIATIONS

PLA	=	Poly(lactic acid)
PBAT	=	Poly(butylene adipate- <i>co</i> -terephthalate)
MA	=	Maleic anhydride
Luperox101	=	2,5-bis(<i>tert</i> -butylperoxy)-2,5 dimethylhexane
PLA- <i>g</i> -MA	=	Poly(lactic acid) grafted with maleic anhydride
%G	=	Graft content
UT	=	Untreated sawdust
AT	=	Alkali treated sawdust
FTIR	=	Fourier transform infrared spectroscopy
SEM	=	Scanning electron microscope
DSC	=	Differential scanning calorimetry
TGA	=	Thermalgravimetric analysis
T ₅	=	Thermal decomposition temperature at 5% weight loss
T ₅₀	=	Thermal decomposition temperature at 50% weight loss
T _d	=	Thermal decomposition temperature

CHAPTER I

INTRODUCTION

1.1 Background

Thermoplastic polymers obtained from petrochemical resources such as polypropylene (PP), polyethylene (PE), and polystyrene (PS) have generally been used in the plastic industries. However, these polymers do not degrade easily in the natural environment resulting in environmental pollution in the eco-system. Increasing concerns about the environmental impact and sustainability of petrochemical polymer materials have motivated academia and industry to develop biodegradable polymers from renewable resources.

Poly(lactic acid) (PLA) is a linear aliphatic biodegradable polyester derived from renewable resources through bioconversion and polymerization. PLA has become a potential candidate for various large scale industrial applications in the areas of packaging, biomedical, and automotive, etc. Moreover, PLA has many advantages such as high strength, high modulus, and commercial availability (Liu and Zhang, 2011). However, its high brittleness and high cost limit its large scale commercial application (Qiang, Yu, and Gao, 2012). One of the possible methods to minimize effective end product costs is to reduce the quantities of polymeric material required by incorporating low cost filler into biodegradable polymers (Dimonie and Rapa, 2010). Lignocellulosic fillers are widely used as reinforcing fillers in thermoplastic composites to provide positive environmental benefits with respect to ultimate disposability. The major advantages of these composite materials are low cost, light weight, high specific

strength, and recyclability (Satyanarayana, Arizaga, and Wypych, 2009). In wood industries, sawdust is wood processing residue from consumer good manufacture. Basically, sawdust is used to make particle board and others furniture products or used as a fuel source. However, in many countries, sawdust is often disposed as landfill or incinerated causing environmental problems. Therefore, using sawdust as reinforcing fillers for polymer composites is an alternative way to add value to sawdust and also benefit the environment (Bettini, Bonse, Melo, and Muñoz, 2010).

Mechanical properties of lignocellulosic filler/polymer composites are determined by several factors including properties of matrix and dispersed phase, shape and orientation of dispersed phase, concentration of dispersed phase, and interfacial adhesion between matrix and dispersed phase (Saheb and Jog, 1999). The main problem of using lignocellulosic filler to reinforce PLA is the incompatibility between lignocellulosic filler and PLA matrix leading to poor mechanical properties of the composites. In order to attain superior mechanical properties, the interfacial adhesion between the filler and the PLA matrix should be improved. The methods to enhance the interfacial adhesion between lignocellulosic fillers and PLA matrix include matrix modification (Wang, Chou, Wu, and Yeh, 2012; Wu, 2012), addition of compatibilizer (Petinakis, Yu, Edward, Dean, Liu, and Scully, 2009; Chen, Liu, Cooke, Hicks, and Zhang, 2008; Lee and Wang, 2006), and filler surface treatment (Qian, Mao, Sheng, Lu, Luo, and Hou, 2013; Chun, Husseinsyah, and Osman, 2012; Aydin, Tozlu, Kemalglu, Aytac, and Ozkoc, 2011). Alkali treatment is found to be an effective method to improve mechanical properties of lignocellulosic filler/PLA composites (Sawpan, Pickering, and Fernyhough, 2011; Hu and Lim, 2007). Alkali treatment can remove a certain amount of lignin, hemicellulose, and surface impurities of the filler.

The removal of surface impurities makes the filler cleaner and rougher than untreated filler. The effective filler surface areas which are available for mechanical interlocking with PLA matrix are increased. This results in the improvement of the adhesion between lignocellulosic filler and PLA matrix leading to improved mechanical properties of the biocomposites.

However, one obstacle that restricts the application of PLA based lignocellulosic filler biocomposites is owing to a remarkable decrease in toughness of the biocomposites. Therefore, the toughness of the PLA biocomposites has to be improved without excessive reduction of stiffness and strength to achieve balance overall properties. Several modifications have been proposed to improve toughness of PLA based lignocellulosic filler biocomposites including plasticization (Rahman, De Santis, Spagnoli, Ramorino, Penco, Phuong, and Lazzeri, 2012; Gregorova, Sedlarik, Pastorek, Jachandra, and Stelzer, 2011) and addition of flexible polymer component (Afrifah and Matuana, 2013; Petinakis et al., 2009; Jiang and Qin, 2006). In the recent year, many considerable interests have focused on toughening lignocellulosic filler/PLA biocomposites with flexible biodegradable polymers, e.g. polycaprolactone (PCL) (Goriparthi, Suman, and Nalluri, 2012), polyhydroxyalkanoates (PHAs) (Qiang et al., 2012), and poly(butylene adipate-*co*-terephthalate) (PBAT) (Lee, 2009) due to their obvious environment friendly properties comparing to conventional non-biodegradable polymers. The addition of PBAT is found to be an effective way to improve toughness of the PLA biocomposites without affecting the biodegradability. With the addition of PBAT, elongation at break of the biocomposites is significantly improved. Thus, in the view of high toughness and biodegradability, PBAT is considered as a good choice for toughening PLA based lignocellulosic filler biocomposites (Liu et al., 2011).

In fact, all of the investigated PLA/PBAT blends are immiscible or only partially miscible leading to poor mechanical properties especially in strength and stiffness properties (Jiang, Wolcott, and Zhang, 2006). Therefore, interfacial adhesion between PLA and PBAT should be improved to achieve balance overall properties including strength, stiffness, and toughness of the PLA biocomposites. Generally, poly(lactic acid) grafted with maleic anhydride (PLA-*g*-MA) is considered to be an effective compatibilizer for improving the compatibility between PLA and PBAT (Teamsinsungvon, Ruksakulpiwat, and Jarukumjorn, 2013; Lee, 2009; Victor, Witold, Wunpen, and Betty, 2009).

1.2 Research objectives

The main objectives of this research are as below :

- (i) To study effect of alkali treatment on chemical compositions, thermal properties, and morphological properties of sawdust.
- (ii) To study effects of sawdust content and alkali treatment on mechanical properties, thermal properties, and morphological properties of sawdust/PLA composites.
- (iii) To study effect of PBAT content on mechanical properties, thermal properties, and morphological properties of sawdust/PLA/PBAT composites.
- (iv) To prepare PLA-*g*-MA and investigate effect of PLA-*g*-MA content on mechanical properties, thermal properties, and morphological properties of sawdust/PLA/PBAT composites.

1.3 Scope and limitation of the study

In this study, sawdust was prepared as untreated and alkali treated sawdust. For alkali treated sawdust, sawdust was treated with 2, 5, and 10% w/v sodium hydroxide (NaOH) solution for 30 and 60 min at room temperature. Filler composition determination, functional group analysis, thermal properties, and morphological properties of sawdust were investigated.

PLA composites at various sawdust contents (20, 30, and 40 wt%) were prepared using a twin screw extruder and then the test specimens were molded by an injection molding machine. The effects of sawdust content and alkali treatment on mechanical, thermal, and morphological properties of the composites were investigated.

Based on the mechanical properties of the sawdust/PLA composites, the composite giving the optimum mechanical properties was selected to further study. PBAT was used to improve toughness of sawdust/PLA composite. PBAT content was varied as 10, 20, and 30 wt%. The effect of PBAT content on mechanical, thermal, and morphological properties of the composites were investigated.

Based on the mechanical properties of the sawdust/PLA/PBAT composites, the composite giving the optimum mechanical properties was selected to study the effect of PLA-g-MA as a compatibilizer. PLA-g-MA content was varied as 3, 5, and 10 wt%. Then, mechanical, thermal, and morphological properties of the compatibilized composites were investigated.

CHAPTER II

LITERATURE REVIEW

The interest in lignocellulosic filler reinforced poly(lactic acid) (PLA) composites is growing rapidly in recent years. The major advantages of these composite materials are low cost, light weight, high specific strength, and biodegradability. Unfortunately, the main problem of using lignocellulosic filler to reinforce PLA is the incompatibility between lignocellulosic filler and PLA matrix leading to poor mechanical properties of the composites. The methods to enhance the interfacial adhesion between lignocellulosic filler and PLA include filler surface treatment, matrix modification, and addition of compatibilizer. In addition, one obstacle that limits the application of PLA based lignocellulosic filler composites is owing to a remarkable decrease of toughness of the composites. The toughness improvement of the PLA composites can be carried out by several modifications such as plasticization and addition of flexible polymer.

2.1 Interfacial modification of lignocellulosic filler/polymer composites

The interfacial modification of lignocellulosic filler/polymer composites includes lignocellulosic filler surface treatment, matrix modification, and addition of compatibilizer.

2.1.1 Filler surface treatment

Filler surface treatment is considered in modifying the filler surface properties to improve interfacial adhesion between filler and polymer matrix. The filler surface treatment can be classified into chemical treatment and physical treatment.

2.1.1.1 Chemical treatment

2.1.1.1.1 Alkali treatment

Alkali treatment is one of the most used chemical treatment of lignocellulosic filler to modify filler surfaces and enhance interfacial adhesion between lignocellulosic filler and polymer matrix. The important modification achieved with alkali treatment is the reduction of a certain amount of lignin, hemicellulose, and impurities covering the external surface of filler. The removal of surface impurities made the filler cleaner and rougher than untreated filler resulting in better mechanical interlocking with polymer matrix. Gomes, Goda, and Ohgi (2004) investigated the effect of alkali treatment on mechanical properties and surface morphology of curaua fiber. Curaua fibers were treated with 5, 10, and 15% w/v sodium hydroxide (NaOH) solution for 1 and 2 h. The results showed that tensile strength of alkali treated curaua fiber decreased with increasing NaOH concentration. This may be attributed to a partial change from crystalline cellulose I into amorphous cellulose II. On the other hand, the fracture strain of alkali treated fibers increased greatly in comparison with untreated fibers. Moreover, curaua fibers treated with the same concentration of NaOH for 1 h showed slightly higher tensile strength than those fibers treated for 2 h. Scanning electron microscope (SEM) micrographs showed that alkali treatment changed the structure of the curaua fiber. The packed structure of fibrils was deteriorated by removing lignin out of the fibrils leading to fibril separation.

Liu, Mohanty, Askeland, Drzal, and Misra (2004)

reported the effect of alkali treatment on structure and surface morphology of indian grass fibers. Chopped grass fibers were treated with 5 and 10% w/v NaOH for 2 and 4 h. The composites with 30 wt% of untreated and alkali treated grass fiber reinforced soy protein based biocomposites were prepared. From digital images, alkali treated grass fibers appeared to be finer, smaller in size, and more entanglement. The extent of shrinkage and entanglement increased with increasing concentration of alkali solution and treatment time. Fourier transform infrared spectroscopy (FTIR) results confirmed that the structure of the fiber changed after alkali treatment. The vibration peak at 1737 cm^{-1} assigned to C=O stretching vibration of carboxylic acid or ester disappeared due to the removal of hemicellulose. The vibration peak at 1515 cm^{-1} assigned to the benzene ring vibration of lignin and the peak at 1254 cm^{-1} corresponded to C-O stretching vibration of acetyl group in lignin reduced. SEM micrographs of untreated fiber revealed that the macro grass fibers were composed of smaller individual single fibers held together by materials in the inter-fibrillar region. After alkali treatment, the materials in the inter-fibrillar region decreased with increasing concentration of alkali solution and treatment time. Based on the FTIR results, the inter-fibrillar materials consisted of hemicellulose and lignin. The removal of hemicellulose and lignin resulted in weak interaction between fibrils leading to easy separation of the grass fiber into finer micro-fibers. As concentration of alkali solution and treatment time were increased, more hemicellulose and lignin were reduced resulting in an increase of fiber aspect ratio. The best tensile and flexural properties were obtained from soy protein based biocomposite filled with fiber treated with 10% w/v NaOH for 4 h. The improvement of mechanical properties was due to a good dispersion of the grass fibers

in the matrix and the enhancement of the interfacial adhesion between the grass fiber and the matrix.

Lui, Mohanty, Drzal, Askel, and Misra (2004) reported the effect of alkali treatment on structure, morphology, and thermal properties of native grass fibers. Native grass fibers were treated with 10% w/v NaOH for 2, 4, 8, and 16 h. FTIR results showed that after alkali treatment, the peak of hemicellulose (1737 cm^{-1}) was absent and the peaks of lignin (1515 , 1254 cm^{-1}) were reduced as they were removed. Moreover, the peak at 2918 cm^{-1} belonging to the C-H stretching vibration in hemicellulose was decreased after alkali treatment due to leaching out of hemicellulose by alkali treatment. With increasing treatment time, hemicellulose and lignin content of the fiber decreased. SEM micrographs of treated fiber showed the separation of the micro-fibrillar structure of the fiber. The removal of hemicellulose and lignin resulted in weak interaction between fibrils leading to easy separation of the fiber into finer micro-fibers. Thermogravimetric analysis (TGA) result showed that thermal decomposition temperature of the alkali treated fiber was higher than that of the untreated fiber. This indicated that alkali treatment improved the thermal stability of the grass fiber due to a reduction of lignin and hemicellulose content. With increasing treatment time, thermal decomposition temperature of the fiber was increased.

Lopattananon, Panawarankul, Sahakaro, and Ellis (2006) studied the effect of alkali treatment on structure and surface morphology of pineapple leaf fibers. Pineapple leaf fibers were treated with 1, 3, 5, and 7% w/v of NaOH solution for 18 h at 28°C . FTIR results showed that the peak of lignin at 1436 cm^{-1} was reduced and the peak of hemicellulose at 1254 cm^{-1} was absent due to complete decomposition of hemicellulose and partial leaching out of lignin by the alkali

treatment. SEM micrograph of treated pineapple leaf fiber showed the separation of the microfibrillar structure of fiber due to the removal of lignin and hemicellulose. The removal of lignin and hemicellulose appeared to increase with increasing concentration of alkali solution.

Bwire, Christian, and Joseph (2007) studied the effect of alkali treatment on chemical compositions of rice husks. Rice husks were treated with 2, 4, 6, and 8% w/v NaOH solution for 24 h at room temperature. Proximate analysis based on the fractionation of organic components of natural fibers was used to investigate the chemical compositions of rice husks against alkali treatment. The results indicated that the proportion of lignin and hemicellulose in rice husks decreased significantly with increasing alkali concentration from 4 to 8% w/v. Lignin and hemicellulose content in rice husks treated with NaOH ranging from 4 to 8% w/v decreased by 96 and 74%, respectively. This revealed that the removal of lignin and hemicellulose was significant when the concentration of NaOH was at least 4% w/v at room temperature.

Edeerozey, Akil, Azhar, and Ariffin (2007) examined the influence of alkali treatment on structure and morphology of kenaf fibers. Kenaf fibers were immersed in NaOH solution with different concentrations (3, 6, and 9% w/v) for 3 h at room temperature. Moreover, kenaf fibers were treated with 6% w/v NaOH at room temperature and 95°C. SEM micrograph of 9% w/v NaOH treated fiber showed the cleanest fiber surface. Tensile strength of the fibers was measured through fiber bundle tensile test. The results showed that alkali treatment significantly improved tensile strength of the fibers. The optimum NaOH concentration was found to be 6% w/v. Moreover, kenaf fibers treated with 6% w/v NaOH at high temperature (95°C)

showed higher tensile strength than that of the fiber treated at room temperature. This was attributed to the effective cleaning process of fiber at high temperature.

Hu and Lim (2007) examined the effects of alkali treatment and fiber content on mechanical properties of hemp fiber/PLA composites. Hemp fibers were treated with 6% w/v NaOH at 40°C for 24 h. The composites with 30, 35, 40, 45, and 50 v% of untreated and treated hemp fibers were prepared. SEM micrographs showed that hemp fiber was separated into finer fibers after alkali treatment due to the removal of non-cellulosic components including hemicellulose, lignin, and pectin. Mechanical properties of the composites were also investigated. The results showed that the composite filled with 40 v% of alkali treated fiber had the best tensile and flexural properties. This indicated that alkali treatment improved the adhesion between the fiber and the matrix.

Liu, Yu, Cheng, and Yang (2009) reported the influence of alkali treatment on structure and chemical compositions of jute fibers. Jute fibers were treated with 5% w/v NaOH solution at room temperature for 4 h. FTIR results showed that after alkali treatment, the strong and sharp peak at 1740 cm^{-1} attributed to C=O stretching vibration of hemicellulose was weakened. Chemical composition analysis also showed that after alkali treatment, the hemicellulose and lignin content decreased whereas the cellulose content increased when compared with untreated jute fiber. This was because hemicellulose and lignin were removed by NaOH solution during alkali treatment. In addition, the removal of lignin and hemicellulose made the fiber cleaner and rougher than the untreated fiber.

Aydin, Tozlu, Kemaloglu, Aytac, and Ozkoc (2011) studied the effect of alkali treatment on surface morphology of flax fibers. Flax fibers

were treated with 10, 20, and 30% w/v NaOH solution for 20 min. SEM micrographs showed that alkali treatment changed the structure of the raw flax fiber. The packed structure of fibrils was deteriorated by removing lignin and waxes out of the fibrils. Fibrils were separated from each other and the surface roughness of the alkali treated flax fibers was increased. This was more pronounced in flax fiber treated with 30% w/v NaOH. The fiber diameter of untreated flax fiber was 40 μm . With increasing concentration of alkali solution up to 30% w/v, the fiber diameter reduced to a range of 10-15 μm . This was attributed to an increase extent of removal of non-cellulosic materials out of the flax fibers.

Tran, Ogihara, and Kobayashi (2011) studied the effects of alkali treatment and fiber content on mechanical properties of coir fiber/poly(butylene succinate) (PBS) composites. Coir fibers were treated with 5% w/v NaOH solution for 72 h at room temperature. The composites with 10, 20, 30, 40, and 50 wt% of untreated and alkali treated coir fibers were prepared. Tensile and flexural properties of alkali treated coir fiber/PBS composites were significantly greater than those of untreated composites at all fiber contents. This was because alkali treatment increased the fiber surface roughness resulting in better mechanical interlocking with PBS matrix. SEM micrographs revealed that alkali treated coir fiber/PBS composites had a good interfacial adhesion between fiber and matrix leading to effective stress transfer throughout the interface. This resulted in an improvement of mechanical properties of alkali treated coir fiber/PBS biodegradable composites.

Tran, Ogihara, Nguyen, and Kobayashi (2011) reported the effect of alkali treatment on surface morphology and mechanical properties of coir fibers and coir fibers/PBS composites. Coir fibers were treated with 5% w/v

NaOH solution for different soaking times (24, 48, 72, and 96 h) at room temperature. SEM micrographs showed that alkali treatment increased surface roughness of coir fibers. Coir fiber treated with 5% w/v NaOH for 72 h showed the highest fiber surface roughness. Moreover, alkali treatment significantly improved tensile properties of the coir fibers. Coir fibers treated with 5% NaOH for 72 h showed the highest interfacial shear strength (IFSS) with 55.6% higher than untreated coir fibers. This was because alkali treated fiber had higher surface roughness than untreated fiber leading to better interfacial fiber-matrix bond. Therefore, the alkali treated fiber with 5% NaOH for 72 h was used to prepare the composites. The fiber contents were 10, 15, 20, 25, and 30 wt%. The alkali treated coir fiber/PBS composites exhibited significantly greater tensile and flexural properties than those of the untreated coir fiber/PBS composites at all fiber contents. This was because alkali treatment enhanced the compatibility between the coir fiber and the PBS matrix.

Williams, Hosur, Theodore, Netravali, Rangari, and Jeelani (2011) studied the effect of alkali treatment time on surface chemistry and morphology of kenaf fibers. The fibers were treated with 7% w/v NaOH solution for 0.5, 1, 2, 4, 8, 16, and 24 h at room temperature. SEM micrographs showed that alkali treatment was successful in removing waxes and surface impurities. As the treatment time was increased beyond 2 h, an increase of surface roughness was observed. This was attributed to the deterioration of lignin and hemicellulose which essentially bound individual fibrils into bundles to form fibers. FTIR results showed that after alkali treatment, the peak of hemicellulose (1730 cm^{-1}) and the peak of lignin (1600 cm^{-1}) structure were reduced. This indicated that hemicellulose and lignin were removed. The sharp decrease of mean hydrogen bond strength (MHBS) for kenaf alkali treated

between 0.5 and 4 h further confirmed the removal of hemicellulose and a part of lignin during alkali treatment.

Qian, Mao, Sheng, Lu, Luo, and Hou (2013) studied the effect of alkali treatment on properties of bamboo particles reinforced PLA composites. Bamboo particles were treated with 0.3 N sodium hydroxide solution with different treatment times (0.25, 0.5, 1, 2, 3, 4, 5, 6, 7, 8, 24 h). The composites with 30 wt% of untreated and alkali treated bamboo particles were prepared. FTIR results revealed that after 3 h of alkali treatment, the peaks located at 3428, 2919, and 1736 cm^{-1} were weakened significantly. The peak at 3428 cm^{-1} assigned to the hydroxyl (-OH) stretching vibration peak was reduced. This indicated that hemicellulose and lignin were removed by mean of a decrease of hydroxyl group. The peak of hydrocarbon (-CH) stretching vibration at 2919 cm^{-1} decreased considerably with the decomposition of hemicellulose and lignin. The peak at 1736 cm^{-1} assigned to carbonyl stretching vibration peak in ester group (-CH₂-COO-) or carboxyl (-COOH) was gradually reduced due to the removal of hemicellulose. Moreover, the composition analysis results indicated that the proportion of hemicellulose in the bamboo particles decreased significantly within 3 h of treatment time. SEM micrographs showed that with increasing treatment time, the surface impurities on the filler surface were eliminated and the surface roughness of the filler was increased. The specific surface area of filler increased significantly and reached the peak value in 3 h of treatment time. The increase of surface roughness of the bamboo particles facilitated mechanical interlocking with PLA matrix. This led to an improvement of mechanical properties of the bamboo particles/PLA composites. Furthermore, DSC analysis showed that alkali

treated bamboo particles/PLA composite had a higher degree of crystallinity than untreated bamboo particles/PLA composite.

2.1.1.1.2 Silane treatment

A variety of silanes are used as coupling agents in the lignocellulosic filler/polymer composites to promote interfacial adhesion and improve the properties of the composites. Silane coupling agents are hydrophilic compounds with different groups attached to silicon that one end interacts with matrix and the other end can react with hydrophilic filler. This reaction performs as a bridge between filler and matrix. Pilla, Gong, O'Neill, Rowell, and Krzysik (2008) studied the effects of silane coupling agent and filler content on mechanical properties and morphologies of pine wood flour (PWF) reinforced PLA composites. PWF was treated with 0.5 wt% of γ -methacryloxypropyltrimethoxysilane. The composites filled with 20 and 40 wt% of untreated and treated PWF were prepared. The results showed that tensile modulus of the untreated PWF/PLA composites increased with increasing PWF content whereas toughness and strain-at-break decreased. However, the composites filled with silane treated PWF showed a slight increase of tensile properties when compared with untreated PWF/PLA composites. SEM micrographs of fracture surface of treated PWF/PLA composites revealed good adhesion between PLA and PWF and good dispersion of PWF in the PLA matrix.

Frone, Berlioz, Chailan, Panaitescu, and Donescu (2011) studied the effect of silane coupling agent on dynamic mechanical thermal properties and morphologies of the composites from PLA and cellulose fiber obtained from mechanical disintegration of regenerated wood fibers (MF). MF was treated with 10 wt% of 3-aminopropyltriethoxysilane (APS) in a mixture of 90/10 ethanol/water

solution for 2 h at room temperature. The composites with 2.5 wt% of silanized and unsilanized cellulose fiber were prepared. FTIR results confirmed the chemical reaction between silane coupling agent and cellulose fiber. The characteristic peaks of amine and siloxane groups were found in the spectra of silane treated fibers. SEM micrographs of the untreated cellulose fiber/PLA composites showed the fibers pulled out from PLA matrix indicating the poor adhesion at fiber-matrix interface. However, the APS treated cellulose fiber/PLA composite showed a better adhesion between cellulose fibers and PLA matrix. Dynamic mechanical thermal analysis (DMTA) showed that both untreated and silane treated fibers led to an improvement of the storage modulus of PLA in the glassy state and a decrease of polymer chains mobility. Furthermore, the storage modulus of PLA composites was significantly enhanced by silanization.

Jandas, Mohanty, Nayak, and Srivastava (2011) evaluated the effect of silane treatment on mechanical properties of banana fiber reinforced PLA composites. Banana fiber was treated with 5 wt% of 3-aminopropyl triethoxysilane (APS) or bis-(3-triethoxysilylpropyl)-tetrasulfane (Si69) for 1 h. The composites with 30 wt% of untreated and silane treated banana fiber were prepared. FTIR spectra of APS banana fiber and Si69 banana fiber exhibited symmetric stretching frequencies of Si-C and Si-O-Si around 784 cm^{-1} and 713 cm^{-1} , respectively. The asymmetric stretching of Si-O-Si and Si-O-C were identified at around 1105 cm^{-1} and 1161 cm^{-1} in the FTIR spectra of silane treated banana fiber. The -Si-O-Si- linkage indicated the deposition of polysiloxanes on the fiber surface and -Si-O-C- confirmed condensation reaction between the silane coupling agent and the fiber. This revealed that silane treatment introduced organosiloxy group to the surface of banana fiber. Moreover, tensile properties of single strand of untreated and silane treated banana fiber

were evaluated. The result showed that silane treatment tend to enhance the tensile properties of the fiber. This might be because the silane can act as a coupling agent between different cellulose strands through covalent and hydrogen bonding. When compared with the untreated banana fiber, the APS and Si69 treated banana fiber exhibited 15 and 35% enhancement of tensile strength and 4 and 13% enhancement of tensile modulus, respectively. The most significant improvement of tensile properties of the composite was observed in case of Si69 treated banana fiber/PLA composites. This was because the ethoxy group of the Si69 reacted with the carbonyl group of the lignocellulosic fiber in ethanol media which further interacted with PLA through hydrogen and covalent bonds. The sulphur atom presented in Si69 can also impart polarity in the system to enhance the interaction with the PLA matrix leading to improved compatibility between banana fiber and PLA matrix.

Chun, Husseinsyah, and Osman (2012) studied the effects of silane coupling agent and filler content on mechanical, thermal, and morphological properties of coconut shell powder (CSP)/PLA biocomposites. CSP was treated with 3% v/v of 3-aminopropyltriethoxysilane (3-APE) for 1 h. The composites with 15, 30, 45, and 60 part per hundred of resin (phr) of untreated and treated CSP were prepared. Tensile strength and elongations at break of the CSP/PLA composites decreased whereas their modulus of elasticity increased with increasing filler content. Tensile strength and modulus of 3-APE treated CSP/PLA composites were better than CSP/PLA composites due to a stronger filler-matrix interaction. SEM micrographs of the 3-APE treated CSP/PLA composites confirmed a better adhesion between CSP and PLA matrix. This may be because silane coupling agent increased the surface functionality of CSP particles and subsequently enabled CSP particles to bond

chemically to PLA matrix. Furthermore, silane treatment improved thermal stabilities of the composites.

Srubar Iii, Pilla, Wright, Ryan, Greene, Frank, and Billington (2012) studied the effect of silane treatment on mechanical properties and morphologies of oak wood flour/poly(hydroxybutyrate)-*co*-poly(β -hydroxyvalerate) (PHBV) composites. 100 g of oak wood flour was treated with 2 ml of trimethoxy(octadecyl)-silane by thermochemical vapor deposition technique. The composites with 10, 20, 30, and 40 v% of untreated and treated oak wood flour were prepared. The results showed that silane treated oak wood flour/PHBV composites had higher stiffness but lower ultimate strength and elongation at break than untreated composites. SEM micrographs also revealed better wetting of silane treated oak wood flour particles in PHBV matrix. This was because the hydrolyzed silane can react with both cellulosic hydroxyl groups and matrix polymer chains. This reaction enhanced wettability and dispersion of oak wood flour particles in PHBV matrix.

Zhao, Qiu, Feng, and Zhang (2012) treated rice straw fiber (RSF) with 5 wt% of four aminosilane coupling agents : 3-aminopropyltrimethoxy silane (APTMS), 3-(2-aminoethylaminopropyl)trimethoxysilane (AEAPTMS), 3-aminopropyltriethoxysilane (APTES), and 3-(2-amino ethylamino-propyl)triethoxy silane (AEAPTES). FTIR and ζ potential results confirmed that amino groups were introduced to the silane treated RSF (TRSF) for all four silane coupling agents. The ethoxy silane treatment was more effective than the methoxy silane treatment because ethoxy silane led to more efficient chemical grafting on RSF. Additionally, the effect of aminosilane on tensile properties and water absorption of RSF reinforced PBS composites was investigated. The composites with 30 wt% of RSF or TRSF were

prepared. FTIR results suggested that aminosilane could form hydrogen bonds with the ester carbonyl of the PBS matrix leading to an improvement of the interaction between RSF and PBS matrix. Therefore, the TRSF/PBS composites had higher tensile strength than that of the RSF/PBS composites. A considerable increase of tensile strength of the composites was found with the presence of AEAPTES. It might be because of the highest amino content of AEAPTES. Moreover, the aminosilane treatment significantly reduced the moisture diffusion coefficient of the TRSF/PBS composites but did not change the mechanism of water adsorption.

2.1.1.1.3 Acrylic acid treatment

Acrylic acid treatment is also reported to be effective in modifying the lignocellulosic filler surface. The main principle of acrylic acid treatment is to react hydroxyl group (-OH) of lignocellulosic filler with carboxyl group (-COOH) of acrylic acid (Suardana, Lokantara, and Lim, 2011). This leads to strong covalent bond formation between lignocellulosic filler and polymer matrix. Suardana, Abdalla, Kim, Choi, and Lim (2011) evaluated the effect of acrylic acid treatment on mechanical properties of coconut fiber/PLA composites. Coconut fibers were treated with 6% w/v NaOH in distilled water at 95°C for 3 h and then treated with solution of 0.5% acrylic acid for 0.5 h. The composites with 35 wt% of untreated and acrylic acid treated coconut fibers were prepared. The results showed that acrylic acid treated fiber/PLA composites had higher tensile, flexural, and impact properties than untreated fiber/PLA composites. This was because acrylic acid treatment provided strong covalent bond formation between coconut fiber and PLA matrix. SEM micrographs of the acrylic acid treated coconut fiber/PLA composites confirmed a better adhesion between coconut fibers and PLA matrix.

Suardana et al. (2011) investigated the effect of acrylic acid treatment on mechanical properties of coconut coir fiber/PLA composites. Coconut coir fibers were treated with 0.5% acrylic acid for 0.5 h at room temperature and 70°C. The composites with 40 wt% of untreated and acrylic acid treated coconut coir fibers were prepared. Tensile and flexural properties of acrylic acid treated coconut coir fiber/PLA composites were improved in comparison to untreated coconut coir fiber/PLA composites. This was because acrylic acid treatment led to strong covalent bond formation between coconut coir fiber and PLA matrix resulting in good filler-matrix interfacial adhesion. In addition, the composite prepared from acrylic acid treated coconut coir fiber at 70°C had higher tensile strength and modulus than the composite prepared from acrylic acid treated coconut coir fiber at room temperature. This was attributed to the effectiveness of graft copolymerization of acrylic acid on the fibers at higher temperature.

2.1.1.2 Physical treatment

2.1.1.2.1 Heat treatment

Heat treatment is an environmental friendly method without impregnating with additional chemicals. Heat treatment of lignocellulosic filler is an effective method to improve the dimensional stability, hygroscopic properties, and durability against biodegradation (Derya and Bilgin, 2008). Rong, Zhang, Liu, Yang, and Zeng (2001) studied the effect of heat treatment on structure and tensile properties of sisal fiber. Sisal fiber was heated at 150°C in air circulating oven for 4 h. FTIR spectra of both untreated and heat treated fibers exhibited almost the same except the slightly diminished intensity at 1650 cm⁻¹ of the heat treated fiber. This was due to the removal of some aromatic lignin from the fiber. Heat treatment improved tensile

strength and tensile modulus of the fiber. This was due to the adjustment in molecular structure at elevated temperature leading to an increase of crystallinity of the fiber.

Ochi (2006) studied the effect of heat treatment on mechanical properties of Manila hemp fiber. The fibers were heated with different temperatures and times (160, 180, and 200°C for 15, 30, 60, and 120 min). Tensile strength of heat treated hemp fiber at 160°C did not decrease even with longer heating times. Moreover, tensile strength of heat treated hemp fiber at 180°C for 30 min was similar to that of non-heat treated fibers due to no degradation of fiber. However, at heating temperature of 200°C, tensile strength of hemp fibers decreased with increasing heating time due to the degradation of fiber.

Cao, Sakamoto, and Goda (2007) studied the effect of heat treatment on tensile strength of kenaf fiber. Kenaf fibers were treated in the vacuum heater at different temperatures (130, 140, 160, 190, and 220°C) for 10 h. With increasing heat treatment temperature, the appearance color of the fibers became brown and gradually black by the observation of naked eye. Moreover, kenaf fibers became easily brittle and broken after heat treatment. Compared with untreated fiber, tensile strength of heat treated kenaf fiber increased at heat temperature of 130 and 140°C then decreased with increasing heat temperature higher than 140°C.

Saikia (2008) evaluated the influence of heat treatment temperature on structural characteristics of sisal fiber. Sisal fiber was heated in a convection oven in an air atmosphere at different temperatures (330, 370, 410, 450, 500, 530, and 600K) for 3 h. X-ray diffraction (XRD) and FTIR studied under ambient conditions showed that sisal fiber had a cellulosic structure in nature. The cellulosic structure of the fiber did not change when heating temperature was up to 450K.

However, the degree of crystallinity of the sisal fiber heated at 450K was decreased by 10.32% from its normal value. Sisal fiber heated at 530K showed a transformation of a crystalline structure to an amorphous state. A decrease of crystallinity of the heat treated sisal fiber could be attributed to the change in dipole interactions. FTIR results of the sisal fiber heated at temperatures from 370 to 600K showed no significant change when compared with native structure of the untreated sisal fibers. However, intensities of the peak resulting from OH in the 3600 to 3125 cm^{-1} regions decreased slightly for the sisal fiber heated at 370K. This was attributed to the removal of water molecules from the fiber after heat treatment.

Yi, Tian, Tong, and Xu (2008) studied thermal stability and mechanical properties of sisal fiber in cycle process of heat treatment. Thermal behavior of fiber was investigated between room temperature and 600°C under a nitrogen atmosphere. From differential thermogravimetric analysis (DTA) curve of sisal fiber, the first peak occurred in the temperature range from 160 to 200°C corresponded to the dehydration as well as degradation of lignin. The second peak of sisal at about 350°C was due to the thermal decomposition of hemicellulose and the cleavage of the glycosidic linkage of cellulose. The third peak at about 550°C of sisal fiber may be due to the further breakage of decomposition products of second stage leading to the information of tar. Moreover, the effect of heat treatment on mechanical properties of sisal fiber was investigated. Sisal fibers were roasted in an oven at 185°C for 5.30, 10.30, 15.30, and 30 min. Tensile strength of sisal fiber decreased gradually with increasing treatment time because some components of the fiber decomposed during thermal cycles.

Kaewkuk, Sutapun, and Jarukumjorn (2013) studied the effects of heat treatment and fiber content on physical properties of sisal fiber/polypropylene (PP) composites. Sisal fiber was treated in an oven at 170°C for 30 min under an atmospheric pressure and a presence of air. The composites with 10, 20, and 30 wt% of untreated and heat treated sisal fiber were prepared. With increasing untreated fiber content, tensile strength and Young's modulus of PP composites increased whereas elongation at break and impact strength decreased. This was due to the reinforcing effect of the fibers. Additionally, tensile properties of heat treated sisal fiber/PP composites were improved in comparison to untreated sisal fiber/PP composites at all fiber contents. This was attributed to the removal of impurities, wax, hemicelluloses, and lignin on fiber surface leading to an enhancement of fiber-matrix interfacial adhesion. Water absorption of the PP composites increased with increasing fiber content. Heat treatment resulted in a reduction of water absorption of the PP composites. This was because wax, impurities, and some hemicelluloses on fiber surface, which were responsible for water absorption of the PP composites, were previously removed by the heat treatment.

2.1.1.2.2 Corona treatment

Corona treatment is one of the most interesting techniques for surface oxidation activation. This process changes the surface energy of the lignocellulosic fillers. Corona discharge treatment is found to be an effective method to enhance the compatibility between hydrophilic fillers and polymer matrix. Gassan, Gutowski, and Bledzki (2000) investigated the effect of corona treatment on surface characteristics of jute fibers. The fiber surface was modified by means of a corona discharge treatment with different corona energy (103, 133, and 200 mJ/mm²).

Corona treatment increased the polarity of the fibers due to an increase of the number of carboxyl and hydroxyl groups. Therefore, the adhesion at the fiber-matrix interface may be increased. The results of surface energy and wetting behavior showed that with increasing corona energy output, the polarity of the flax fibers increased up to corona energy of 133 mJ/mm² and subsequently remained constant.

Ma, Huang, Cao, and Xu (2010) examined the influence of temperature of corona discharge treatment on surface properties of cotton fibers. Corona discharge treatment was applied to modify cotton fibers at temperature of 20, 50, 90, and 110°C. After corona discharge treatment, cotton fiber surface was rougher than the untreated fiber. Moreover, surface oxygen content increased at lower temperature (20°C) and then decreased when temperature was increased. Breaking strength of corona discharge treated cotton fiber increased in certain degree then decreased greatly when the applied temperature was increased up to 110°C. The highest breaking strength of treated cotton fiber was obtained when applied temperature was 50°C. Weight loss rate of cotton fiber increased significantly when temperature was increased. This indicated that cotton fiber was etched severely at higher temperature. These results suggested that the treatment temperature played an important role in surface properties of the fiber.

Ragoubi, George, Molina, Bienaimé, Merlin, Hiver, and Dahoun (2012) studied the effect of corona discharge treatment on mechanical and thermal properties of miscanthus fibers/PLA composites. SEM and X-ray photoelectron spectroscopy (XPS) results showed that corona treatment resulted in a surface oxidation and an etching effect on corona treated fibers. SEM micrographs also showed that corona treatment led to an improvement of compatibility between PLA matrix and

fibers. Therefore, tensile strength and tensile modulus of the composites made from corona treated fibers were remarkably enhanced. Moreover, TGA results showed that corona treatment slightly increased thermal stability of the composites.

2.1.1.2.3 Plasma treatment

Plasma surface treatment is one of environmentally friendly treatments of lignocellulosic fillers. Plasma treatment is an effective method to increase filler-matrix interfacial adhesion by creating free radicals and active groups on fiber surface. Moreover, plasma treatment may be used in order to remove organic surface contamination from the filler which would result in an increase of filler surface roughness. Khammatova (2005) examined the effect of high frequency capacitive discharge plasma (HFC) on structure and mechanical properties of flax fiber. XRD results showed that degree of crystallinity of treated flax fiber was higher than untreated flax fiber. Moreover, it was found that plasma treatment increased tensile strength of the fibers by 55-64%.

Xu, Wang, Zhang, Jing, Yu, and Wang (2006) studied the effect of plasma treatment on surface properties of bamboo fiber. Argon plasma at atmospheric pressure was used to improve wettability of bamboo fibers. SEM and scanning probe microscopy (SPM) results showed that fiber surface became rougher after plasma treatment. Surface roughness of bamboo fiber was increased with increasing treatment time because of the plasma bombardment and etching. These results revealed that atmospheric pressure argon plasma treatment was an effective method to improve surface wettability of bamboo fibers.

Demir, Seki, Bozaci, Sarikanat, Erden, Sever, and Ozdogan (2011) investigated the effect of atmospheric air plasma treatment on

mechanical properties of jute fiber reinforced polyester composites. Jute fibers were subjected to different plasma powers (60, 90, and 120 W) for the exposure times of 1, 3, and 6 min. The effects of plasma powers and exposure times on interlaminar shear strength (ILSS), tensile strength, and flexural strength of jute fibers/polyester composites were evaluated. The highest ILSS values was obtained from the jute fiber treated with plasma power 120 W. After plasma treatment at plasma power 120 W for 1, 3, and 6 min, the ILSS values increased about 122, 144, and 171%, respectively. This can be explained by an increase of surface roughness of jute fiber which caused a better mechanical interlocking with polymer matrix. This led to an improvement of the interfacial adhesion between jute fiber and polyester matrix. The greatest tensile strength and flexural strength values were obtained at 120 W for 1 min and at 60 W for 3 min, respectively. However, the atmospheric air plasma treatment of jute fiber at longer exposure time (6 min) made a detrimental effect on tensile and flexural properties of jute fibers reinforced polyester composites due to the loss of fiber strength.

2.1.2 Matrix modification

Matrix modification can be used to improve the compatibility between lignocellulosic filler and polymer matrix. The main principle of matrix modification is to graft reactive functional groups onto polymer matrix backbone to enhance the filler-matrix interfacial adhesion. Arbelaiz, Fernández, Valea, and Mondragon (2006) studied the effect of poly(ϵ -caprolactone) (PCL) modification on mechanical properties of flax fiber/PCL composites. The grafting reaction of maleic anhydride (MA) onto PCL polymer was carried out in a presence of dicumyl peroxide as an initiator. The results showed that flax fiber/PCL-g-MA composites exhibited higher tensile and flexural properties when compared with flax fiber/PCL composites. This may be due to the

formation of chemical bonds between anhydride groups of PCL-*g*-MA and hydroxyl groups of flax fiber leading to enhanced stress transfer from the matrix to the fiber. SEM micrographs of fracture surface confirmed the adhesion improvement between flax fiber and PCL-*g*-MA matrix.

Wu (2011) evaluated mechanical properties and biodegradability of poly(butylene adipate-*co*-terephthalate) (PBAT) and acrylic acid grafted PBAT (PBAT-*g*-AA) filled with sisal fiber. Tensile strength of sisal fiber/PBAT composites decreased markedly with increasing sisal fiber content. This was attributed to poor dispersion of sisal fiber in the PBAT matrix. However, mechanical properties of the sisal fiber/PBAT-*g*-AA composites, especially tensile strength were higher than that of the sisal fiber/PBAT composites. This behavior was likely due to enhanced dispersion of sisal fiber in the PBAT-*g*-AA matrix resulting from the ester formation and the creation of branched or cross-linked macromolecules. FTIR results confirmed the formation of ester groups due to reactions between hydroxyl groups in sisal fiber and anhydride carboxyl groups in PBAT-*g*-AA. SEM micrograph of sisal fiber/PBAT-*g*-AA composites also confirmed good adhesion between sisal fiber phase and PBAT-*g*-AA matrix. Moreover, biodegradation results demonstrated that the addition of sisal fiber enhanced the biodegradability of the composites.

Wu, Yen, and Wang (2011) studied the effect of polybutylene-terephthalate (PBT) modification on mechanical and morphological properties of sisal fiber/PBT composites. Acrylic acid (AA) was grafted onto molten PBT. SEM micrographs of sisal fiber/PBT composites showed that sisal fiber tended to agglomerate into bundles and was unevenly distributed in the matrix. Poor wetting in sisal fiber/PBT composites was due to large differences in surface energy between sisal

fiber and PBT matrix. However, sisal fiber/PBT-*g*-AA composite showed more homogeneous dispersion and improved sisal fiber wetting in PBT-*g*-AA matrix. This was due to the formation of ester linkage between carboxyl groups of PBT-*g*-AA and hydroxyl groups of sisal fiber leading to enhanced adhesion between sisal fiber and PBT-*g*-AA matrix. Thus the AA modified PBT composites exhibited better mechanical properties than the unmodified PBT composites.

Wu (2012) evaluated mechanical properties and biodegradability of poly(butylene-succinate-*co*-adipate) (PBSA) and acrylic acid-modified PBSA (PBSA-*g*-AA) filled with rice husk (RH). FTIR and nuclear magnetic resonance (NMR) results revealed the formation of ester groups in the resulting composite formed by reactions between the hydroxyl groups in RH and the carboxyl groups of PBSA-*g*-AA. RH/PBSA-*g*-AA composites exhibited noticeably superior mechanical properties when compared with those of RH/PBSA composites. SEM micrographs of RH/PBSA-*g*-AA composites also showed a good interfacial adhesion between RH particle and PBSA-*g*-AA matrix. Moreover, water resistance of RH/PBSA-*g*-AA composites was higher than those of RH/PBSA composites. On the other hand, biodegradation rate of RH/PBSA-*g*-AA composites was lower than that of RH/PBSA composites.

Wu and Liao (2012) studied mechanical and thermal properties of rice straw fiber (RSF)/PCL and RSF/maleic anhydride grafted polycaprolactone (PCL-*g*-MA) composites. RSF/PCL-*g*-MA composites exhibited better tensile properties than RSF/PCL composites due to greater compatibility between PCL-*g*-MA and RSF. SEM micrographs showed that the dispersion of RSF in the PCL-*g*-MA matrix was highly homogeneous. This was due to ester formation between the

anhydride groups of PCL-*g*-MA and the hydroxyl groups of RSF that resulted in the formation of branched and cross-linked macromolecules.

2.1.3 Addition of compatibilizer

Generally, the compatibility between lignocellulosic filler and polymer matrix can be improved with the presence of compatibilizer. The compatibilizer attends at the filler-matrix interface and plays the roles of strengthening interfacial adhesion resulting in an improvement of the properties of the lignocellulosic filler/polymer composites. Lee and Wang (2006) studied tensile properties and water resistance of both bamboo fiber/PLA and bamboo fiber/PBS composites. Lysine-based diisocyanate (LDI) was used as a compatibilizer. Tensile properties and water resistance of both bamboo fiber/PLA and bamboo fiber/PBS composites were improved with the addition of LDI. This may be attributed to enhanced interfacial adhesion between the polymer matrix and the bamboo fiber. Enzymatic degradation result showed that biodegradability of bamboo fiber/PLA and bamboo fiber/PBS composites could be quickly decomposed by enzyme whereas the addition of LDI delayed the degradation.

Avella, Gaceva, Buz̄arovska, Errico, Gentile, and Grozdanov (2007) examined the effect of maleic anhydride grafted poly(3-hydroxybutyrate-*co*-3-hydroxyvalerate) (PHBV-*g*-MA) as a compatibilizer on mechanical properties of kenaf fiber/PHBV composites. PHBV-*g*-MA was obtained by grafting maleic anhydride onto PHBV. PHBV-*g*-MA induced a strong interfacial adhesion between kenaf fiber and PHBV matrix leading to enhanced mechanical properties of the composite. SEM micrographs of the compatibilized composite confirmed a significant enhancement of the adhesion between fibers and matrix. Kenaf fibers were wetted by PHBV matrix and the fiber pull out from matrix was minimum. This may be attributed to the formation

of ester linkage between MA groups grafted onto PHBV backbones and hydroxyl groups of kenaf fibers during mixing.

Chen, Liu, Cooke, Hicks, and Zhang (2008) studied the effect of polymeric diphenylmethane diisocyanate (pMDI) as a compatibilizer on mechanical properties and water resistance of biocomposite from PLA and sugar beet pulp (SBP). Mechanical properties and water resistance of SBP/PLA composites were improved when pMDI was incorporated. As the pMDI concentration gradually increased from 0.5 to 2%, tensile strength of the composites increased and approached that of neat PLA. The microstructure of the composites indicated that the addition of pMDI remarkably improved the wettability of the SBP particles by PLA and increased the penetration of PLA into the porous SBP. Consequently, the failure of the composites in mechanical testing changed from extensive debonding without pMDI to progressive rupture of the SBP particles with pMDI.

Petinakis, Yu, Edward, Dean, Liu, and Scully (2009) investigated the effect of methylenediphenyl-diisocyanate (MDI) as a compatibilizer on mechanical properties of wood flour/PLA composites. The addition of MDI into the composites resulted in 10% increase of tensile strength and 135% increase of tensile modulus of the composites. This indicated that the addition of MDI enhanced filler-matrix interfacial adhesion. SEM micrographs also revealed an improvement of interfacial adhesion between PLA and wood flour particles with the addition of MDI.

2.2 Toughness improvement of lignocellulosic filler/polymer composites

The remarkable reduction in toughness of lignocellulosic filler/PLA composites limits the application of the composites. Therefore, the toughness of the PLA composites has to be improved to achieve balance overall properties. Several methods have been proposed to improve toughness of PLA based lignocellulosic filler composites including plasticization and addition of flexible polymer component into PLA composites.

2.2.1 Toughness improvement of lignocellulosic filler/polymer composites by adding plasticizer

Plasticizers are used not only to improve the processability of polymers but also to enhance flexibility and ductility of polymers by increasing polymer chain flexibility and resistance to fracture. Haq, Burgueño, Mohanty, and Misra (2008) enhanced toughness of hemp fiber/unsaturated polyester (UPE) composites using epoxidized soybean oil. The weight ratios of UPE/epoxidized soybean oil were 100/0, 90/10, and 80/20 while the content of hemp fiber was maintain at 21 wt% based on the total composite weight. The addition of epoxidized soybean oil increased toughness of the hemp fiber/polyester composite, which was observed experimentally as larger elongation at break and higher impact strength. With increasing epoxidized soybean oil content, elongation at break and impact strength of the composites increased continuously. This indicated that epoxidized soybean oil acted as a plasticizer that weakened the interaction between polymer macromolecules and improved the flexibility and mobility of polymer chains. However, stiffness and ultimate tensile

stress of the composites decreased continuously with increasing epoxidized soybean oil content.

Li, Zhou, and Pei (2011) improved toughness of sisal fiber reinforced PLA composites using polyethylene glycol (PEG) as a plasticizer. PLA composite and PEG-plasticized PLA composite with 30 wt% of sisal fiber were prepared. The incorporation of PEG increased the toughness of sisal/PLA composite. PEG plasticized PLA composite exhibited higher impact strength than PLA composite. This may be attributed to the plasticization effect of PEG that weakened the interaction between PLA macromolecules and improved the chains mobility of PLA. However, flexural strength and flexural modulus of the PEG-plasticized PLA composite were lower than the composite without plasticizer.

Rahman, De Santis, Spagnoli, Ramorino, Penco, Phuong, and Lazzeri, (2012) used PEG to improve toughness of softwood kraft lignin/poly-L-lactic acid (PLLA) composites. PEG was used at different contents (15, 20, and 30 wt%) and softwood kraft lignin content was fixed at 15 wt% in all composites. The results showed that the composites prepared from 30 wt% PEG plasticized PLLA exhibited higher deformability in comparison with the unplasticized PLLA composites. This may be attributed to the plasticization effect of PEG that improved the chains mobility of PLA. Thus, the composites with higher amount of PEG provided a good balance between flexibility and stiffness.

2.2.2 Toughness improvement of lignocellulosic filler/polymer composites by adding flexible polymer component

Adding flexible polymer component into lignocellulosic filler/polymer composites is an effective way to improve the toughness of the composites. This

method is regarded as a useful and economical way to produce new materials with a wide range of properties. Sombatsompop, Yotinwattanakumtorn, and Thongpin (2005) investigated the effect of ethylene octene copolymer on mechanical properties of sawdust/PP composites. Ethylene octene copolymer contents were varied between 0 and 11.1 wt% based on the total composite weight. Sawdust contents were also varied from 0 to 30 wt%. With increasing sawdust content, the overall tensile strength and toughness of the composites were reduced. However, toughness of the sawdust/PP composites could be regained by adding an ethylene octene copolymer. Elongation at break and impact strength of the composites increased with increasing ethylene octene copolymer content. The toughening mechanism of sawdust/PP composites was caused by the improvement ability of the rubber phase to deform plastically. SEM micrographs of impact fracture surface of the composite with ethylene octene copolymer showed elongated PP matrix on the fracture surface and along the filler, which indicated a ductile deformation.

Liu, Wu, Han, Yao, Kojima, and Suzuki (2008) investigated morphologies and mechanical properties of bamboo flour (BF)/high density polyethylene (HDPE) composites toughening with semi-crystalline maleated ethylene/propylene elastomers (sEPR-*g*-MA), amorphous maleated ethylene/propylene elastomers (aEPR-*g*-MA), maleated polyethylene (PE-*g*-MA), and their combinations. The concentrations of each toughening agent were varied between 0 and 8.3 wt% based on the total composite weight while HDPE/BF ratio was fixed at 60/40 w/w. The incorporation of either PE-*g*-MA or sEPR-*g*-MA enhanced tensile strength, flexural strength, and impact toughness of the composites. Tensile and flexural strength of the composites toughening with either PE-*g*-MA or sEPR-*g*-MA increased with the amount

of toughening agent. However, this effect began to level off when its concentration exceeded 2.9 wt%. aEPR-g-MA showed a negative effect on tensile and flexural strengths but had a moderate enhancement of impact toughness when compared to the composite without toughening agents. The impact toughness of the aEPR-g-MA toughened composites initially increased with aEPR-g-MA loading up to 2.9 wt% and then gradually decreased beyond this level. The combination of PE-g-MA/sEPR-g-MA with 2:1 weight ratio improved impact toughness while simultaneously maintained tensile and flexural strength of the composite at an acceptable level when compared to the composites with either PE-g-MA or sEPR-g-MA alone.

Petinakis et al. (2009) studied the effect of poly(ethylene-acrylic acid) (PEAA) on mechanical properties of wood flour/PLA composites. The composites with 5, 10, 20, 30, and 40 wt% of wood flour were prepared with 3 wt% of PEAA. The addition of PEAA to wood flour/PLA composites resulted in improvement of elongation at break and impact strength of the composites. This was attributed to the presence of more resilient PEAA in the polymer composite resulting in a more ductile polymer matrix. However, tensile strength of the composites decreased with the incorporation of PEAA.

Cai, Wang, Nie, Tian, Zhu, and Zhou (2011) investigated the effect of toughening agents on mechanical properties of bamboo fiber/PP composites. Three toughening agents, namely glycidyl methacrylate grafted poly(ethylene-1-octene) (MPOE), maleic anhydride grafted poly(ethyleneoctene) (POE-g-MAH), and poly(ethylene-butylacrylate-glycidyl methacrylate) (PTW) were used to improve impact toughness of the bamboo/PP composites. The concentrations of each toughening agent were varied between 0 and 8 wt% based on the total composite weight while

bamboo fiber/PP ratio was fixed at 50/50 w/w. With the addition of toughening agent, impact strength of the composites was significantly improved. The part of POE in POE-*g*-MAH and MPOE can form a cavitation effect, which would result in material change in stress state and gave rise to shear yielding leading to improve flexibility of the composites. For PTW toughening agent, butylacrylate segment in PTW had a good low temperature performance. Therefore, the impact strength of bamboo fiber/PP composites increased via the deformation of butylacrylate chain when suffered from external shocks. Moreover, when the content of toughening agents was controlled between 6 and 8 wt%, impact strength of bamboo fiber/PP composites was remarkably improved while tensile and flexural properties were less affected.

Jiang and Qin (2006) studied the effect of polyethylene octene elastomer (POE) on mechanical properties of wood flour/PP composites. POE contents were varied between 15 and 30 wt% of PP while wood flour content was fixed at 60 wt%. Impact strength of the composites increased with increasing POE content. This indicated that the presence of POE in the wood/PP composites prevented the propagation of the crack. However, the stiffness of the composites decreased with the addition of POE.

Lee (2009) evaluated the effect of PBAT content on mechanical properties of bamboo flour (BF)/PLA composites. PBAT contents were varied between 5 and 20 wt% and BF contents were also varied from 10 to 30 wt%. The results showed that as the BF content was increased, the overall tensile strength, flexural strength, and toughness of the composites decreased. The addition of PBAT led to an increase of deformability of the BF/PLA composites which was observed experimentally as larger elongation at break. This was probably due to the presence of soft elastomeric phase.

Goriparthi, Suman, and Nalluri (2012) studied the effect of PCL on impact property and damping capacity of jute fiber/PLA biocomposites. The weight ratios of PLA/PCL/jute fiber were 50/0/50, 45/5/50, 40/10/50, and 35/15/50. Mechanical, thermal, and biodegradation properties of the biocomposites were investigated. The addition of PCL into jute fiber/PLA biocomposite led to recovery of the impact strength and damping capacity of the biocomposites without much reduction in stiffness and strength. Biocomposite with 10 wt% PCL attained an optimum balance between stiffness and toughness. Degree of crystallinity of the composites decreased with increasing PCL content. Furthermore, the addition of PCL also resulted in an improvement of biodegradation rate of biocomposites thereby making them more environmental friendly.

Qiang, Yu, and Gao (2012) investigated the effect of polyhydroxyalkanoates (PHAs) on mechanical, thermal, and morphological properties of pine wood flour/PLA composites. PLA, wood flour, and PHAs were mixed together with different weight ratios of 80/20/0, 65/10/25, 55/20/25, and 45/30/25. The addition of PHAs into the wood flour/PLA composites led to an increase of impact strength but a decrease of tensile strength. The brittle-ductile transition of impact strength of the wood flour/PLA composites toughened with PHAs was observed when the content of wood flours was between 15 and 35 wt%. The results demonstrated that PHAs can be used to tune mechanical properties of the wood flour/PLA composites. SEM images showed that the fracture surfaces of the wood flour/PLA composites toughened with PHAs were rougher than that of their nontoughened composites. However, TGA results indicated that the PHAs reduced the thermal stability of the wood flour/PLA composites.

Afrifah and Matuana (2013) studied the effect of ethylene acrylate copolymer (EAC) content on fracture toughness of wood flour/PLA composites using fracture mechanics analysis. The contents of EAC were varied between 0 and 20 wt% and wood flour/PLA ratio was fixed at 40/60 w/w. J-integral at crack initiation (J_{in}) and fracture energy per unit surface area (J_f) were evaluated as the fracture properties. The results showed that J_{in} and J_f were notably increased with the addition of flexible EAC into wood flour/PLA composites. This was because EAC acted as stress concentrators that initiated local yielding of the matrix around crack tips resulting in an enhancement of toughness of the composites. With increasing EAC content, J_{in} and J_f of the composites increased continuously. SEM micrographs of impact fractured surfaces revealed that EAC was presented as a separate phase in the PLA matrix of the composite. This immiscibility allowed the rubbery nature of EAC to induce energy dissipation mechanisms into PLA, which retarded crack initiation and propagation resulting in an improvement of fracture toughness of the toughened composites.

CHAPTER III

EXPERIMENTAL

3.1 Materials

Poly(lactic acid) (PLA, 3052D) was supplied from Nature Works LLC. Poly(butylene adipate-*co*-terephthalate) (PBAT, Ecoflex FBX 7011) was purchased from BASF Co., Ltd. Iron wood (*Hopea odorata* Roxb) sawdust was supplied from Piyarat sawmill, Nakhon Ratchasima, Thailand. Sodium hydroxide (NaOH, Carlo Erba) was purchased from Italmar (Thailand) Co., Ltd. Maleic anhydride (MA monomer) and 2,5-bis(*tert*-butylperoxy)-2,5 dimethylhexane (Luperox 101) were purchased from Sigma-Aldrich. Tris(2,4-di-*tert*-butylphenyl) phosphite antioxidant (Irgafos 168, Ciba) and pentaerythritol tetrakis(3-(3,5-di-*tert*-butyl-4-hydroxyphenyl) propionate) antioxidant (Irganox 1010, Ciba) were purchased from Merit Solution Co., Ltd.

3.2 Experimental

3.2.1 Preparation of sawdust

Sawdust was sieved with a screen system equipped with 50 mesh screens (particle size between 300 and 425 μm) then dried in an oven at 70°C for 24 h. This sawdust was called untreated sawdust (UT). The untreated sawdust was treated with 2, 5, and 10% w/v sodium hydroxide solution with vigorous stirring for 30 and 60 min at room temperature. Then, the sawdust was washed with water for several times

until pH7 was attained. After that the sawdust was dried at 70°C for 24 h. This sawdust was called alkali treated sawdust (AT).

3.2.2 Characterization of sawdust

3.2.2.1 Filler composition determination

The filler composition : cellulose, hemicellulose, and lignin of untreated and alkali treated sawdust was carried out according to wood industry sector methods (Sarkar, Mazumdar, and Pal, 1948; Chattopadhyay and Sarkar, 1946). The sawdust was dewaxed with a mixture of benzene/ethanol taken in the ratio of 2:1 at 70°C for 3 h. Filler to liquor ratio was 1:50. The dewaxed sawdust was washed with ethanol for 30 min, then dried at 105°C and weighed.

The dewaxed sawdust was boiled for 2 h in 0.7% sodium chlorite solution (adjusted to a pH4 using buffer solution) at 75°C by maintaining a filler to liquor ratio of 1:50. After that the samples were washed with 5% sodium bisulphate solution and distilled water, then dried at 105°C in a hot air oven and weighted. In this step, the lignin was removed, thus the weight difference after this step corresponded to the lignin content while the remaining weight was holocellulose content (hemicellulose and cellulose). The percentage of lignin was calculated using equation (3.1):

$$\% \text{ Lignin} = \frac{W \text{ (g)} - W_1 \text{ (g)}}{W \text{ (g)}} \times 100 \quad (3.1)$$

Where W is the dry weight of dewaxed sample, W₁ is the dry weight of remaining holocellulose in sample.

The remaining holocellulose sawdust was treated with 17.5% sodium hydroxide solution for 30 min at room temperature to eliminate alkali soluble

hemicellulose. After that the samples were washed with acetic acid solution and distilled water, then dried at 105°C and weighted. The remaining weight and weight loss corresponded to the contents of cellulose and hemicellulose, respectively. The percentage of cellulose and hemicellulose were calculated using equation (3.2) and (3.3), respectively:

$$\% \text{ Cellulose} = \frac{W_2 \text{ (g)}}{W \text{ (g)}} \times 100 \quad (3.2)$$

$$\% \text{ Hemicellulose} = \frac{W_1 \text{ (g)} - W_2 \text{ (g)}}{W \text{ (g)}} \times 100 \quad (3.3)$$

Where W is the dry weight of dewaxed sample, W_1 is the dry weight of remaining holocellulose in sample, and W_2 is the dry weight of remaining cellulose in sample.

3.2.2.2 Functional group analysis

FTIR spectra of untreated and alkali treated sawdust were recorded in an air atmosphere using Fourier transform infrared spectrometer (Bruker, Tensor 27) in the wavenumber range from 4000 to 600 cm^{-1} , operating in attenuated total reflectance (ATR) mode. Thirty two scans were used at a resolution of 4 cm^{-1} .

3.2.2.3 Thermal properties

Thermal stability of untreated and alkali treated sawdust was analyzed by a thermogravimetric analyzer (Perkin Elmer, SDT 2960). Sawdust was heated from room temperature to 800°C with a heating rate of 10°C/min under a nitrogen atmosphere. The weight of specimens between 10 to 15 mg was used.

3.2.2.4 Morphological properties

Surface morphologies of untreated and alkali treated sawdust were examined using a scanning electron microscope (JEOL, JCM6010). Acceleration voltage of 10 keV was used to collect scanning electron microscopic (SEM) images of the samples. The sawdust was coated with gold before analysis.

3.2.3 Preparation of poly(lactic acid) grafted with maleic anhydride

PLA pellets were dried at 70°C for 4 h before mixing. Poly(lactic acid) grafted with maleic anhydride (PLA-*g*-MA) was prepared in an internal mixer (Haake Rheomix, 3000P) at 170°C for 10 min. The rotor speed was 50 rpm. Maleic anhydride and 2,5-bis(*tert*-butylproxy)-2,5 dimethylhexane were 5.0 and 1.0 wt%, respectively (Teamsinsungvon, 2010).

3.2.4 Characterization of poly(lactic acid) grafted with maleic anhydride

3.2.4.1 Determination of maleic anhydride content

The quantity of maleic anhydride content on PLA was determined by a titration of acid groups derived from anhydride functions using phenolphthalein as an indicator. Samples were dissolved in chloroform and precipitated with methanol to remove residual MA and initiator. Then, the grafted PLA was accurately weighed and completely dissolved in chloroform:methanol (80:20 v/v) and it was titrated immediately with potassium hydroxide solution (KOH). The acid number and the graft content (%G) were calculated using equation (3.4) and (3.5), respectively. Pure PLA without MA was also titrated under the same condition to obtain blank value (Wu, 2003).

$$\text{Acid number (mg KOH/g)} = \frac{V_{\text{KOH}} (\text{ml}) \times N_{\text{KOH}} (\text{N})}{\text{sample (g)}} \times 56.11 \quad (3.4)$$

$$\%G = \frac{(\text{Acid number} - M_0)}{2 \times 561} \times 98.06 \quad (3.5)$$

Where N is the normality (mol/l), V is the volume (ml), 56.11 is the molecular weight of KOH, M_0 is the blank titration value of pure PLA, and 98.06 is the molecular weight of MA.

3.2.4.2 Fourier transform infrared spectroscopy

Infrared spectrum of PLA-g-MA was investigated and compared with the spectrum of PLA using a Fourier transform infrared spectrometer (Bruker, Tensor 27) in the wavenumber range from 4000 to 600 cm^{-1} , operating in attenuated total reflectance (ATR) mode. Thirty two scans were used at a resolution of 4 cm^{-1} .

3.2.5 Preparation of sawdust/PLA composites

Before mixing, PLA and sawdust were dried at 70°C for 4 and 24 h, respectively to minimize the moisture content. PLA, untreated or alkali treated sawdust, and antioxidants were mixed using a co-rotating intermeshing twin screw extruder (Brabender, DSE 35/17D) at the barrel temperature of 175/170/165/160/155°C. The screw speed was 15 rpm. Sawdust contents were 20, 30, and 40 wt%. The antioxidants (Irganox 1010 and Irgafos 168 as a weight ratio 1:1) were used at content of 1 phr for all composites. After exiting die, the extrudate was cooled in air before being granulated by a pelletizer. After that, granulated composites were dried at 70°C for 4 h. Test specimens were prepared by an injection molding machine (Chuan Lih Fa, CLF 80T).

The injection was processed at a melting temperature of 170°C, an injection speed of 46 mm/s, a holding pressure of 1,400 kg/cm², and a mold temperature of 30°C.

3.2.6 Preparation of sawdust/PLA/PBAT composites and compatibilized sawdust/PLA/PBAT composites

Based on mechanical properties of the sawdust/PLA composites, the alkali treated sawdust/PLA composite with the ratio of 30:70 giving the optimum mechanical properties was chosen to study the effect of PBAT content on the properties of the sawdust/PLA/PBAT composites. The ratio of alkali treated sawdust/PLA was kept at 30:70 and PBAT contents were varied as 10, 20, and 30 wt%. Moreover, based on the mechanical properties of sawdust/PLA/PBAT composites, the composite with 20 wt% of PBAT giving the optimum mechanical properties was selected to study the effect of PLA-g-MA content on the properties of the composites. The ratio of alkali treated sawdust/PLA was kept at 30:70, PBAT content was fixed at 20 wt%, and the compatibilizer contents were varied as 3, 5, and 10 wt%. Before compounding, PLA, PBAT, and PLA-g-MA were dried at 70°C for 4 h in an oven. Moreover, sawdust was dried at 70°C for 24 h to minimize the moisture content. The composites were prepared using a co-rotating intermeshing twin screw extruder (Brabender, DSE 35/17D) at the barrel temperature of 175/170/165/160/155°C. The screw speed was 15 rpm. The antioxidants (Irganox 1010 and Irgafos 168 as a weight ratio 1:1) were used at content of 1 phr for all composites. After exiting die, the extrudate was cooled in air before being granulated by a pelletizer. After that, granulated composites were dried at 70°C for 4 h. Test specimens were prepared by an injection molding machine (Chuan Lih Fa, CLF 80T). The injection was processed at a melting temperature of 170°C, an injection speed of 46 mm/s, a holding pressure of 1,400 kg/cm², and a mold temperature of 30°C.

3.2.7 Characterization of PLA, sawdust/PLA, sawdust/PLA/PBAT, and compatibilized sawdust/PLA/PBAT composites

3.2.7.1 Mechanical properties

Tensile properties of PLA and PLA composites were obtained according to ASTM D638 using a universal testing machine (Instron, 5565) with a load cell of 5 kN and a crosshead speed of 5 mm/min.

Flexural properties of PLA and PLA composites were obtained according to ASTM D790 using a universal testing machine (Instron, 5565) with a load cell of 5 kN, a span length of 53 mm, and a crosshead speed of 1.4 mm/min.

Izod impact strength of PLA and PLA composites were performed according to ASTM D256 using an impact testing machine (Atlas, BPI). Unnotched impact strength was tested using the impact pendulum with impact energy of 2.7 J.

All the mechanical properties were performed at room temperature and five samples were tested for each composition.

3.2.7.2 Thermal properties

Thermogravimetric analysis of PLA and PLA composites was analyzed using a thermogravimetric analyzer (Perkin Elmer, SDT 2960). The weight of specimens between 10 to 15 mg was used. The specimens were heated from room temperature to 600°C with a heating rate of 10°C/min under a nitrogen atmosphere.

Thermal properties of PLA and PLA composites were investigated using a differential scanning calorimeter (NETZSCH, DSC 204F1). All samples were heated from -50 to 200°C with a heating rate of 5°C/min (1st heating scan) and kept isothermal for 5 min under a nitrogen atmosphere to erase previous thermal

history. Then, the sample was cooled to -50°C with a cooling rate of $5^{\circ}\text{C}/\text{min}$ and heated again to 200°C with a heating rate of $5^{\circ}\text{C}/\text{min}$ (2nd heating scan). The crystallinity of PLA (χ_c) was estimated using the following equation:

$$\chi_c = \frac{\Delta H_m}{w_f \times \Delta H_m^0} \times 100\% \quad (3.6)$$

Where ΔH_m is the enthalpy of melting during the heating, ΔH_m^0 is the enthalpy for 100% crystalline of PLA (93.7 J/g) (Garlotta, 2001), and w_f is the weight fraction of PLA component in composites.

3.2.7.3 Morphological properties

Morphological properties of PLA and PLA composites were performed by a scanning electron microscope (JEOL, JCM6010). Acceleration voltage of 10 keV was used to collect scanning electron microscopic (SEM) images of the samples. The impact and tensile fractured surface of the specimens were coated with gold before analysis.

CHAPTER IV

RESULTS AND DISCUSSION

4.1 Effect of alkali treatment on properties of sawdust

4.1.1 Filler composition

Filler compositions of untreated sawdust (UT) and alkali treated sawdust (AT) are listed in Table 4.1. The contents of cellulose, hemicellulose, and lignin of untreated sawdust were 64.06, 19.59, and 16.36%, respectively. Obviously, after alkali treatment with 2% w/v sodium hydroxide (NaOH) solution for 30 min, hemicellulose and lignin contents of alkali treated sawdust were decreased whereas cellulose content was increased. This was because hemicellulose and lignin were removed during alkali treatment (Kargarzadeh, Ahmad, Abdullah, Dufresne, Zainudin, and Sheltami, 2012; Joseph, Joseph, and Thomas, 1999). Brígidaa et al. (2010) also reported that the alkali treated coconut fiber had higher cellulose content than the untreated coconut fiber. This might be due to partial removal of hemicellulose and lignin during alkali treatment. Moreover, Liu et al. (2009) found that alkali treatment can remove a certain amount of lignin and hemicellulose of jute fiber. With further increasing NaOH concentration to 5 and 10% w/v, the quantity of hemicellulose and lignin slightly decreased while cellulose content slightly increased. Obi Reddy, Shukla, Uma Maheswari, and Varada Rajulu (2012) also reported that cellulose content of borassus fine fibers increased with increasing NaOH concentration from 2 to 20% w/v because of the removal of hemicellulose and surface impurities.

At the same concentration of NaOH solution, hemicellulose and lignin contents slightly decreased whereas cellulose content slightly increased with increasing treatment time from 30 to 60 min as seen in Table 4.1. Qian, Mao, Sheng, Lu, Luo, and Hou (2013) also found that hemicellulose and lignin contents of bamboo flour slightly decreased while cellulose slightly increased with increasing treatment time.

Table 4.1 Filler composition of untreated sawdust and alkali treated sawdust.

Treatment conditions	Cellulose (%)	Hemicellulose (%)	Lignin (%)
Untreated sawdust (UT)	64.06	19.59	16.36
Alkali treated 2% w/v for 30min (AT2%_30min)	72.43	15.40	12.17
Alkali treated 5% w/v for 30min (AT5%_30min)	73.22	14.89	11.89
Alkali treated 10% w/v for 30min (AT10%_30min)	74.64	14.22	11.14
Alkali treated 2% w/v for 60min (AT2%_60min)	73.29	15.12	11.60
Alkali treated 5% w/v for 60min (AT5%_60min)	74.32	14.23	11.45
Alkali treated 10% w/v for 60min (AT10%_60min)	74.99	14.08	10.93

4.1.2 Functional group analysis

Fourier transform infrared spectroscopy (FTIR) spectrum of untreated sawdust is shown in Figure 4.1 and assigned positions for absorption bands are summarized in Table 4.2. FTIR spectrum of the untreated sawdust exhibited absorption bands of chemical group characteristic of lignocellulosic filler compounds : cellulose, hemicellulose, and lignin. The peak located in 3334 cm^{-1} was corresponded to the

characteristic O-H stretching vibration peak which mainly existed in cellulose, hemicellulose, and lignin. The peaks at 2919 and 2856 cm^{-1} were the characteristic band for the C-H stretching vibration of CH and CH_2 in cellulose, hemicellulose, and lignin. The peak located in 1728 cm^{-1} was belonged to the C=O stretching vibration of linkage of carboxylic acid in lignin or ester group in hemicellulose. The absorption peaks at 1603 and 1508 cm^{-1} in the spectrum were attributed to C=C stretching of aromatic ring of lignin. The peak at 1456 cm^{-1} was associated to the CH_2 symmetric bending in cellulose. The absorption peaks observed at 1363 and 1328 cm^{-1} were associated to the bending vibration of C-H and C-O groups of the aromatic ring in polysaccharides, respectively. The peak located in 1234 cm^{-1} was corresponded to the C-O stretching vibration of the acetyl group in hemicellulose component. A little shoulder located in 1160 cm^{-1} was due to the antisymmetrical stretching of the C-O-C band in cellulose. The peak observed at 1030 cm^{-1} was attributed to the C-O and O-H stretching vibration which belonged to polysaccharide in cellulose. Moreover, the peak located in 894 cm^{-1} was correspond to the presence of β -glycosidic linkages between the monosaccharides (Qian, Mao, Sheng, Lu, Luo, and Hou, 2013; De Rosa, Kenny, Puglia, Santulli, and Sarasini, 2010; Das and Chakraborty, 2006; Schwanninger, Rodrigues, Pereira, and Hinterstoisser, 2004).

Table 4.2 Infrared main transitions for untreated sawdust (Qian et al., 2013; De Rosa et al., 2010; Das et al., 2006; Schwanninger et al., 2004).

Wavenumber (cm ⁻¹)	Vibration	Source
3334	O-H stretching	cellulose, hemicellulose, and lignin
2919	C-H stretching	cellulose, hemicellulose, and lignin
2856	CH ₂ stretching	cellulose, hemicellulose, and lignin
1728	C=O stretching	linkage of carboxylic acid in lignin or ester group in hemicellulose
1603, 1508	C=C stretching	aromatic ring of the lignin
1456	CH ₂ symmetric bending	cellulose
1363	C-H bending	aromatic ring in polysaccharides
1328	C-O bending	aromatic ring in polysaccharides
1234	C-O stretching	acetyl group in hemicellulose
1160	C-O-C antisymmetrical stretching	cellulose
1031	C-O and O-H stretching	polysaccharide in cellulose
893	β-glycosidic linkages	polysaccharide

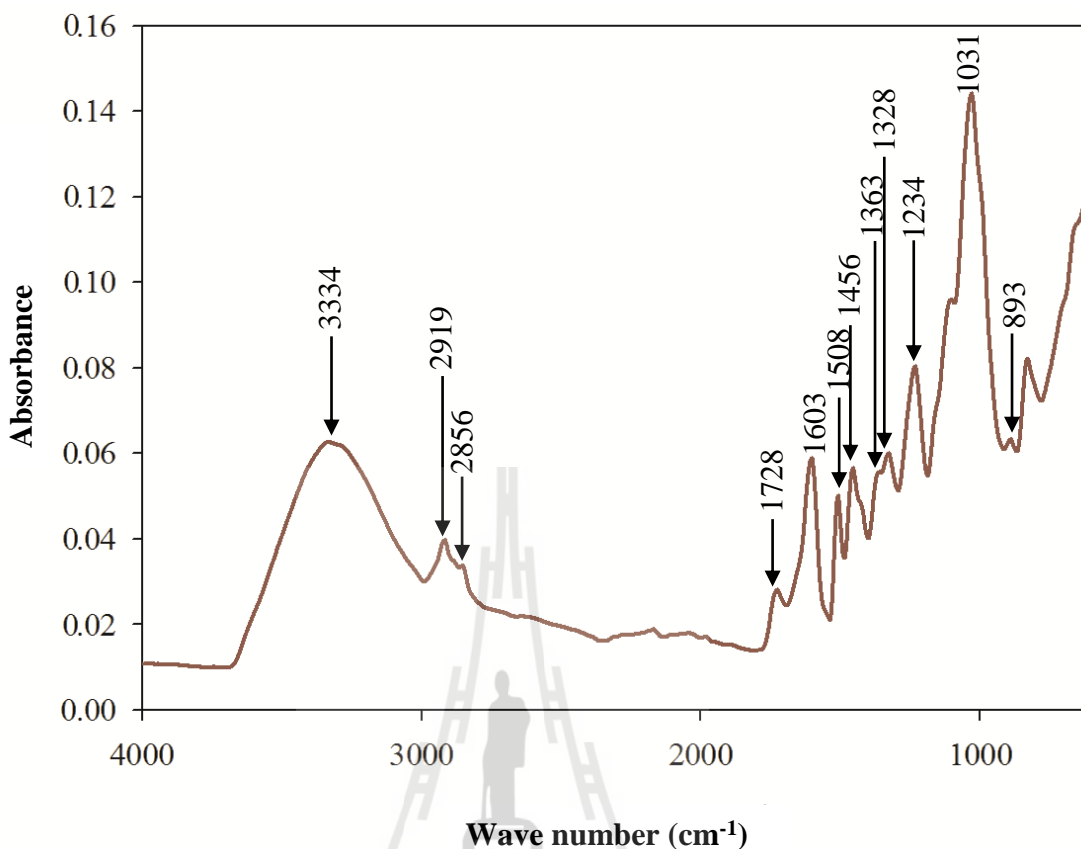


Figure 4.1 ATR-FTIR spectrum of untreated sawdust.

FTIR spectra of untreated sawdust and alkali treated sawdust with different NaOH concentrations and treatment times are shown in Figure 4.2. After alkali treatment, the absorption peak in several locations, i.e. 3334, 2919, 2856, 1728, 1603, and 1508 cm⁻¹ were decreased significantly. The peak at 3334 cm⁻¹ assigned to the hydroxyl (O-H) stretching vibration peak of cellulose, hemicellulose, and lignin was reduced. Since cellulose is fairly resistant to alkali solution, the reduction of this peak intensity was possibly due to the removal of hemicellulose and lignin (Qian et al., 2013). The peaks of hydrocarbon (C-H) stretching vibration at 2919 and 2856 cm⁻¹ decreased considerably with the decomposition of hemicellulose and lignin (Lui, Mohanty, Drzal, Askel, and Misra, 2004). The peak at 1728 cm⁻¹ assigned to carbonyl

stretching vibration peak in ester group (-CH₂-COO-) or carboxyl (-COOH) was gradually reduced due to the removal of hemicellulose and lignin (Qian et al., 2013; Williams, Hosur, Theodore, Netravali, Rangari, and Jeelani, 2011; Liu et al., 2009). In addition, the absorption peaks at 1603 and 1508 cm⁻¹ belonged to the C=C bonds of aromatic ring in the lignin were also remarkably decreased after alkali treatment. It was expected due to lignin were removed during alkali treatment (Williams et al., 2011). Similar investigation was also reported by Liu et al. (2004). They observed that after alkali treatment of native grass fibers, the peak of hemicellulose (1737 cm⁻¹) was absent and the peak of lignin (1515, 1254 cm⁻¹) structure was reduced as they were removed from the fiber. Furthermore, the peak at 2918 cm⁻¹ belonging to the C-H stretching vibration in hemicellulose and lignin was decreased after alkali treatment due to a leaching out of hemicellulose and lignin by alkali treatment.

Additionally, it was interesting to note that the intensity of peaks at 3334, 2919, 2856, 1728, 1603, and 1508 cm⁻¹ was remarkably decreased after alkali treatment with 2% w/v NaOH solution for 30 min. With further increasing NaOH concentration, the intensity of these peaks insignificantly changed. Moreover, treatment time had little effect on the peak intensity. This result was corresponded to filler composition results in previous section.

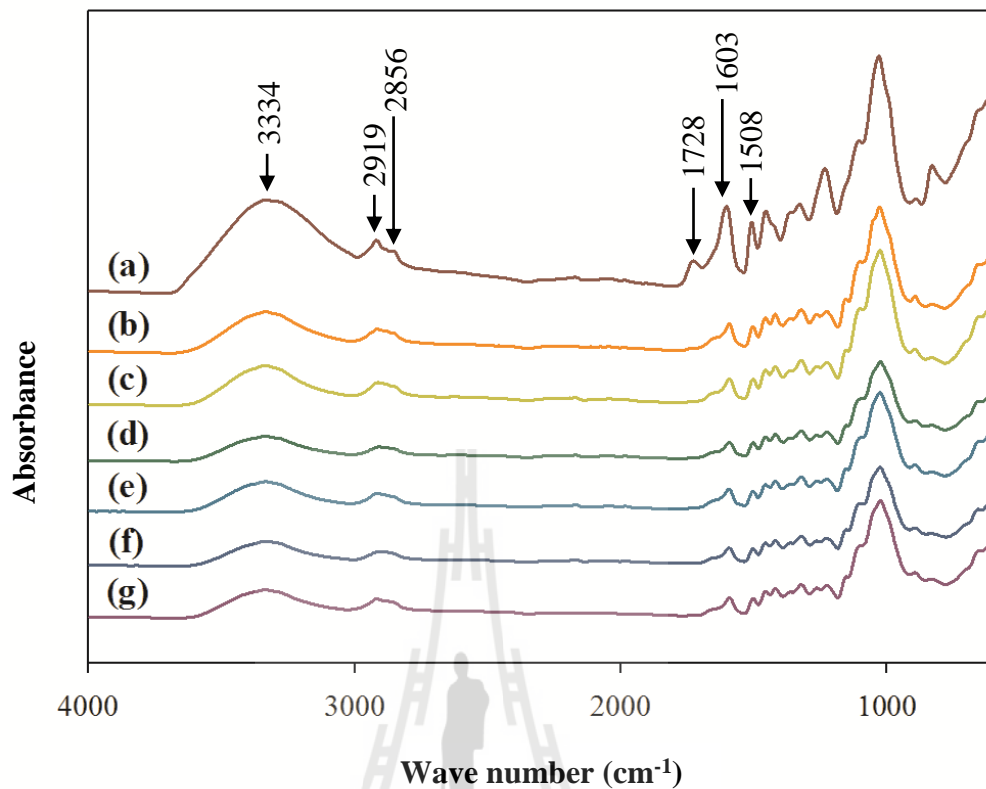


Figure 4.2 ATR-FTIR spectra of (a) UT, (b) AT2%_30min, (c) AT5%_30min, (d) AT10%_30min, (e) AT2%_60min, (f) AT5%_60min, and (g) AT10%_60min.

4.1.3 Thermal properties

Thermogravimetric analysis (TGA) curve and differential thermogravimetric analysis (DTA) curve of untreated sawdust are shown in Figure 4.3. It can be observed that the untreated sawdust exhibited three stages of decomposition process. An initial weight loss around 65°C was corresponded to the evaporation of moisture. The first transition of untreated sawdust started to undergo initial weight loss and showed peak transition about 175 and 292°C, respectively. This step involved the decomposition of low molecular weight compositions (e.g. wax, pectin, and others

surface impurities contained in the sawdust) and hemicellulose (Obi Reddy et al., 2012; Bwire et al., 2007). The second transition of untreated sawdust at 360°C was belonged to the decomposition of cellulose (Obi Reddy et al., 2012; Rachini, Le Troedec, Peyratout, and Smith, 2009). The third transition of untreated sawdust was observed as a small shoulder around 421°C corresponding to lignin decomposition (Mohan, Pittman, and Steele, 2006). Generally, it was well known that lignin had complex structure which composed of aromatic rings with various branches. Thus, the lignin decomposition in lignocellulosic filler was occurred slowly within the wide temperature which begin at 280°C and continues to 450-500°C (De Rosa et al., 2010; Mohan et al., 2006). De Rosa et al. (2010) also found that the decomposition temperature of okra fiber was in three stages. The first one occurred between 220 and 310°C was attributed to the thermal degradation of pectin and hemicellulose. The second stage was observed between 310 and 390°C corresponding to thermal degradation of cellulose. The third stage was the decomposition of lignin which occurred slowly within the whole temperature range (280-500°C). Additionally, from Table 4.3, it can be observed the residual weight of untreated sawdust at 800°C was 8.42%.

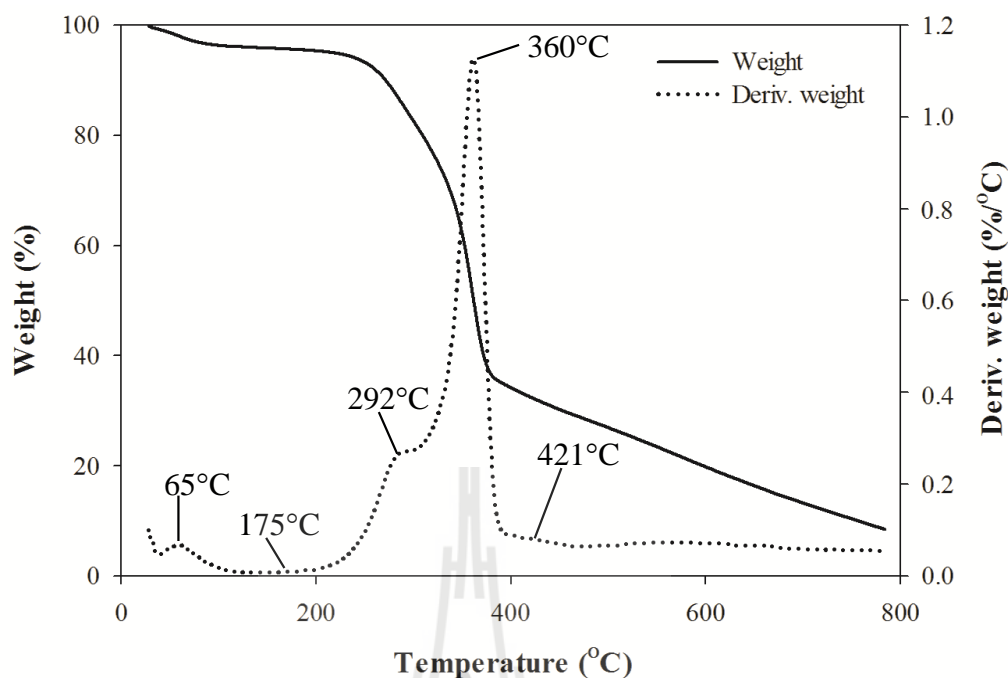


Figure 4.3 TGA and DTA curve of untreated sawdust.

Thermal decomposition temperatures of untreated sawdust and alkali treated sawdust with different NaOH concentrations and treatment times are shown in Table 4.3. TGA and DTA curves of untreated sawdust and alkali treated sawdust with different NaOH concentrations and treatment times are shown in Figure 4.4 and 4.5, respectively. All DTA curves showed the moisture evaporation around 65°C. It can be seen that weight loss percentage of the moisture evaporation of alkali treated sawdust was lower than untreated sawdust. This might be because alkali treatment reduced the numbers of OH groups of lignocellulosic filler. Therefore, the lignocellulosic filler became less hydrophilic and retain less moisture compared to untreated filler (Yılmaz, 2013). This result was corresponded with the FTIR results which showed the reduction of peak intensity at 3334 cm^{-1} related to the decrease of OH groups in sawdust after alkali treatment. Zaini, Jonoobi, Tahir, and Karimi (2013) also found that water content

of alkali treated kenaf bast fibers was decreased by alkali treatment. From Figure 4.5, the onset temperature of the first transition of untreated sawdust and alkali treated sawdust was remarkably different. All alkali treated sawdust had higher onset temperature than that of untreated sawdust about 25°C as shown in Table 4.3. This was due to the removal of low molecular weight compositions, e.g., wax, pectin, and others surface impurities during alkali treatment. These substances degraded at a lower temperature thus this removal led to an improvement of thermal stability of the sawdust (Rojo, Alonso, Domínguez, Saz-Orozco, Oliet, and Rodriguez, 2013). Moreover, an absence of the first peak transition was observed after alkali treatment. This characteristic was attributed to the removal of hemicellulose during alkali treatment (Obi Reddy et al., 2012; Bwire et al., 2007). For the second transition of the sawdust, it was found that the decomposition temperature of cellulose of alkali treated sawdust was slightly higher than that of untreated sawdust. This indicated that thermal stability of alkali treated sawdust was enhanced due to removal of hemicellulose and low molecular weight compositions which had low thermal stability (Lu and Oza, 2013; Arifuzzaman Khan, and Shamsul Alam, 2012; Liu et al., 2004). In addition, it can be seen that the third transition associated with lignin decomposition disappeared for alkali treated sawdust. This result confirmed the removal of lignin in sawdust during alkali treatment. Moreover, alkali treated sawdust showed higher percentage of residue weight at 800°C than untreated sawdust as seen in Figure 4.4. This was because the presence of more amount of crystalline nature (cellulose crystal) increased the proportion of carbon (Kumar, Negi, Choudhary, Bhardwaj, 2014; Mohamad Haafiz, Eichhorn, Hassan, and Jawaaid, 2013). In fact, the formation of char residue of lignocellulosic filler was increased as carbon content increased (Kumar et al., 2014). Therefore, the char residue

of alkali treated sawdust increased due to the increased of cellulose proportion in sawdust as seen in Table 4.1. Reddy, Maheswari, Reddy, and Rajulu (2009) reported that initial degradation temperature (T_i), final degradation temperature (T_f), 25% degradation temperature (T_{25}), 50% degradation temperature (T_{50}), and char content of alkali treated Napier grass fibers were higher than those of the untreated fibers. This might be due to the removal of hemicellulose and low molecular weight components from the fibers after alkali treatment.

However, with increasing NaOH concentration and treatment time, the decomposition temperatures and residue weight content of all alkali treated sawdust insignificantly changed as seen in Table 4.3. A similar observation was reported by Obi Reddy et al. (2012). They found that the DTA thermogram of the alkali treated Borassus fruit fibers showed similar trend under different alkali treatment conditions (2-15% w/v NaOH). Ray, Sarkar, Basak, and Rana (2002) reported that thermal decomposition temperatures and residue weight at 600°C of alkali treated jute fiber insignificantly changed with increasing treatment time from 2-8 h.

It can be seen that thermal properties of the sawdust were corresponded with the filler composition results and functional group analysis results in previous sections.

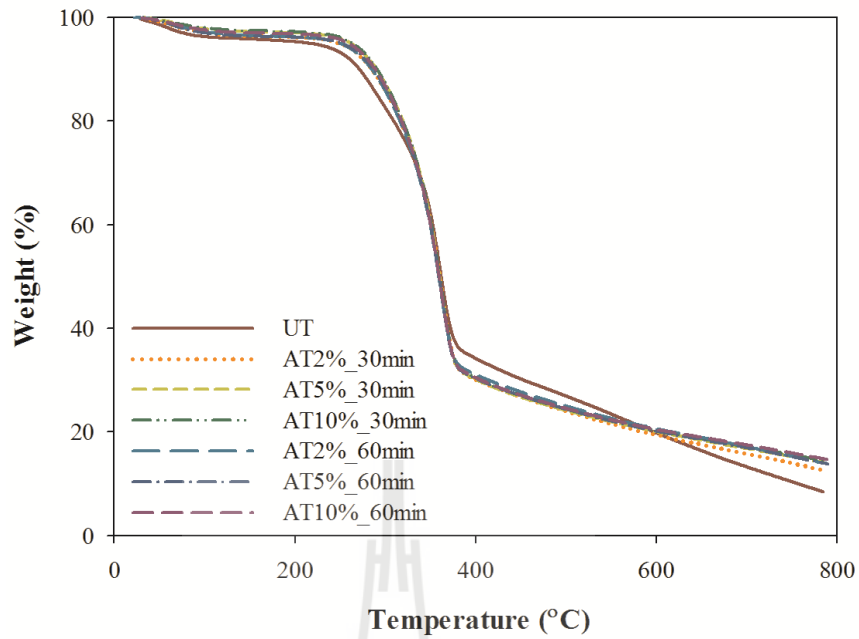


Figure 4.4 TGA curves of untreated sawdust and alkali treated sawdust with different NaOH concentrations and treatment times.

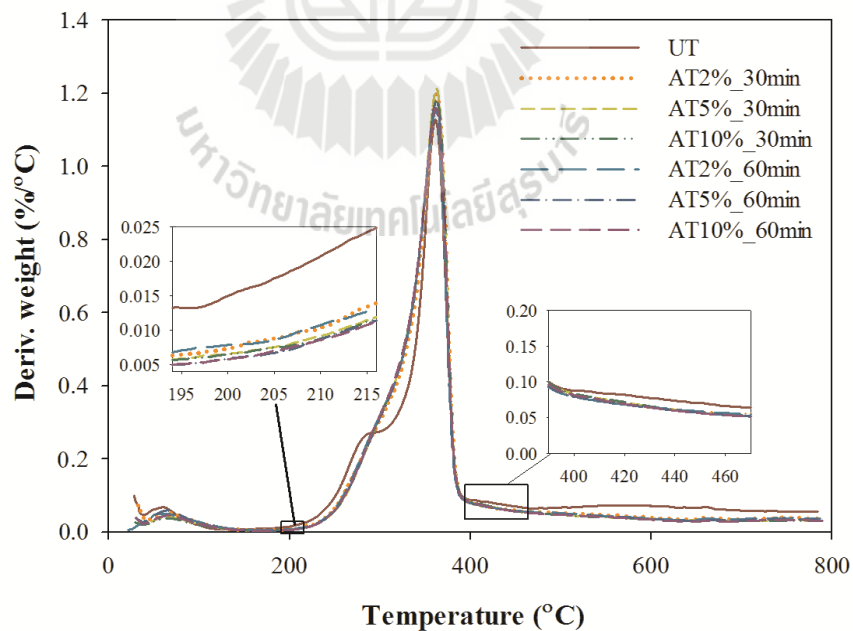


Figure 4.5 DTA curves of untreated sawdust and alkali treated sawdust with different NaOH concentrations and treatment times.

Table 4.3 Thermal decomposition temperatures of untreated sawdust and alkali treated sawdust with different NaOH concentrations and treatment times.

Treatment conditions	Water evaporation			1 st Transition		2 nd Transition	3 rd Transition	Residue weight at 800°C (%)
	Onset (°C)	Peak (°C)	Weight loss (%)	Onset (°C)	Peak (°C)	Peak (°C)	Peak (°C)	
UT	39.70	65.58	4.241	175.74	292.05	360.14	421.28	8.42
AT2%_30min	40.23	66.37	3.651	201.98	-	363.29	-	12.50
AT5%_30min	40.12	66.94	2.874	200.78	-	362.82	-	13.95
AT10%_30min	39.47	66.92	2.588	199.15	-	362.80	-	14.34
AT2%_60min	39.04	65.31	3.561	199.77	-	362.10	-	13.32
AT5%_60min	38.66	65.82	2.776	199.58	-	362.63	-	13.80
AT10%_60min	37.34	65.63	2.463	199.75	-	362.45	-	14.63

4.1.4 Morphological properties

SEM micrographs of untreated sawdust and alkali treated sawdust with different NaOH concentrations and treatment times at 200x and 500x magnification are shown in Figure 4.6 and 4.7, respectively. According to Figure 4.6 (a) and 4.7 (a), it can be observed that the untreated sawdust contained considerable amounts of surface impurities on its surface. After alkali treatment, the surface of alkali treated sawdust was cleaner and rougher than the untreated sawdust as seen in Figure 4.6 (b)-(g) and 4.7 (b)-(g). Liu et al. (2009) also reported that alkali treatment can remove surface impurities covering the external surface of jute fiber. This made the fiber surface cleaner and rougher when compared with the untreated jute fiber.

When compared to the untreated sawdust, sawdust treated with 2% w/v NaOH for 30 min had cleaner and rougher surface than the untreated sawdust. This was attributed to the removal of surface impurities, lignin, and hemicellulose by alkali treatment (Obi Reddy et al., 2012; Lopattananon, Panawarangkul, Sahakaro, and Ellis, 2006). With further increasing NaOH concentration more than 2% w/v, surface roughness of sawdust was insignificantly changed (Figure 4.7 (c)-(d)). As the treatment time was approached 60 min, surface roughness of sawdust slightly increased and its surface started to develop cracks as seen in Figure 4.7 (e)-(g). Generally, an increase of filler cracking resulted in an adverse effect on mechanical properties of lignocellulose filler reinforced polymer composites (Srisuwan, 2012). Thus, it appeared that alkali treatment with low sodium hydroxide concentration (2% w/v) and short treatment time (30 min) was successful with removing the surface impurities and increasing surface roughness of the sawdust. Williams et al. (2011) treated kenaf fiber with 7% w/v NaOH solution at various treatment times. They found that with increasing treatment time, an

increase of surface roughness was observed due to the removal of hemicellulose and lignin. Nonetheless, the fiber cracking on the fiber surface was observed. This resulted in a noticeable decrease of mechanical properties of the fiber.

From results of filler composition, functional group analysis, thermal properties, and morphological properties, the optimum alkali treatment condition was 2% w/v NaOH for 30 min. This condition was used to treat the sawdust for further study.



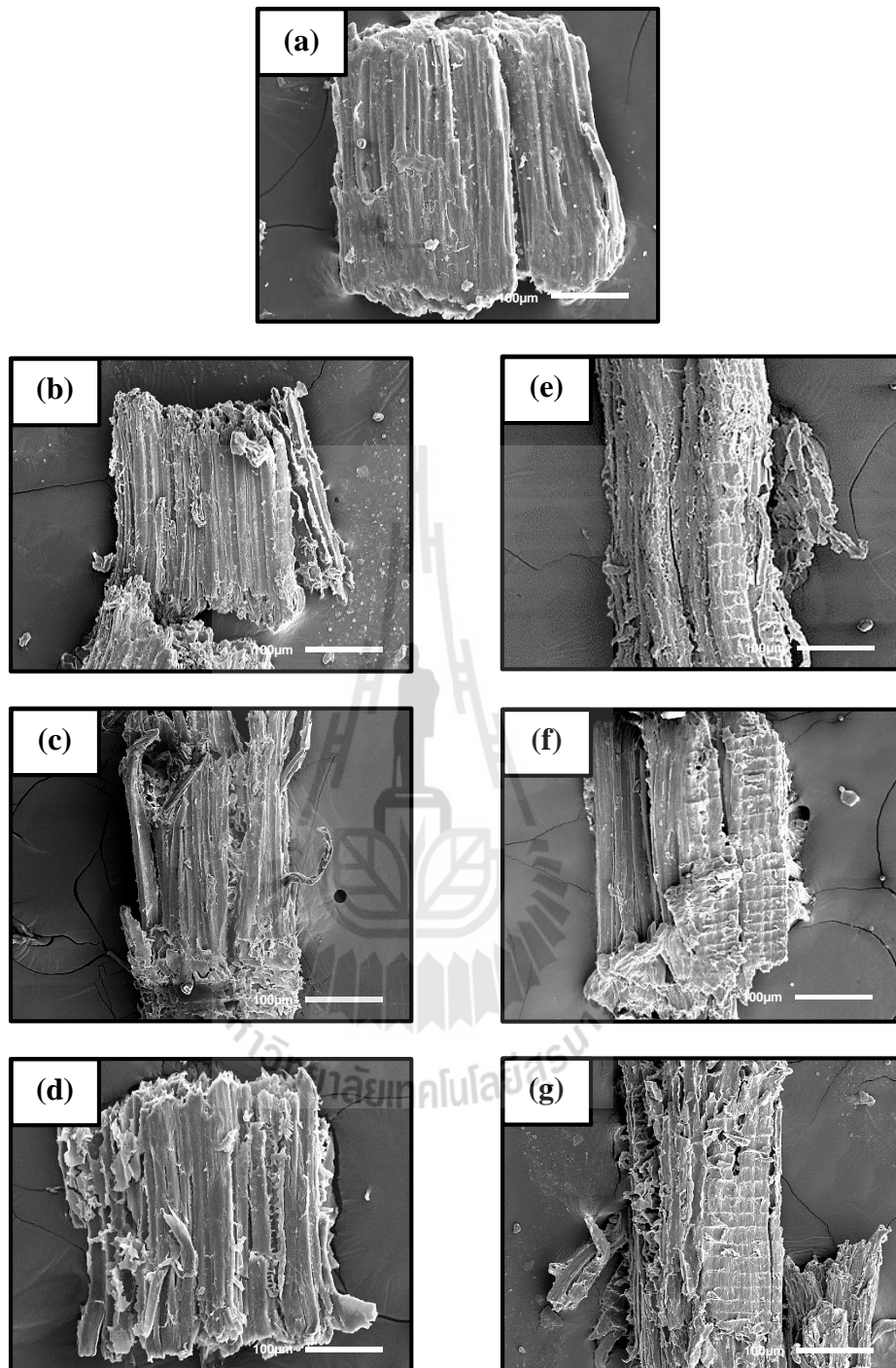


Figure 4.6 SEM micrographs at 200x magnification of (a) UT, (b) AT2%_30min, (c) AT5%_30min, (d) AT10%_30min, (e) AT2%_60min, (f) AT5%_60min, and (g) AT10%_60min.

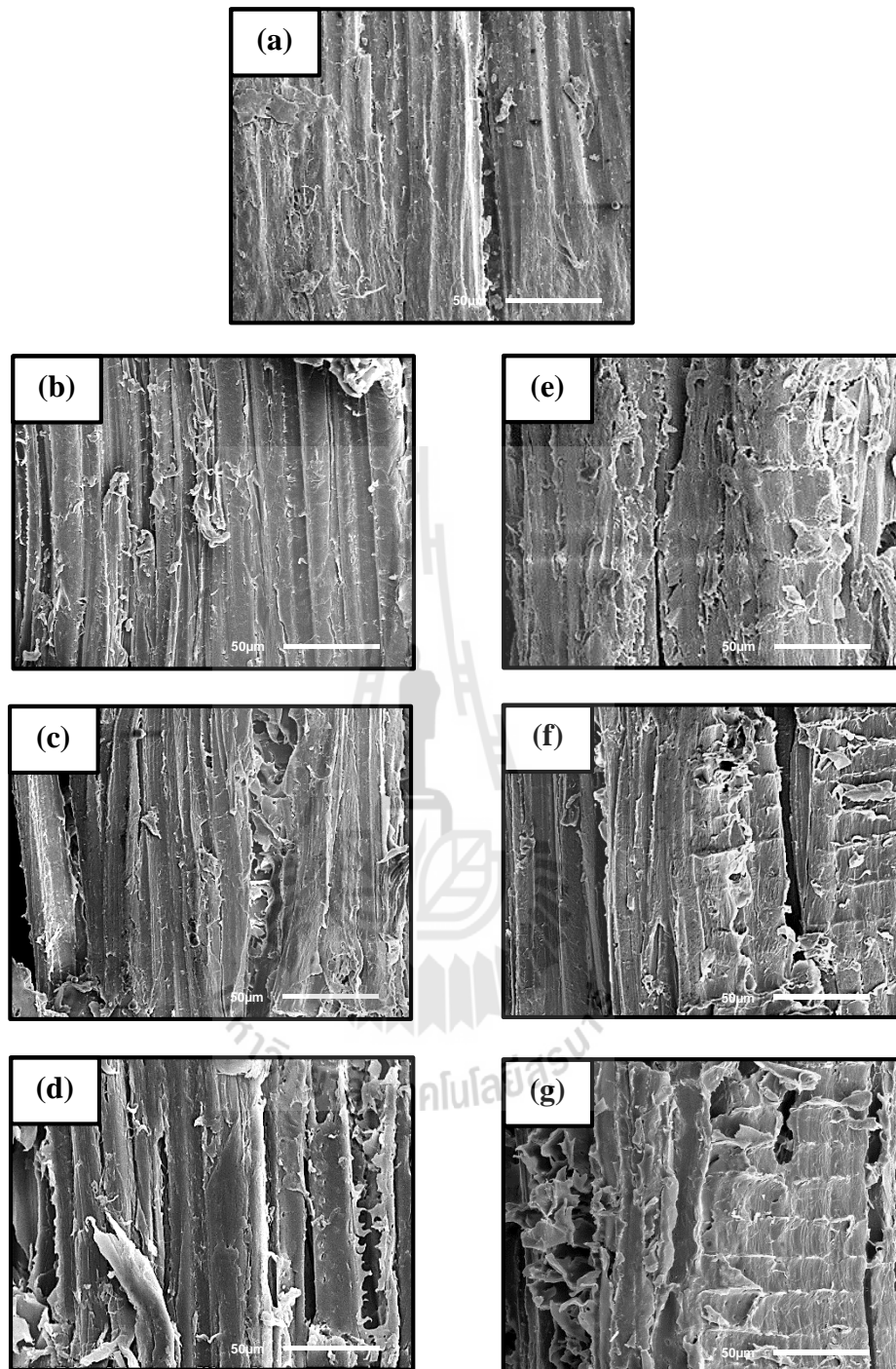


Figure 4.7 SEM micrographs at 500x magnification of (a) UT, (b) AT2%_30min, (c) AT5%_30min, (d) AT10%_30min, (e) AT2%_60min, (f) AT5%_60min, and (g) AT10%_60min.

4.2 Characterization of PLA-g-MA

PLA-g-MA was prepared by an internal mixer. Graft content of MA on PLA was determined by a titration of acid groups derived from anhydride functions. The graft content of PLA-g-MA with MA monomer 5.0 wt% and Luperox101 1.0 wt% was 0.86%.

FTIR was used to identify the grafting reaction of PLA-g-MA. FTIR spectra of PLA, PLA-g-MA, and MA in the range of 2000-1000 cm^{-1} are shown in Figure 4.8. Generally, succinic anhydride groups exhibited an intensive absorption band near 1780 cm^{-1} and a weak band near 1850 cm^{-1} which were attributed to the symmetric stretching and the asymmetric stretching of C=O (Zhu, Liu, and Zhang, 2012; Mani, Bhattacharya, and Tang, 1999). From Figure 4.8, it can be seen that the absorption at 1780 cm^{-1} was weak and might be overlapped with the large carbonyl peak of PLA. Moreover, the absorption at 1850 cm^{-1} was hardly noted. Therefore, the second derivative of FTIR spectra were used for improving resolution of strongly overlapping peaks.

Figure 4.9 shows the second derivative IR spectra of PLA, PLA-g-MA, and MA in the range of 2000-1000 cm^{-1} . The spectrum of PLA-g-MA exhibited the absorption at 1780 cm^{-1} corresponding to the symmetric stretching of C=O due to the cyclic anhydride group absorption. The absorption at 1850 cm^{-1} (asymmetric stretching of C=O) was observed as a small shoulder peak in the PLA-g-MA spectrum. This result confirmed that MA was grafted onto PLA successfully (Zhu et al., 2012; Teamsinsungvon, 2010).

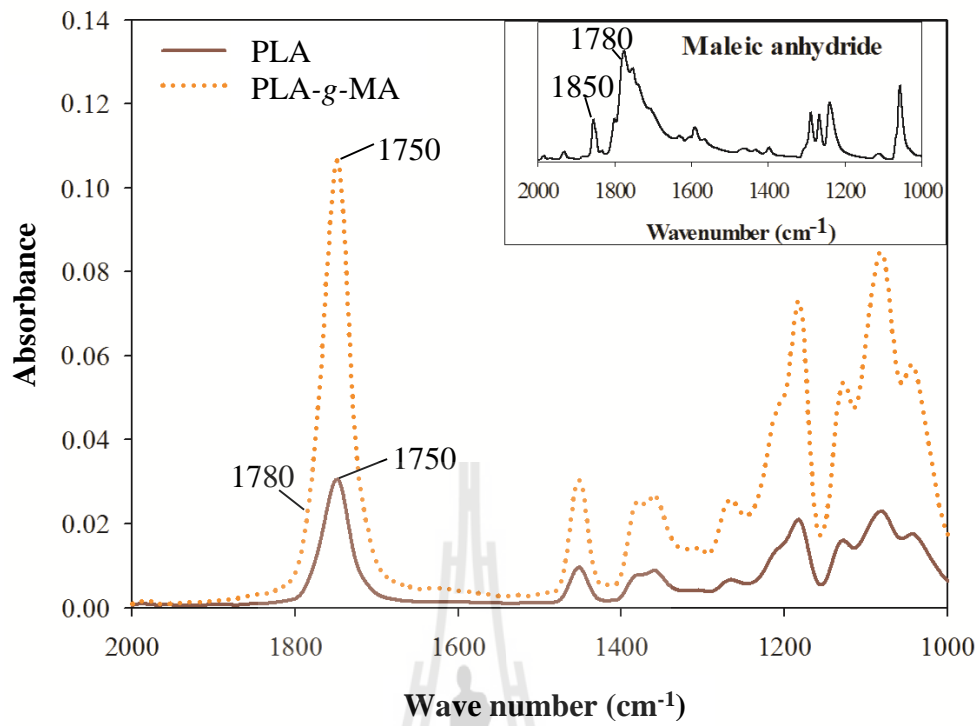


Figure 4.8 FTIR spectra of PLA, PLA-g-MA, and MA.

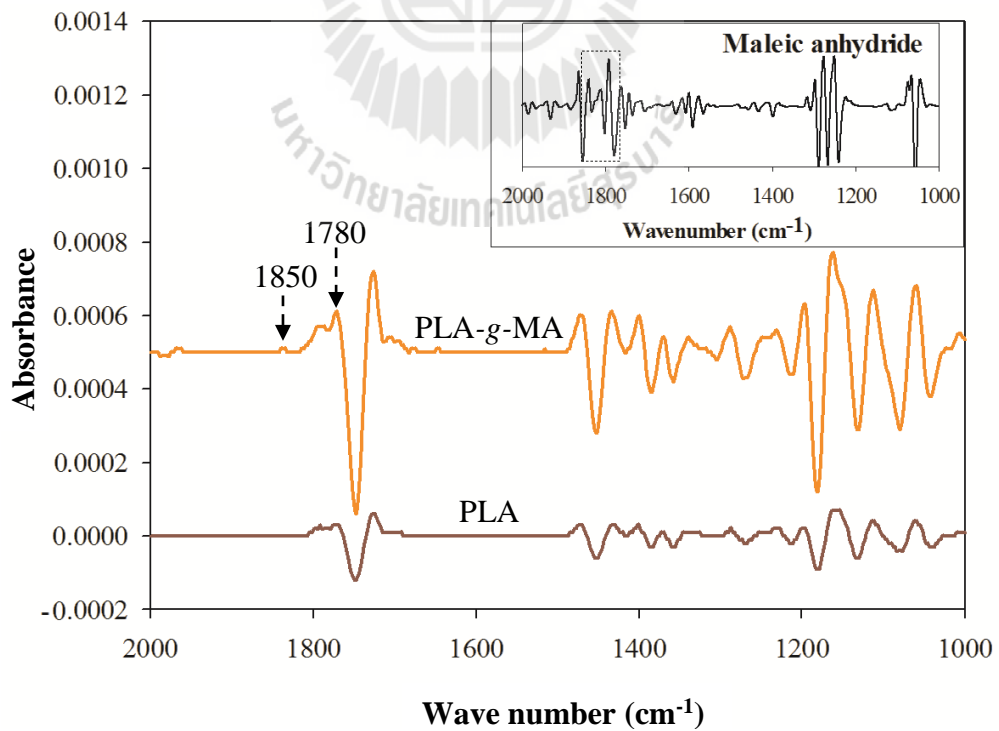


Figure 4.9 FTIR second derivative spectra of PLA, PLA-g-MA, and MA.

4.3 Effects of alkali treatment and sawdust content on properties of sawdust/PLA composites

4.3.1 Mechanical properties

4.3.1.1 Tensile properties

Tensile properties of PLA, untreated sawdust/PLA composites, and alkali treated sawdust/PLA composites with different sawdust contents are shown in Table 4.4. With the addition of untreated sawdust into PLA, tensile strength and elongation at break of PLA were decreased whereas tensile modulus was increased. Tensile strength of untreated sawdust/PLA composites slightly decreased with increasing sawdust content from 20 to 40 wt% as shown in Figure 4.10. This was due to poor dispersion of sawdust in PLA matrix and poor interfacial adhesion between sawdust and PLA matrix (Srubar Iii et al., 2012; Ming-Zhu, Chang-Tong, Xu-Bing, and Yun-Lei, 2011). SEM micrographs of untreated sawdust/PLA composites (Figure 4.19 (a)-(c)) showed that at high sawdust content, poor dispersion of sawdust was found. Moreover, at higher magnification, poor filler-matrix interfacial adhesion was clearly observed (Figure 4.20 (a)-(c)). This resulted in a decrease of tensile strength of the composites.

However, tensile modulus gradually increased with increasing sawdust content as shown in Figure 4.11. This was due to the reinforcement of sawdust in PLA matrix (Sombatsompop, Yotinwattanakumtorn, and Thongpin, 2005). Chun, Husseinsyah, and Osman (2012) also observed a decrease of tensile strength and an increase of tensile modulus of coconut shell powder/PLA composites with increasing filler content.

Elongation at break of the composites decreased when the sawdust was added into the PLA matrix and decreased continuously with increasing sawdust content as shown in Figure 4.12. This may be due to decreased deformability of a rigid interphase between the sawdust and the PLA matrix (Ming-Zhu et al., 2011). Pilla, Gong, O'Neill, Rowell, and Krzysik (2008) also reported that elongation at break of pine wood flour/PLA composites decreased as pine wood flour content was increased because the deformability of the matrix was reduced.

Tensile strength, tensile modulus, and elongation at break of alkali treated sawdust/PLA composites also showed the same trend as the untreated sawdust/PLA composites as shown in Figure 4.10-4.12, respectively. However, at the same sawdust content, the composites filled with alkali treated sawdust exhibited higher tensile properties than the composites filled with untreated sawdust. This was because alkali treatment can remove a certain amount of lignin, hemicellulose, wax, and pectin covering the external surface of filler. The removal of surface impurities made the filler cleaner and rougher than untreated filler which resulted in better mechanical interlocking with PLA matrix (Aydin, Tozlu, Kemaloglu, Aytac, and Ozkoc, 2011; Tran, Ogihara, Nguyen, and Kobayashi, 2011). This explanation can be substantiated by considering the SEM micrographs which showed better dispersion of the alkali treated sawdust in the PLA matrix (Figure 4.19 (d)-(f)) and a good filler-matrix interfacial adhesion (Figure 4.20 (d)-(f)). The strong adhesion at the sawdust-PLA interface led to effective stress transfer and load distribution throughout the interface (Islam, Pickering, and Foreman, 2010).

When compared with the untreated sawdust/PLA composites, the alkali treated sawdust/PLA composites at 20, 30, and 40 wt% sawdust content

exhibited 20, 28, and 19% enhancement of tensile strength and 5, 12, and 7% enhancement of tensile modulus, respectively. Moreover, elongation at break of the composites filled with alkali treated sawdust at 20, 30, and 40 wt% were 12, 13, and 9% higher than that of the composites filled with untreated sawdust, respectively. Tran, Ogiwara, and Kobayashi (2011) also found that mechanical properties of alkali treated coir fiber/poly(butylene succinate) (PBS) composites were significantly greater than those of untreated composites. This was because alkali treatment increased the fiber surface roughness resulting in better mechanical interlocking with PBS matrix.

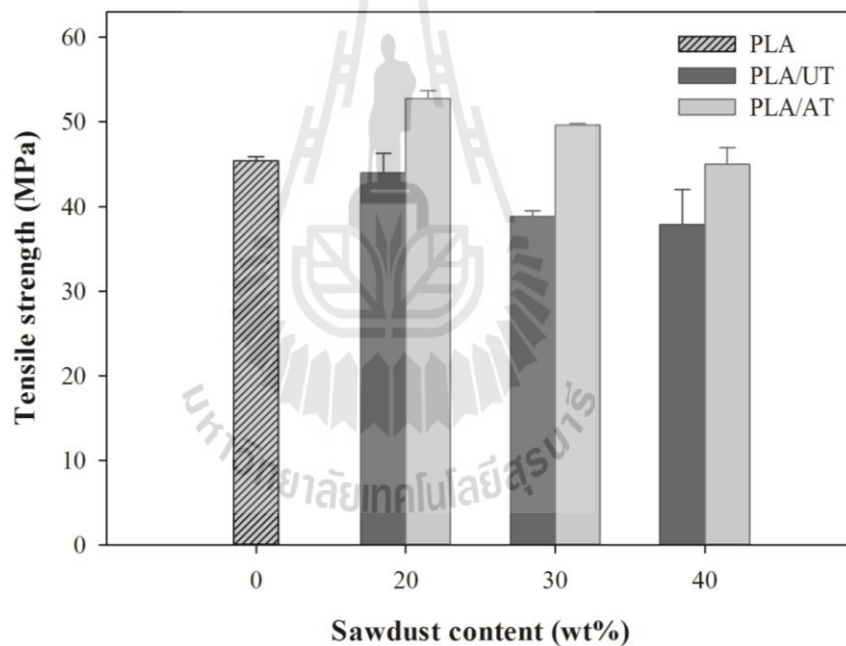


Figure 4.10 Tensile strength of PLA, untreated sawdust/PLA composites, and alkali treated sawdust/PLA composites with different sawdust contents.

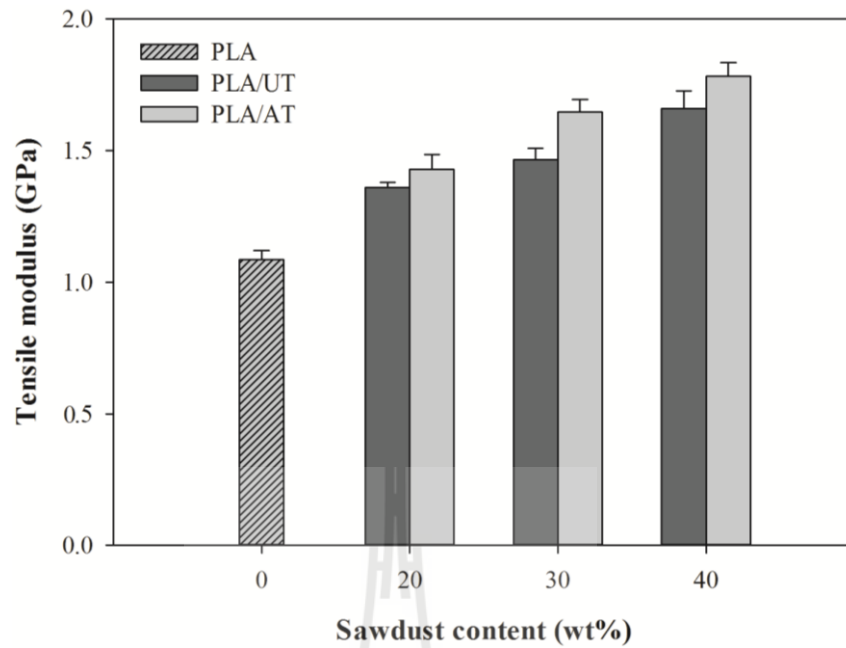


Figure 4.11 Tensile modulus of PLA, untreated sawdust/PLA composites, and alkali treated sawdust/PLA composites with different sawdust contents.

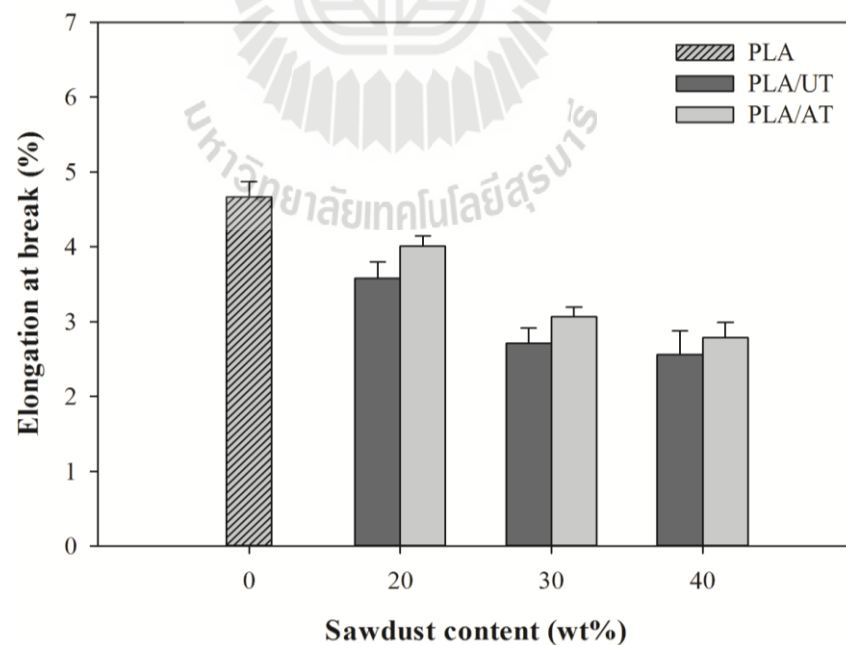


Figure 4.12 Elongation at break of PLA, untreated sawdust/PLA composites, and alkali treated sawdust/PLA composites with different sawdust contents.

4.3.1.2 Flexural properties

Flexural strength and flexural modulus of PLA, untreated sawdust/PLA composites, and alkali treated sawdust/PLA composites with different sawdust contents are shown in Table 4.4. Flexural properties also showed the same trend as tensile properties of sawdust/PLA composites. Flexural strength of the composites decreased with increasing sawdust content as shown in Figure 4.13. This was because of a poor filler-matrix interfacial adhesion and filler agglomeration at high sawdust content which resulted in difficult stress transfer from matrix to filler (Ming-Zhu et al., 2011). On the other hand, flexural modulus increased with the addition of sawdust and increased continuously with increasing sawdust content from 20 to 40 wt% as shown in Figure 4.14. This was attributed to the addition of the rigid filler into the matrix (Sombatsompop et al., 2005). Tran et al. (2011) also observed a decrease of flexural strength and an increase of flexural modulus of short coir fiber/PBS composites with increasing fiber content from 20 to 50 wt%.

It was interesting to note that flexural strength and flexural modulus of alkali treated sawdust/PLA composites were significantly greater than those of untreated sawdust/PLA composites. This was due to a good dispersion of sawdust in PLA matrix and an enhancement of the interfacial adhesion between sawdust and PLA matrix through mechanical interlocking (Islam et al., 2010). The flexural strength of alkali treated sawdust/PLA composites at 20, 30, and 40 wt% sawdust content were 21, 31, and 26% higher than those of the untreated composites, respectively. Moreover, when compared to the untreated composites, the composites filled with alkali treated sawdust at 20, 30, and 40 wt% exhibited 18, 19, and 10% enhancement of flexural modulus, respectively. Tran et al. (2011) also found that PBS composites made from

alkali treated jute fiber exhibited higher flexural strength and flexural modulus than the composites made from untreated jute fiber. This was attributed to the improvement of interfacial adhesion between jute fiber and PBS matrix.

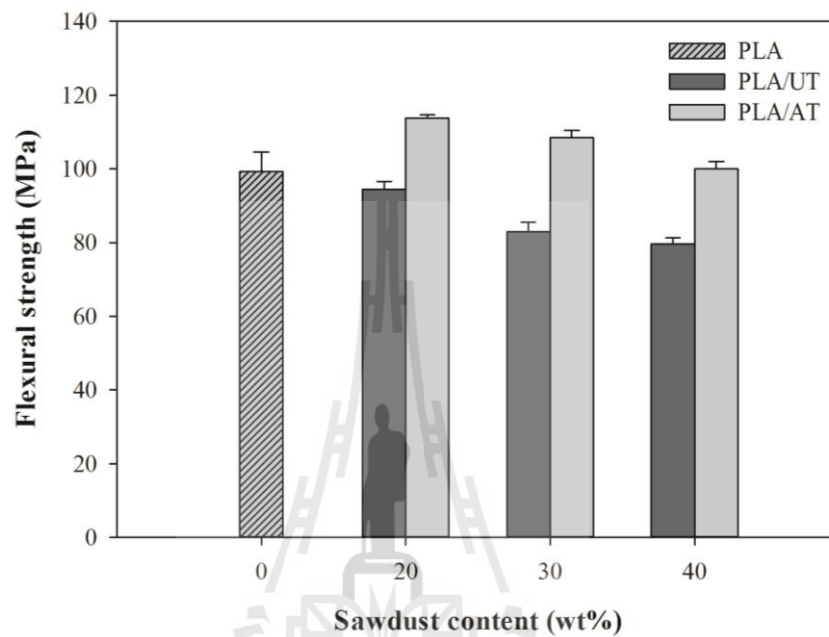


Figure 4.13 Flexural strength of PLA, untreated sawdust/PLA composites, and alkali treated sawdust/PLA composites with different sawdust contents.

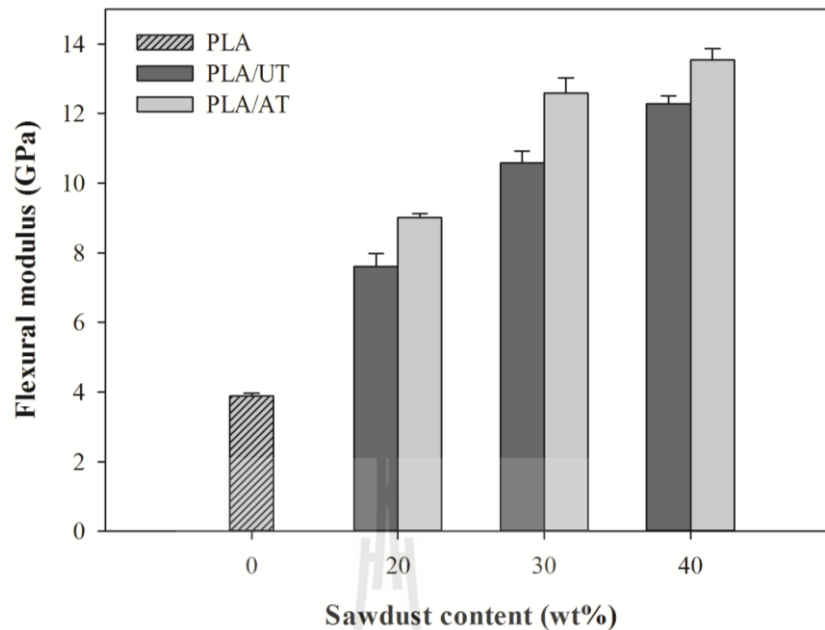


Figure 4.14 Flexural modulus of PLA, untreated sawdust/PLA composites, and alkali treated sawdust/PLA composites with different sawdust contents.

4.3.1.3 Impact properties

Impact strength of PLA, untreated sawdust/PLA composites, and alkali treated sawdust/PLA composites with different sawdust contents are shown in Figure 4.15. It was seen that impact strength of PLA decreased with the addition of sawdust. As sawdust content was increased from 20 to 40 wt%, impact strength of the composites was reduced. This may be due to an increase of filler agglomeration which created regions of stress concentration requiring less energy to initiate cracks. This stress concentration could be generated from the filler and the matrix at the interface region (Tawakkal, Talib, Abdan, and Ling, 2012). Huda, Drzal, Misra, and Mohanty (2006) also found that impact strength of wood fiber/PLA composites decreased with increasing wood fiber from 20 to 40 wt% due to insufficient stress-transfer properties between the matrix and the fiber.

However, the improvement of impact strength was observed in the composites prepared from alkali treated sawdust. This was attributed to a good interfacial adhesion between the sawdust and the PLA matrix which allowed better matrix to fillers stress transfer during testing. The composites prepared from 20, 30, and 40 wt% alkali treated sawdust showed an improvement of impact strength by 17, 31, and 24% compared to those of untreated sawdust/PLA composites.

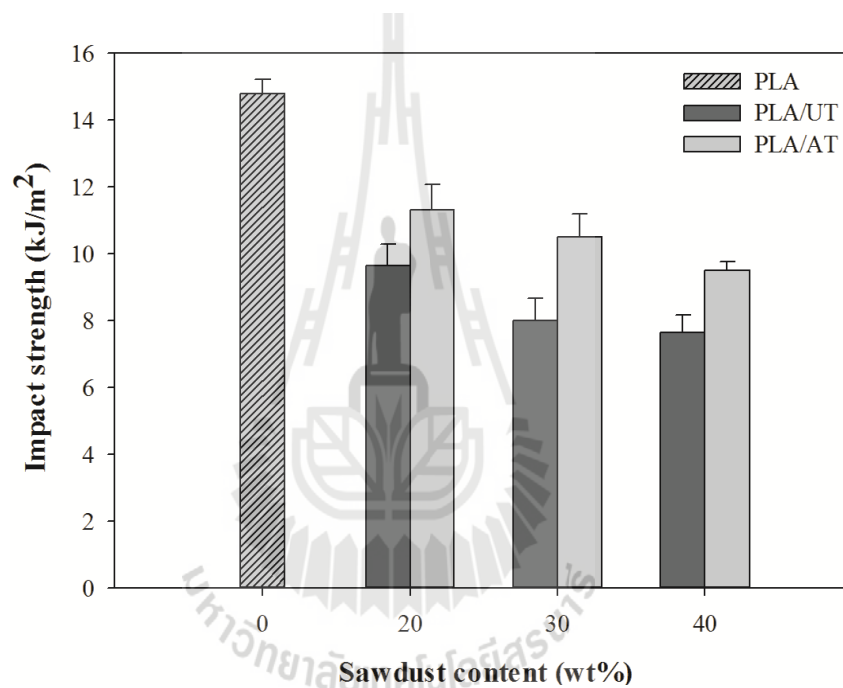


Figure 4.15 Impact strength of PLA, untreated sawdust/PLA composites, and alkali treated sawdust/PLA composites with different sawdust contents.

Table 4.4 Mechanical properties of PLA, untreated sawdust/PLA composites, and alkali treated sawdust/PLA composites with different sawdust contents.

Formulation	Tensile strength (MPa)	Young's modulus (GPa)	Elongation at break (%)	Flexural strength (MPa)	Flexural modulus (GPa)	Impact strength (kJ/m²)
PLA	45.44±0.44	1.09±0.03	4.67±0.20	99.27±5.30	3.89±0.08	14.79±0.42
PLA/UT20	43.98±2.32	1.36±0.02	3.58±0.22	94.39±2.10	7.61±0.37	9.64±0.64
PLA/UT30	38.85±0.61	1.47±0.04	2.71±0.20	82.90±2.55	10.58±0.35	8.00±0.66
PLA/UT40	37.89±4.11	1.66±0.07	2.56±0.32	79.56±1.76	12.28±0.23	7.65±0.52
PLA/AT20	52.73±0.96	1.43±0.06	4.01±0.14	113.76±0.88	9.02±0.11	11.32±0.75
PLA/AT30	49.63±0.17	1.65±0.05	3.07±0.19	108.49±1.91	12.60±0.43	10.49±0.71
PLA/AT40	44.99±1.96	1.78±0.05	2.79±0.21	100.01±1.92	13.55±0.32	9.51±0.26

4.3.2 Thermal properties

TGA and DTA curves of PLA, untreated sawdust/PLA composites, and alkali treated sawdust/PLA composites with different sawdust contents are shown in Figure 4.16 and 4.17, respectively. Thermal decomposition temperature at 5% weight loss (T_5), thermal decomposition temperature at 50% weight loss (T_{50}), and thermal decomposition temperature (T_d) of PLA, untreated sawdust/PLA composites, and alkali treated sawdust/PLA composites with different sawdust contents are listed in Table 4.5. From DTA curve of pure PLA in Figure 4.17, a single stage decomposition process of PLA was observed. T_5 , T_{50} , and T_d of pure PLA were 333.87, 371.82, and 375.77°C, respectively. Moreover, it could be seen that the decomposition process of sawdust/PLA composite was also in a single stage, as the decomposition stage of sawdust was overlapped with the decomposition stage of PLA (Chun, Husseinsyah, and Osman, 2013). Incorporation of untreated sawdust significantly decreased the thermal decomposition temperature of PLA. As sawdust content increased, T_5 , T_{50} , and T_d of the untreated sawdust/PLA composites decreased continuously as shown in Table 4.5. This was because thermal decomposition temperatures of the components of untreated sawdust (Table 4.3.), i.e., low molecular weight compositions (e.g. wax, pectin, and others surface impurities) (Rojo et al., 2013; Bwire et al., 2007), hemicellulose, and cellulose were lower than PLA. This led to a deterioration in thermal stability of the composites (Wenjia, Kaushlendra, and John, 2013; Jandas, Mohanty, Nayak, and Srivastava, 2011). Furthermore, poor interfacial adhesion between the PLA matrix and the sawdust might contribute to decrease thermal decomposition temperature of PLA (Lee, Kang, Doh, Yoon, Park, and Wu, 2008). The char residue content at 600°C

increased with an increase of sawdust loading as shown in Table 4.5. Seong et al. (2012) found that PLA showed better thermal stability than kenaf fiber/PLA composites. The residue after thermal degradation at 600°C increased with increasing kenaf fiber content. Huda et al. (2006) also reported that the thermal stability of PLA was decreased with the addition of wood flour due to poor interfacial adhesion between wood flour and PLA. With increasing wood flour content, T_5 , T_{25} , T_{50} , and T_{75} of the composites were decreased.

Alkali treated sawdust/PLA composites exhibited higher T_5 , T_{50} , and T_d than untreated sawdust/PLA composites at all sawdust contents. This was due to the fact that some components of the sawdust such as low molecular weight compositions and hemicellulose which degraded at a lower temperature, were extracted out during alkali treatment. This led to an improvement of thermal stability of the composites (Rosa et al., 2009). Moreover, the enhancement of thermal stability of alkali treated sawdust/PLA composites was probably due to the improvement of interfacial adhesion between the PLA matrix and the sawdust (Jandas et al., 2011). Yu, Ren, Li, Yuan, and Li (2010) also found that alkali treatment improved thermal stability of ramie fiber/PLA composites due to a good interfacial adhesion between PLA matrix and ramie fiber.

Additionally, it can be seen that char residue at 600°C of the alkali treated sawdust/PLA composites was higher than those of the untreated composites at all sawdust contents as seen in Table 4.5. This was due to the fact that char residue of alkali treated sawdust was higher than untreated sawdust. Moreover, char residue of the composites was formed by the pyrolysis of lignocellulosic filler component. These resulted in an increase of char residue content of the alkali treated sawdust/PLA

composites. Bachtiar, Sapuan, Zainudin, Khalina, and Dahlan (2013) also reported that residue content at 600°C of alkali treated sugar palm fiber/high impact polystyrene composites was higher than that of untreated composites.

Table 4.5 Thermal decomposition temperatures of PLA, untreated sawdust/PLA composites, and alkali treated sawdust/PLA composites with different sawdust contents.

Formulation	T₅ (°C)	T₅₀ (°C)	T_d (°C)	Residue at 600°C (%)
PLA	333.87	371.82	375.77	0.00
PLA/UT20	298.96	362.95	364.40	3.52
PLA/UT30	295.58	358.69	360.52	4.20
PLA/UT40	284.71	356.10	356.87	6.59
PLA/AT20	315.99	366.69	368.22	4.36
PLA/AT30	306.12	363.83	365.54	6.49
PLA/AT40	293.33	361.00	361.76	9.78

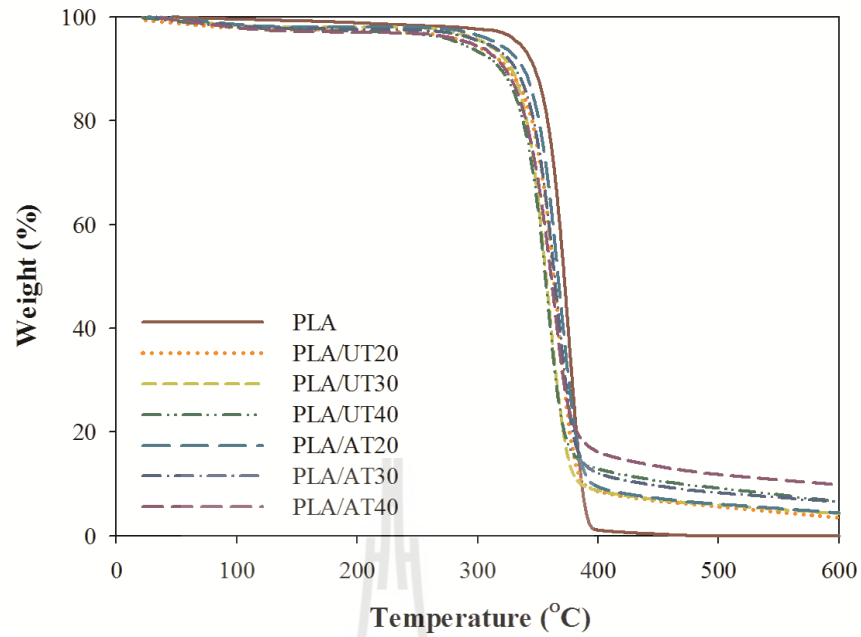


Figure 4.16 TGA curves of PLA, untreated sawdust/PLA composites, and alkali treated sawdust/PLA composites with different sawdust contents.

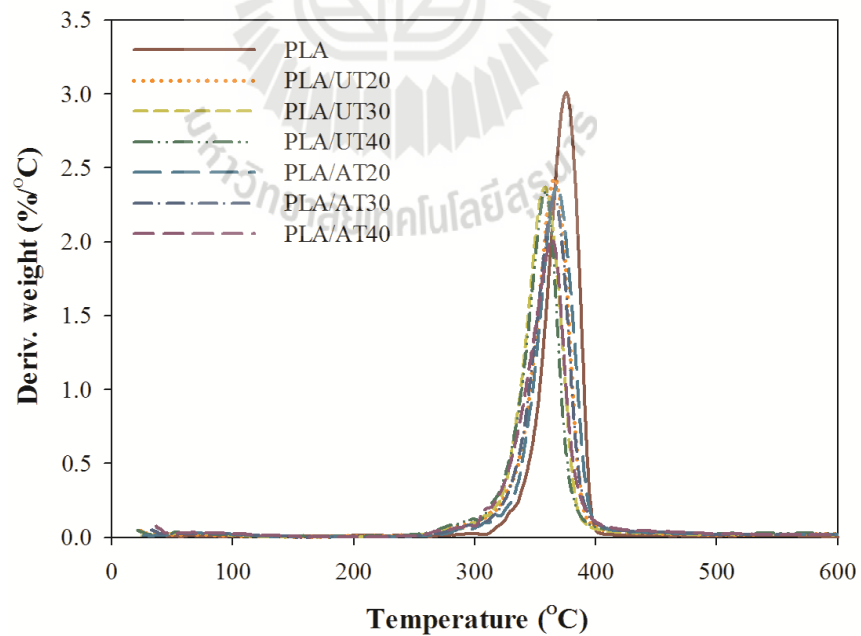


Figure 4.17 DTA curves of PLA, untreated sawdust/PLA composites, and alkali treated sawdust/PLA composites with different sawdust contents.

DSC thermograms of PLA, untreated sawdust/PLA composites, and alkali treated sawdust/PLA composites with different sawdust contents are shown in Figure 4.18. The second heating curves of melt-quenched samples were chosen in order to remove previous thermal history and make glass transition (T_g) more clear and obvious. The determined data of thermal characteristics of PLA, untreated sawdust/PLA composites, and alkali treated sawdust/PLA composites with different sawdust contents are summarized in Table 4.6. On second heating, T_g , cold crystallization temperature (T_{cc}), and melting temperature (T_m) of PLA and PLA composites were observed. PLA exhibited T_g , T_{cc} , T_{m1} , and T_{m2} at 52.2, 99.8, 138.6, and 150.5°C, respectively. The double melting endotherm of PLA was attributed to the different size and/or perfection of ordering of PLA. The peak at low temperature (T_{m1}) was attributed to re-melting of newly formed crystallite during heating (Way, Dean, Wu, and Palombo, 2011; Sarasua, Prud'homme, Wisniewski, Le Borgne, and Spassky, 1998).

T_g of PLA component in the untreated sawdust/PLA composites did not noticeably change with increasing sawdust content. Sawpan (2009) also found similar result in hemp fiber/PLA composites. T_{cc} of PLA component in the composites decreased with the addition of 20 wt% of untreated sawdust. Generally, the lignocellulosic filler can either act as nucleation sites for the crystallization of the polymer or restrict the mobility of the polymer chains. Thus, the decrease of T_{cc} indicated that the nucleation by the sawdust was probably dominant (Mofokeng, 2010). As sawdust content was increased to 30 and 40 wt%, T_{cc} of PLA component in the composites shifted to higher temperature suggesting that sawdust restricted the mobility of the polymer chains during the crystallization (Mofokeng, 2010). This phenomenon may be due to the occurrence of filler agglomeration at higher filler content (Chun et

al., 2012). T_{m1} and T_{m2} of the untreated sawdust/PLA composites were close to T_{m1} and T_{m2} of PLA indicating that sawdust content showed no effect on T_m of PLA. Additionally, it can be seen that heat of crystallization (ΔH_c) and heat of fusion (ΔH_m) of the composites increased with incorporating untreated sawdust because of the nucleation effect of the filler (Mofokeng, 2010). Nevertheless, ΔH_c and ΔH_m of the composites decreased with increasing sawdust content. This may be due to the restriction of chain mobility of PLA by the filler (Mofokeng, 2010). Degree of crystallinity (χ_c) of the composites increased with the addition of sawdust due to the nucleating effect of the lignocellulosic filler. Islam et al. (2010) also found that the addition of hemp fiber to PLA resulted in an increase of percentage crystallinity of the PLA matrix. This can be explained by the nucleating ability of hemp fiber allowing the crystallization of PLA. However, χ_c of the composites tend to decrease with increasing sawdust content as seen in Table 4.6. This was due to the restriction of chain mobility of PLA by the filler agglomeration (Chun et al., 2012).

When compared with untreated sawdust/PLA composites, T_{cc} of PLA component in alkali treated sawdust/PLA composites decreased while T_g , T_{m1} , and T_{m2} insignificantly changed at all sawdust contents. A reduction of T_{cc} was due to the nucleating effect of alkali treated sawdust indicating an enhancement of crystalline ability of PLA (Qian et al., 2013). χ_c of alkali treated sawdust/PLA composites was higher than that of the untreated sawdust/PLA composites at all sawdust contents. This can be explained by the nucleating ability of alkali treated sawdust which allowed the crystallization of PLA. After alkali treatment, lignin, hemicellulose, wax, and surface impurities covering the external surface of lignocellulosic filler were removed. This

made the filler surface cleaner and rougher than untreated filler resulting in better mechanical interlocking with PLA matrix. An increase of filler-matrix interaction could facilitate the filler surface to act as nucleation sites for the crystallization of PLA. This promoted the growth and formation of transcrystalline regions around the filler normal to the filler surface (Sawpan et al., 2011; Islam et al., 2010). Thus, the composites prepared from alkali treated sawdust showed an increase of χ_c when compared to the composites filled with untreated sawdust. Moreover, the alkali treated sawdust/PLA composites exhibited higher ΔH_c and ΔH_m than that of the untreated composites at the same sawdust content indicating an increase of the degree of PLA crystallinity (Sawpan, 2009).

Table 4.6 Thermal characteristics of PLA, untreated sawdust/PLA composites, and alkali treated sawdust/PLA composites with different sawdust contents.

Formulation	T_g (°C)	T_{cc} (°C)	T_{m1} (°C)	T_{m2} (°C)	ΔH_c (J/g)	ΔH_m (J/g)	χ_c (%)
PLA	52.2	99.8	138.6	150.5	22.93	32.92	35.13
PLA/UT20	51.2	97.5	139.0	149.7	27.41	34.45	45.96
PLA/UT30	52.3	101.9	139.7	149.0	26.71	28.50	43.45
PLA/UT40	53.7	100.6	139.2	149.2	20.22	23.47	41.75
PLA/AT20	51.7	94.2	139.1	150.4	30.00	37.38	49.87
PLA/AT30	52.3	97.4	140.7	151.0	32.07	33.59	51.21
PLA/AT40	51.7	98.0	139.0	150.3	27.98	29.50	52.47

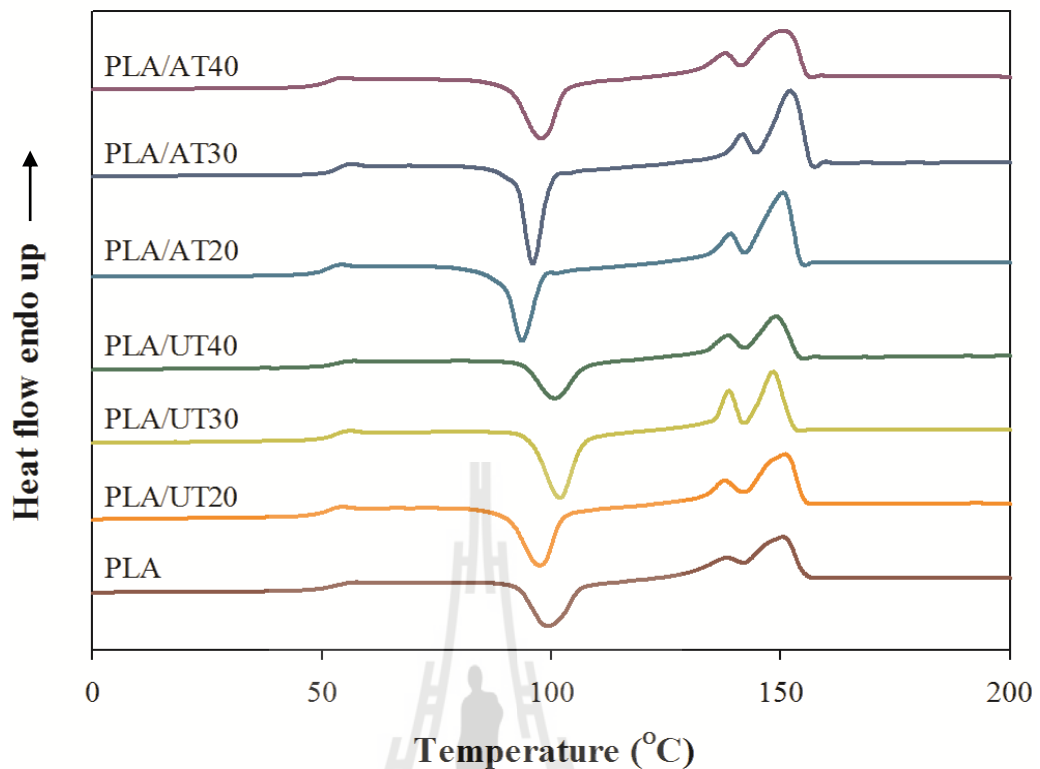


Figure 4.18 DSC thermograms of PLA, untreated sawdust/PLA composites, and alkali treated sawdust/PLA composites with different sawdust contents (the second heating, heating rate 5°C/min).

4.3.3 Morphological properties

Tensile fractured surface morphologies of untreated sawdust/PLA composites and alkali treated sawdust/PLA composites at 100x and 300x magnification are shown in Figure 4.19 and 4.20, respectively. As shown in Figure 4.19 (a)-(c), visible gaps were observed between untreated sawdust and PLA matrix. Moreover, SEM micrographs of the untreated sawdust/PLA composites also showed holes that left after the untreated sawdust was pullout from PLA matrix. These characteristics indicated poor interfacial adhesion between the untreated sawdust and the PLA matrix. With

increasing sawdust content, the agglomeration of sawdust in PLA matrix was observed as shown in Figure 4.19 (b) and (c). This caused a reduction in tensile strength, flexural strength, and impact strength of the composites.

SEM micrographs of the untreated sawdust/PLA composites at higher magnification (300x) are shown in Figure 4.20 (a)-(c). It was clearly observed typical pulled-out traces and a poor filler-matrix interfacial adhesion. However, for all composites filled with alkali treated sawdust, good interfacial adhesion between the sawdust and the PLA matrix was observed as shown in Figure 4.20 (d)-(f). These results suggested that alkali treatment improved the compatibility between sawdust and PLA matrix. Furthermore, the filler agglomeration was not observed in the composites filled with alkali treated sawdust as shown in Figure 4.19 (d)-(f) indicating that alkali treatment enhanced the dispersion of sawdust in PLA matrix. This resulted in an improvement of mechanical properties of alkali treated sawdust/PLA composites.

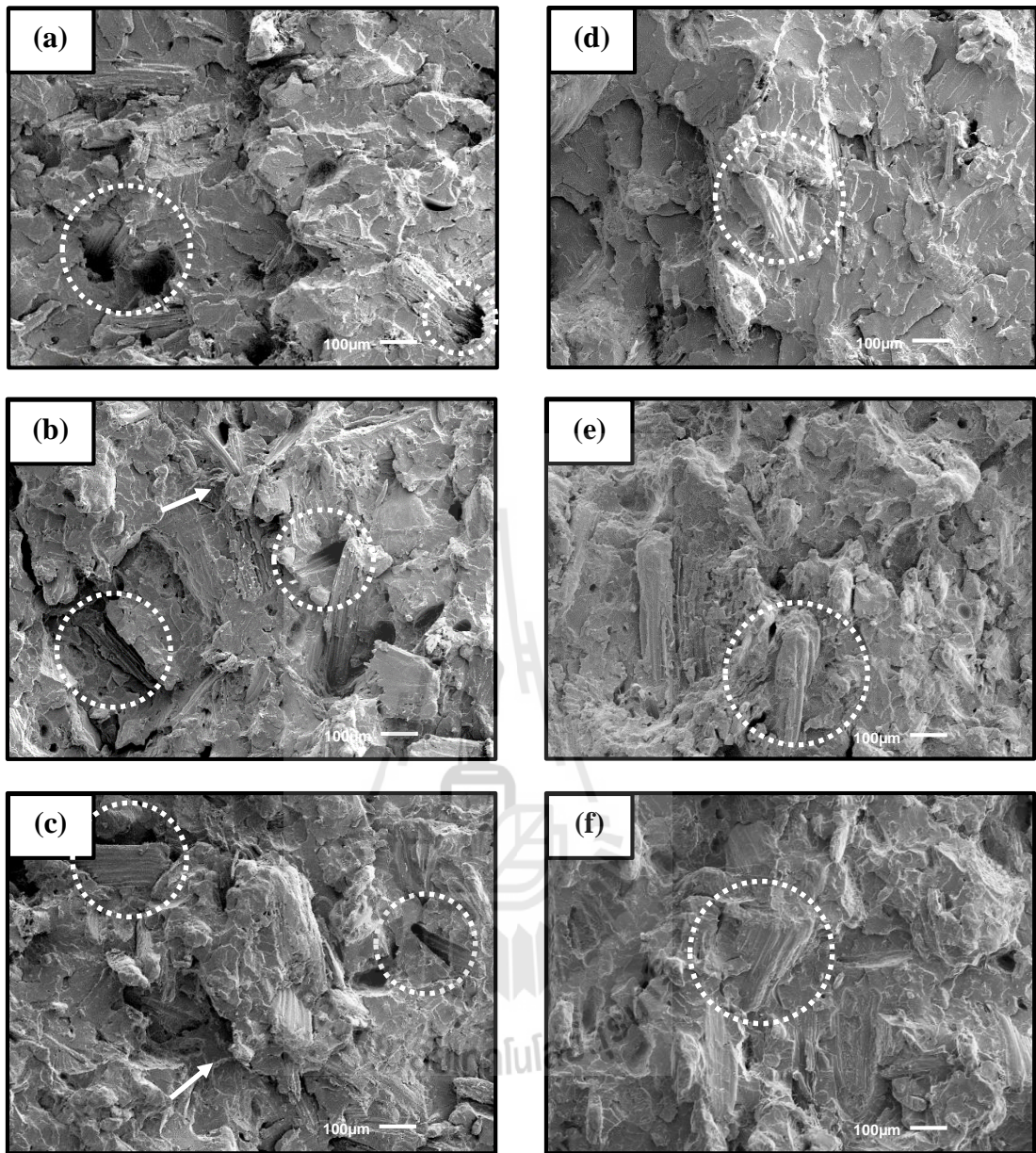


Figure 4.19 SEM micrographs at 100x magnification of (a) PLA/UT20, (b) PLA/UT30, (c) PLA/UT40, (d) PLA/AT20, (e) PLA/AT30, and (f) PLA/AT40 composites.

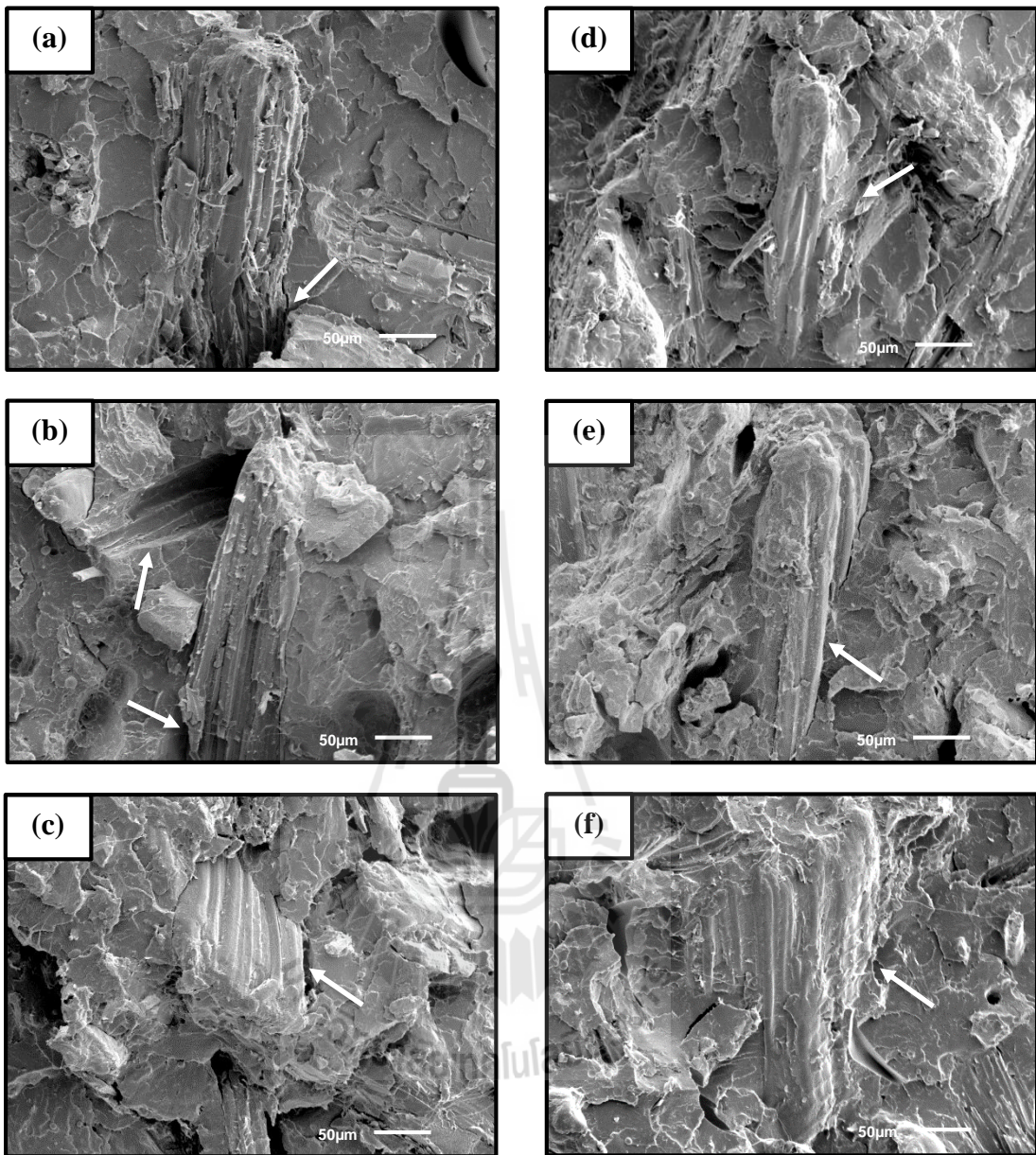


Figure 4.20 SEM micrographs at 300x magnification of (a) PLA/UT20, (b) PLA/UT30, (c) PLA/UT40, (d) PLA/AT20, (e) PLA/AT30, and (f) PLA/AT40 composites.

4.4 Effect of poly(butylene adipate-co-terephthalate) (PBAT) content on properties of sawdust/PLA composites

To study the effect of PBAT content on mechanical, thermal, and morphological properties of the sawdust/PLA/PBAT composites, the PLA composite filled with 30 wt% alkali treated sawdust was chosen due to the highest percentage increase of mechanical properties after alkali treatment.

4.4.1 Mechanical properties

4.4.1.1 Tensile properties

Tensile properties of sawdust/PLA composite and sawdust/PLA/PBAT composites with different PBAT contents are listed in Table 4.7. With increasing PBAT content, tensile strength and tensile modulus of the composites decreased continuously as shown in Figure 4.21 and 4.22, respectively. This was expected by two factors, i.e., low stiffness of PBAT and incompatibility between constituents of the composites (Goriparthi, Suman, and Nalluri, 2012). In fact, PLA exhibited high tensile strength and tensile modulus whereas PBAT had moderate tensile strength and high elongation at break (Jiang, Wolcott, and Zhang, 2006). So the addition of flexible PBAT reduced brittleness characteristics of the sawdust/PLA composites. Moreover, SEM micrographs of toughened PLA composites (Figure 4.30 (b)-(d)) revealed the incompatibility between PLA and PBAT which resulted in deterioration in tensile strength of the composites. Similar result was also found by Petinakis, Yu, Edward, Dean, Liu, and Scully (2009); Jiang and Qin (2006). Petinakis et al. (2009) observed that the addition of poly(ethylene-acrylic acid) as a toughening agent into wood flour/PLA composites resulted in a substantial reduction in tensile strength when compared with wood flour/PLA composites without poly(ethylene-acrylic acid). This was

attributed to poor interfacial adhesion between constituents of the composites. Jiang et al. (2006) also reported that tensile strength and tensile modulus of wood flour/polypropylene (PP) composites decreased with the addition of polyethylene octene elastomer and decreased continuously with increasing polyethylene octene elastomer content from 15 to 30 wt%.

Elongation at break of sawdust/PLA composites toughened with PBAT was higher than that of sawdust/PLA composite. With increasing PBAT content from 10 to 30 wt%, the elongation at break of the PLA composites increased continuously as shown in Figure 4.23. The addition of PBAT at contents of 10, 20, and 30 wt% exhibited 36, 68, and 81% enhancement of elongation at break of the PLA composites, respectively. The toughening mechanism of sawdust/PLA composite by adding the elastomeric PBAT was caused by the improvement of energy absorption during testing (Kfoury et al., 2013). This explanation can be substantiated by considering SEM micrographs in Figure 4.30 (b)-(d), which showed the impact fractured surfaces of the sawdust/PLA composites toughened with PBAT. It can be seen that PBAT evenly dispersed in PLA matrix. Since PBAT had different elastic properties compared with PLA matrix, its particles served as sites of local stress concentrators under tensile stress. These sites can be initiated crazing, shear yielding, cavitation, or debonding which are the major energy absorption mechanism during testing (Kumar, Mohanty, Nayak, and Rahail Parvaiz, 2010; Teamsinsungvon, 2010; Zhao, Liu, Wu, and Ren, 2010; Jiang et al., 2006). This resulted in an improvement of elongation at break of the toughened composites. Additionally, the enhancement of ductile deformation of the composites was confirmed by SEM micrographs of tensile fractured surface of the toughened PLA composites. It can be seen that morphologies of the

composites toughened with PBAT showed some elongated matrix during tensile testing which indicated a ductile deformation (Figure 4.32 (b)-(d)) whereas this did not occur in the composite without PBAT (Figure 4.32 (a)). Lee (2009) observed that the addition of PBAT led to an increase of deformability of bamboo flour/PLA composites which was observed experimentally as larger elongation at break. This was probably due to the presence of soft elastomeric phase. Petinakis et al. (2009) also found that elongation at break of wood flour/PLA composites increased with the addition of poly(ethylene-acrylic acid) as a toughening agent. The improvement of elongation at break of the composites was attributed to the presence of more resilient poly(ethylene-acrylic acid) in the polymer composite resulting in a more ductile polymer matrix. Sombatsompop et al. (2005) also reported that toughness of the sawdust/PP composites could be regained by adding ethylene octene copolymer as an impact modifier. Elongation at break of the composites increased with increasing ethylene octene copolymer content. The toughening mechanism of sawdust/PP composites was caused by the enhancement ability of the rubber phase to deform plastically.

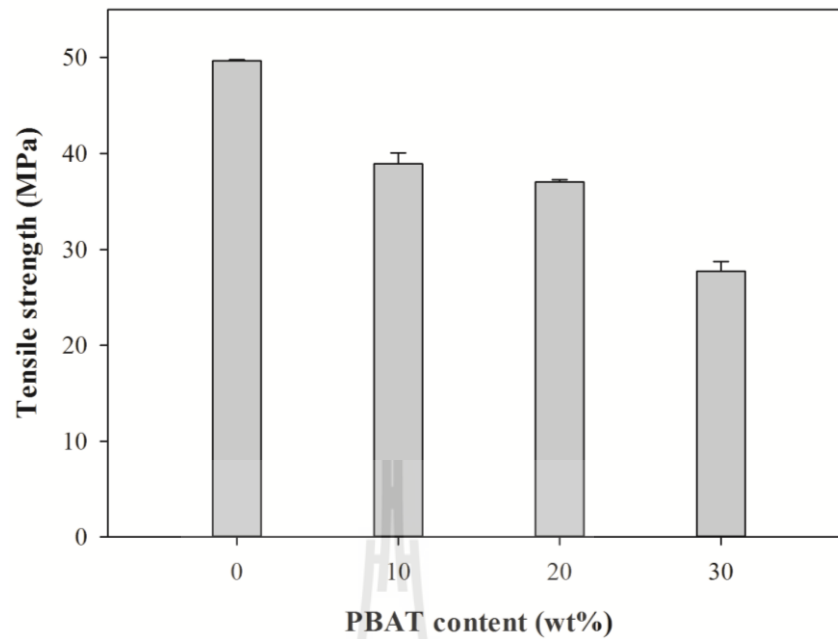


Figure 4.21 Tensile strength of sawdust/PLA composite and sawdust/PLA/PBAT composites with different PBAT contents.

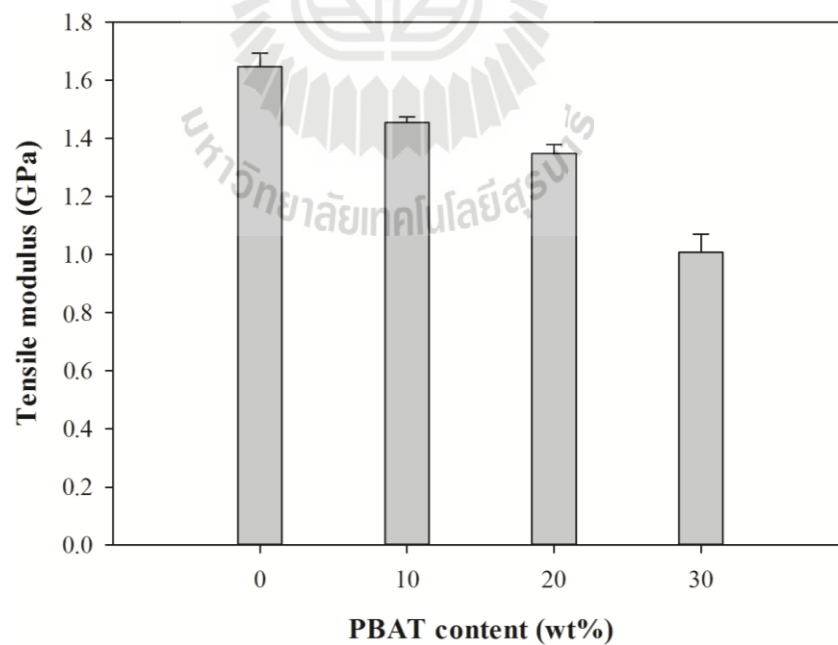


Figure 4.22 Tensile modulus of sawdust/PLA composite and sawdust/PLA/PBAT composites with different PBAT contents.

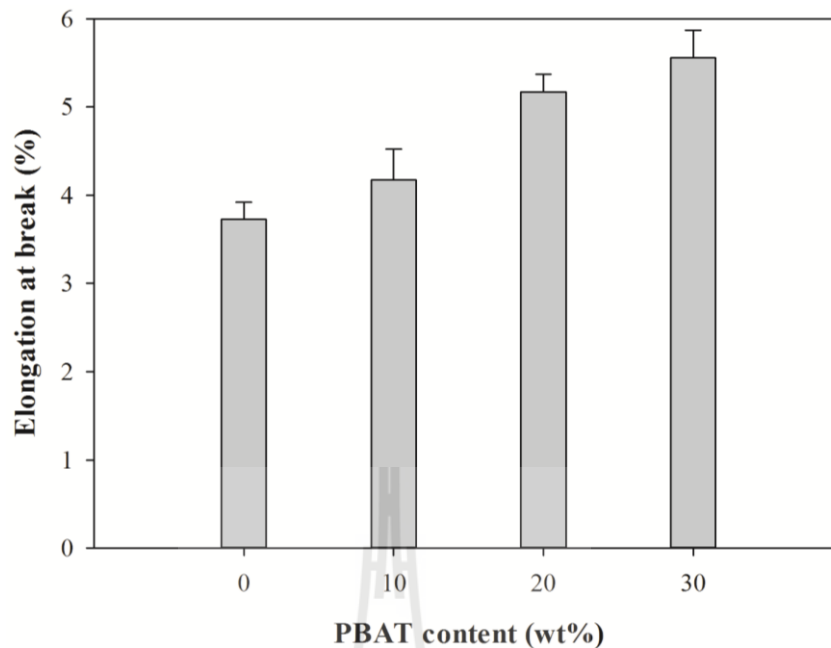


Figure 4.23 Elongation at break of sawdust/PLA composite and sawdust/PLA/PBAT composites with different PBAT contents.

4.4.1.2 Flexural properties

Flexural properties of sawdust/PLA composite and sawdust/PLA/PBAT composites with different PBAT contents are listed in Table 4.7. Flexural strength and flexural modulus of sawdust/PLA composite and sawdust/PLA/PBAT composites with different PBAT contents are shown in Figure 4.24 and 4.25, respectively. It was found that flexural properties showed the same trend as the tensile properties of the composites. Both flexural strength and flexural modulus of sawdust/PLA composites toughened with PBAT were lower than that of the composite without PBAT. With increasing PBAT content, flexural strength and flexural modulus of the sawdust/PLA composites decreased gradually. This was because the fact that PBAT had high flexibility but low strength and stiffness (Jiang et al., 2006). Thus, the addition of flexible PBAT into sawdust/PLA composite led to a reduction in brittleness

characteristics of the composite. Furthermore, the incompatibility between PLA and PBAT might contribute to decrease flexural strength of toughened composites. Yao, Wu, Liu, Lei, and Zhou (2011) found a similar result in rice straw fiber/high density polyethylene (HDPE) composite toughening with unfunctionalized ethylene/propylene copolymer (uEPR). They observed that flexural strength and flexural modulus of the composites decreased with increasing uEPR content due to the presence of soft elastomeric phase. Sombatsompop et al. (2005) also reported that flexural modulus and flexural strength of wood flour/PP composites decreased progressively with increasing ethylene octene copolymer content from 2 to 11.1 wt%. This was because flexural modulus and flexural strength of ethylene octene copolymer were less than those of the unmodified wood flour/PP composites.

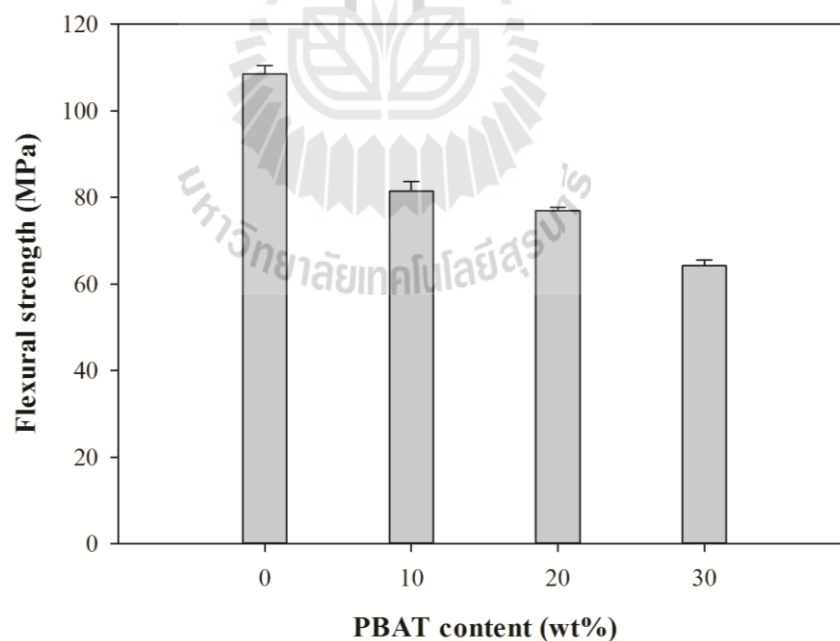


Figure 4.24 Flexural strength of sawdust/PLA composite and sawdust/PLA/PBAT composites with different PBAT contents.

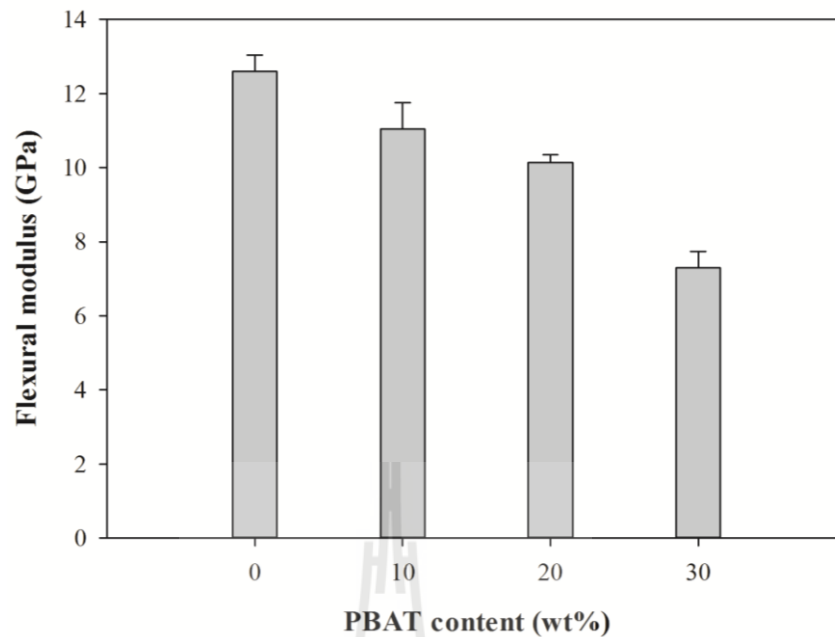


Figure 4.25 Flexural modulus of sawdust/PLA composite and sawdust/PLA/PBAT composites with different PBAT contents.

4.4.1.3 Impact properties

Impact strength of sawdust/PLA composite and sawdust/PLA/PBAT composites with different PBAT contents are shown in Figure 4.26. Impact strength of the sawdust/PLA composite was significantly improved with the incorporation of PBAT. As PBAT content was increased, the impact strength of the composites was continuously increased. The addition of PBAT at content of 10, 20, and 30 wt% increased the impact strength of the composites by approximately 35, 114, and 148%, respectively. The improvement of the impact strength of sawdust/PLA/PBAT composites was attributed to the presence of soft elastomeric phase that exhibited high toughness (Afrifah and Matuana, 2013; Qiang, Yu, and Gao, 2012; Cai, Wang, Nie, Tian, Zhu, and Zhou, 2011). Goriparthi et al. (2012) observed the similar result in jute fiber/PLA composites toughened with polycaprolactone (PCL). They found that the

addition of PCL into jute fiber/PLA composite led to recovery of the impact strength of the composites. Qiang et al. (2012) also reported that the addition of polyhydroxyalkanoates (PHAs) improved impact strength of PLA based wood plastic composites. The brittle-ductile transition of impact strength of the PLA based wood plastic composites toughened with PHAs was observed when the content of wood flour was between 15 and 35 wt%. The results demonstrated that PHAs recovered the impact properties of the PLA based wood plastic composites.

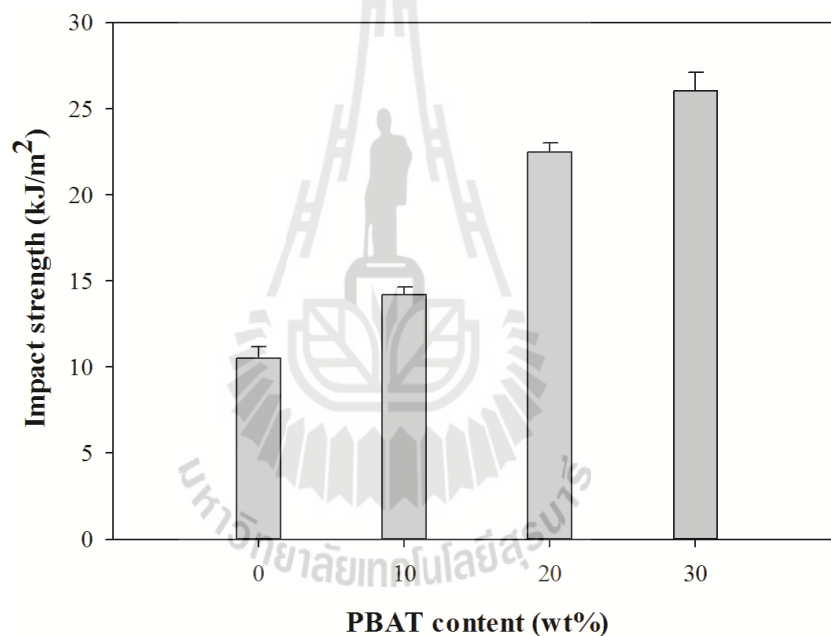


Figure 4.26 Impact strength of sawdust/PLA composite and sawdust/PLA/PBAT composites with different PBAT contents.

Table 4.7 Mechanical properties of sawdust/PLA composite and sawdust/PLA/PBAT composites with different PBAT contents.

Formulation	Tensile strength (MPa)	Young's modulus (GPa)	Elongation at break (%)	Flexural strength (MPa)	Flexural modulus (GPa)	Impact strength (kJ/m²)
PLA/AT30	49.63±0.17	1.65±0.05	3.07±0.19	108.49±1.91	12.60±0.43	10.49±0.71
PLA/AT30/PBAT10	38.93±1.14	1.45±0.02	4.17±0.35	81.40±2.30	11.04±0.71	14.21±0.46
PLA/AT30/PBAT20	37.05±0.21	1.35±0.03	5.17±0.20	76.89±0.83	10.13±0.22	22.47±0.54
PLA/AT30/PBAT30	27.73±1.02	1.01±0.06	5.56±0.31	64.21±1.35	7.29±0.44	26.04±1.07



4.4.2 Thermal properties

Thermal decomposition temperatures of PBAT, sawdust/PLA composite, and sawdust/PLA/PBAT composites with different PBAT contents are summarized in Table 4.8. TGA and DTA curves of PBAT, sawdust/PLA composite, and sawdust/PLA/PBAT composites with different PBAT contents are shown in Figure 4.27 and 4.28, respectively. From DTA curves in Figure 4.28, it was evident that the thermal degradation of PBAT showed only single step of weight loss. T_5 , T_{50} , and T_d of pure PBAT were at 372.00, 412.69, and 413.82°C, respectively. Moreover, a single stage of decomposition process of sawdust/PLA composite was observed. T_5 , T_{50} , and T_d of sawdust/PLA composite were 306.12, 363.83, and 365.54°C, respectively.

With the addition of PBAT into the sawdust/PLA composite, all of the sawdust/PLA/PBAT composites displayed two stages of the decomposition process with the first decomposition temperature ($T_{d,1}$) of sawdust and PLA at about 370°C and the second decomposition temperature of PBAT ($T_{d,2}$) at about 413°C. T_5 , T_{50} , and $T_{d,1}$ of the sawdust/PLA composites toughened with PBAT were higher than that of the sawdust/PLA composite without PBAT. This was because PBAT had higher thermal decomposition temperature than PLA (Kumar et al., 2010; Teamsinsungvon, 2010). With increasing PBAT content, T_5 , T_{50} , and $T_{d,1}$ of the composites further increased whereas $T_{d,2}$ did not change significantly as shown in Table 4.8. Char residue at 600°C significantly changed with increasing PBAT content as seen in Table 4.8. Ko, Hong, Park, Gupta, Choi, and Bhattacharya (2009) found that thermal stability of the multi-walled carbon nanotube/PLA/PBAT composites increased with increasing PBAT content from 10 to 50 wt%. This was because PBAT had higher thermal decomposition temperature than PLA. This led to an increase of thermal stability of the composites.

On the other hand, PBAT content had no significant effect on char residue content of multi-walled carbon nanotube/PLA/PBAT composites.

Table 4.8 Thermal decomposition temperatures of PBAT, sawdust/PLA composite, and sawdust/PLA/PBAT composites with different PBAT contents.

Formulation	T ₅ (°C)	T ₅₀ (°C)	T _{d,1} (°C)	T _{d,2} (°C)	Residue at 600°C (%)
PBAT	372.00	412.69	-	413.82	5.82
PLA/AT30	306.12	363.83	365.54	-	6.49
PLA/AT30/PBAT10	309.16	369.43	370.66	413.21	7.20
PLA/AT30/PBAT20	314.18	374.76	372.00	413.82	7.35
PLA/AT30/PBAT30	319.74	380.16	374.22	413.60	7.65

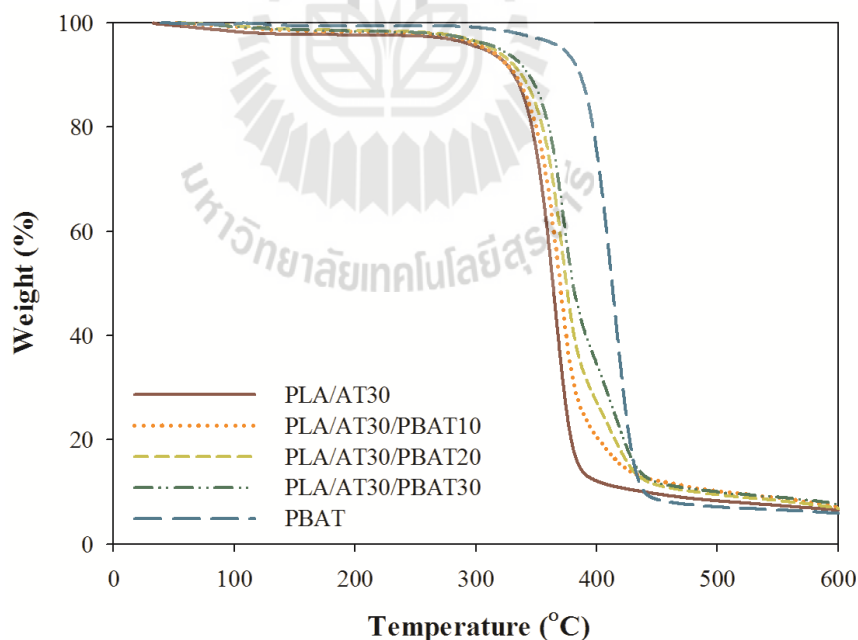


Figure 4.27 TGA curves of PBAT, sawdust/PLA composite, and sawdust/PLA/PBAT composites with different PBAT contents.

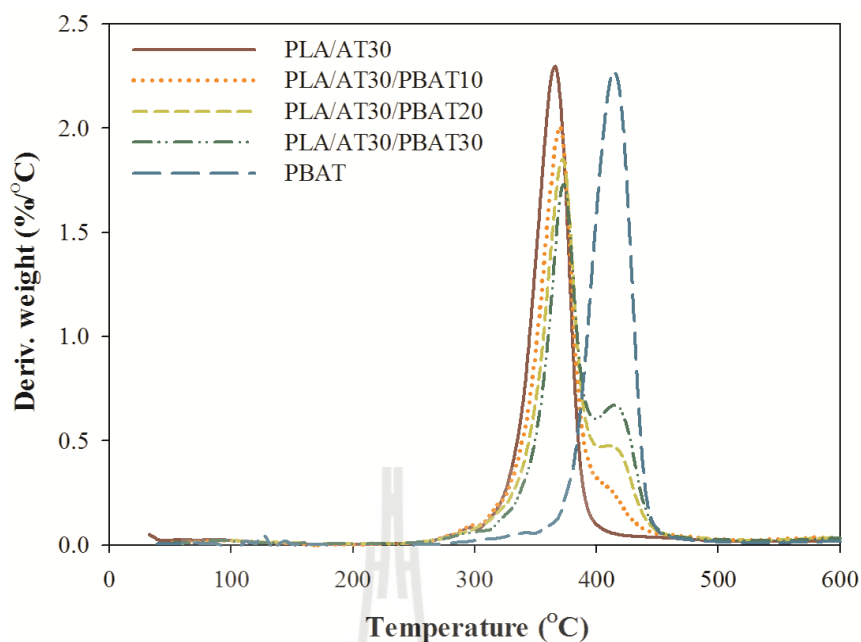


Figure 4.28 DTA curves of PBAT, sawdust/PLA composite, and sawdust/PLA/PBAT composites with different PBAT contents.

Thermal characteristics of PBAT, sawdust/PLA composite and sawdust/PLA/PBAT composites with different PBAT contents are summarized in Table 4.9 and their DSC thermograms are shown in Figure 4.29. PBAT showed T_g at -40.3°C and broad endothermic melting peak at 120°C . The sawdust/PLA composite exhibited T_g , T_{cc} , T_{m1} and T_{m2} at 52.3 , 97.4 , 140.7 , and 151.0°C , respectively. It can be seen that the T_g of PLA component in sawdust/PLA and sawdust/PLA/PBAT composites was similar. With increasing PBAT content, T_g of PLA component in sawdust/PLA/PBAT composites did not change significantly. This indicated that PLA and PBAT were not thermodynamically compatible (Teamsinsungvon, Ruksakulpiwat, and Jarukumjorn, 2013; Zhao et al., 2010). T_{cc} of the composites decreased with the incorporation of PBAT suggesting an enhancement of crystalline ability of PLA (Teamsinsungvon et al., 2013; Zhao et al., 2010). Lee 2009 also found that T_{cc} of

bamboo flour/PLA composite decreased with the addition of PBS. This indicated that crystallization occurred at lower temperature during the heating process due to the easy motion of PLA chains. Furthermore, the addition of PBAT into sawdust/PLA composites did not affect T_{m1} and T_{m2} of the PLA composite. ΔH_c and ΔH_m decreased with incorporating PBAT and decreased continuously with increasing PBAT content. This could be attributed to the reduction of PLA fraction in the sawdust/PLA/PBAT composites (Qiang et al., 2012). Moreover, χ_c of PLA in the composite increased with adding PBAT into sawdust/PLA composite and increased continuously with increasing PBAT content. This could be because PBAT acted as a heterogeneous nucleation agent and increased the degrees of crystallinity of the PLA component in the composites (Dong, Zou, Yan, Ma, and Chen, 2013; Xiao, Lu, and Yeh, 2009). Shakoor (2013) also found that χ_c of wood flour/PLA composites increased with increasing copolymer content.

Table 4.9 Thermal characteristics of PBAT, sawdust/PLA composite and sawdust/PLA/PBAT composites with different PBAT contents.

Formulation	T_g (°C)	T_{cc} (°C)	T_{m1} (°C)	T_{m2} (°C)	ΔH_c (J/g)	ΔH_m (J/g)	χ_c (%)
PBAT	-40.3	-	120.0	-	-	14.24	-
PLA/AT30	52.3	97.4	140.7	151.0	32.07	33.59	51.21
PLA/AT30/PBAT10	52.9	94.8	141.4	152.5	28.93	32.98	55.87
PLA/AT30/PBAT20	53.9	95.8	142.4	153.5	26.93	31.64	60.30
PLA/AT30/PBAT30	53.7	95.1	142.5	153.0	20.32	28.43	61.92

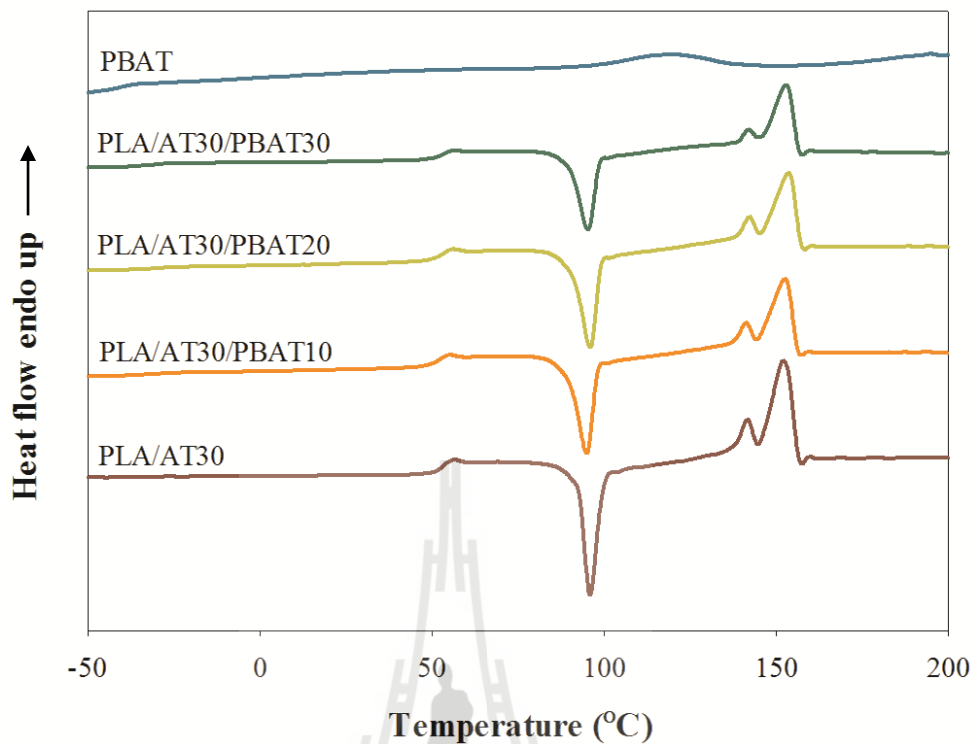


Figure 4.29 DSC thermograms of PBAT, sawdust/PLA composite and sawdust/PLA/PBAT composites with different PBAT contents (the second heating, heating rate 5°C/min).

4.4.3 Morphological properties

To study the toughening mechanism of sawdust/PLA composites toughened with PBAT, SEM micrographs of impact and tensile fractured surfaces were investigated. Impact fractured surface morphologies of sawdust/PLA composite and sawdust/PLA/PBAT composites with different PBAT contents at 1500x magnification are shown in Figure 4.30. SEM micrograph of sawdust/PLA composite exhibited a smooth fractured surface as shown in Figure 4.30 (a). This was attributed to brittle failure of the matrix system (Goriparthi et al., 2012; Zhao et al., 2010). With the addition of PBAT into sawdust/PLA composite, PBAT droplets were found in the PLA

matrix indicating that the matrix was a kind of an immiscible two-phase system. Moreover, the size of PBAT phase increased with increasing PBAT content as shown in Figure 4.30 (b)-(d). This was due to coalescence of PBAT droplets in the matrix of the composites which resulted in deterioration in tensile and flexural strength (Teamsinsungvon, 2010; Hong, Namkung, Ahn, Lee, and Kim, 2006).

The enhancement of ductile deformation of the matrix was confirmed by SEM micrographs of tensile fractured surface of sawdust/PLA/PBAT composites as shown in Figure 4.31 and 4.32. The tensile fractured surface morphologies of PLA composites toughened with PBAT showed some features of ductile fracture. This was evidence from rougher fractured surface (at 200x) and longer fibrils pulled out during tensile testing at high magnification (1500x) as shown in Figure 4.31 (b)-(d) and 4.32 (b)-(d), respectively whereas this did not occur in the composite without PBAT (Figure 4.31 (a) and 4.32 (a)). This indicated that the matrix of PLA composites toughened with PBAT was tougher than the composites without PBAT (Goriparthi et al., 2012). Moreover, with increasing PBAT content, SEM micrographs of the composites revealed more ductile deformation which indicated by extensive elongated matrix on the fracture surface as shown in Figure 4.32 (b)-(d). This resulted in an increase of elongation at break and impact strength of the toughened composites with increasing PBAT content.

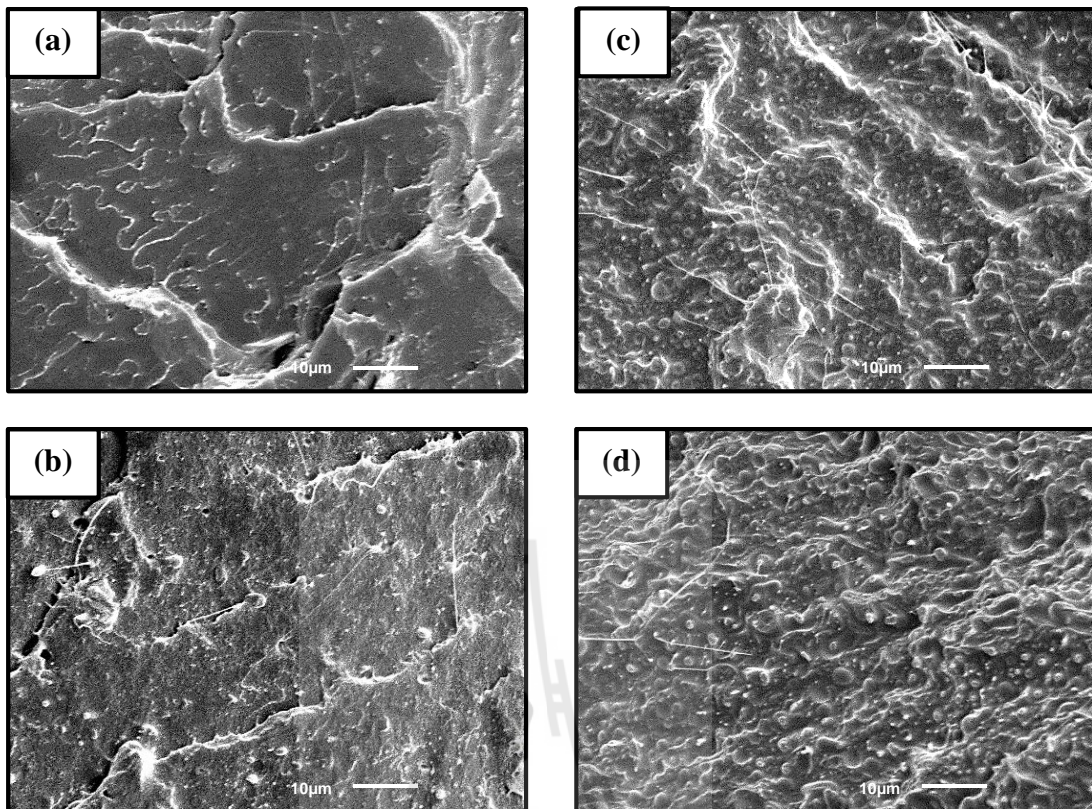


Figure 4.30 SEM micrographs of impact fractured surface at 1500x magnification of (a) PLA/AT30, (b) PLA/AT30/PBAT10, (c) PLA/AT30/PBAT20, and (d) PLA/AT30/PBAT30 composites.

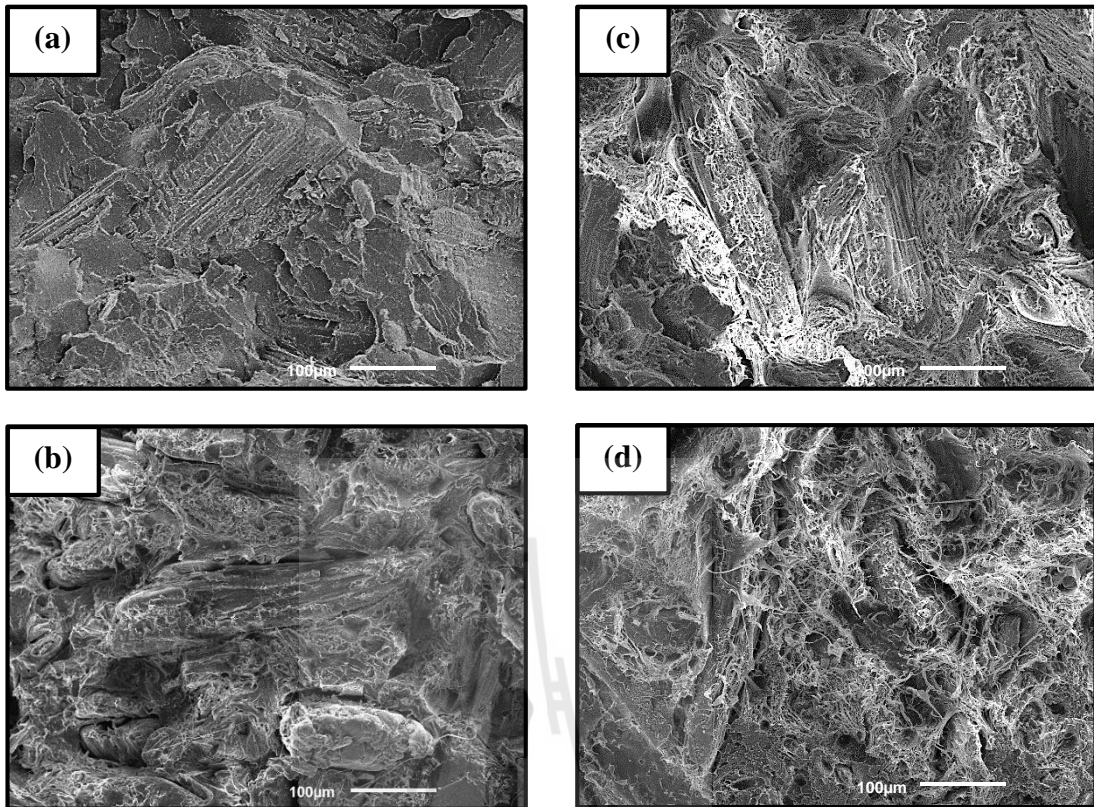


Figure 4.31 SEM micrographs of tensile fractured surface at 200x magnification of (a) PLA/AT30, (b) PLA/AT30/PBAT10, (c) PLA/AT30/PBAT20, and (d) PLA/AT30/PBAT30 composites.

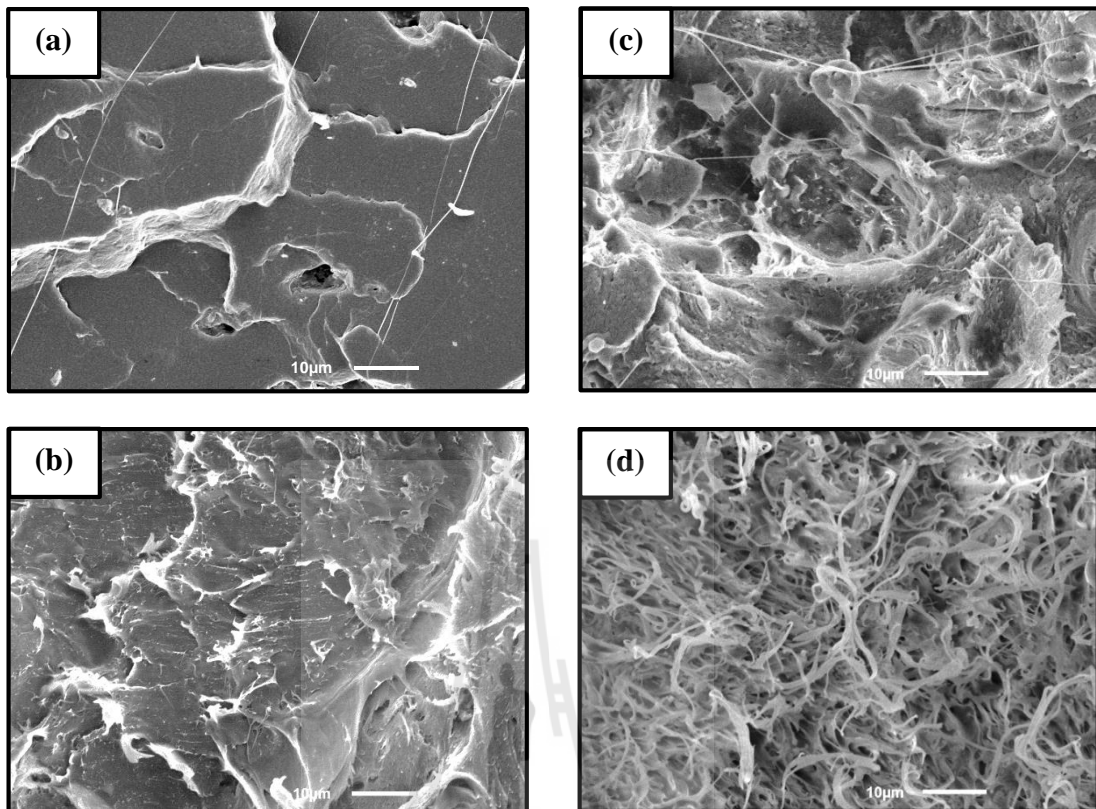


Figure 4.32 SEM micrographs of tensile fractured surface at 1500x magnification of (a) PLA/AT30, (b) PLA/AT30/PBAT10, (c) PLA/AT30/PBAT20, and (d) PLA/AT30/PBAT30 composites.

Based on the mechanical properties of the sawdust/PLA/PBAT composites, the composite filled with 20 wt% of PBAT was selected to study the effect of compatibilizer content on the mechanical, thermal, and morphological properties of the sawdust/PLA/PBAT composites.

4.5 Effect of poly(lactic acid) grafted with maleic anhydride (PLA-g-MA) content on properties of sawdust/PLA/PBAT composites

4.5.1 Mechanical properties

4.5.1.1 Tensile properties

Tensile properties of uncompatibilized sawdust/PLA/PBAT composite and compatibilized sawdust/PLA/PBAT composites with different PLA-g-MA contents are shown in Table 4.10. The uncompatibilized sawdust/PLA/PBAT composite exhibited lower tensile strength, tensile modulus, and elongation at break than that of the compatibilized sawdust/PLA/PBAT. This was due to incompatibility between the constituent polymers in the composite system which resulted in phase separation and deterioration in tensile properties (Kumar et al, 2010). Adding 3 wt% of PLA-g-MA enhanced tensile strength, tensile modulus, and elongation at break of sawdust/PLA/PBAT composite. This may be due to improved interfacial adhesion between polymer constituents of the composites by formation of intermolecular interaction between PLA-g-MA and polymer backbone (Lee, 2009; Yuan, Liu, and Ren, 2009). As PLA-g-MA content was increased up to 5 wt%, the highest tensile properties were obtained. When compared with the uncompatibilized sawdust/PLA/PBAT composite, the addition of 5 wt% PLA-g-MA improved tensile strength, tensile modulus, and elongation at break of the composite up to 35, 23, and 171%, respectively. The enhancement of tensile properties of the compatibilized sawdust/PLA/PBAT composites was confirmed by phase morphology in Figure 4.42 (b)-(d), which showed a good compatibility between PLA and PBAT. Lee (2009) also reported that the tensile strength and elongation at break of bamboo flour/PLA/PBS

composite were improved significantly with the incorporation of 3 wt% PLA-g-MA as a compatibilizer.

Unfortunately, tensile strength, tensile modulus, and elongation at break of the composites slightly decreased with further increasing PLA-g-MA content up to 10 wt% as shown in Figure 4.33-4.35, respectively. In fact that PLA-g-MA molecules contained anhydride moieties which can be brought about some side reactions during melt mixing. This anhydride group was reactive to induce chain scissions of polymer which contained ester bonds via a hydrolysis mechanism. This resulted in a reduction in chain length of the PLA phase in the composites and contributed to a decrease of mechanical properties of the composite (Wootthikanokkhan, Kasemwananimit, Sombatsompop, Kositchaiyong, Isarankura na Ayutthaya, and Kaabbuathong, 2012). Sis, Ibrahim, and Yunus (2013) also reported the similar result in kenaf fiber/PLA/PBAT composites compatibilized with (3-aminopropyl)-trimethoxysilane. They found that tensile properties of compatibilized kenaf fiber/PLA/PBAT composites increased with the addition of 2 wt% APTMS due to a good compatibility between the constituents of the composites. With further increasing APTMS content more than 2 wt%, the tensile properties of the kenaf fiber/PLA/PBAT composites tend to decrease.

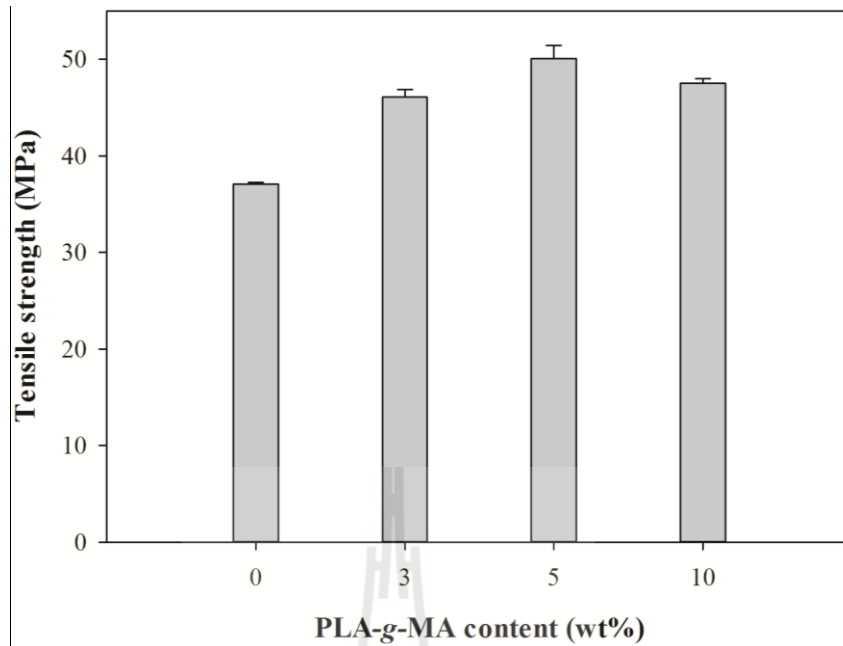


Figure 4.33 Tensile strength of sawdust/PLA/PBAT composites with different PLA-g-MA contents.

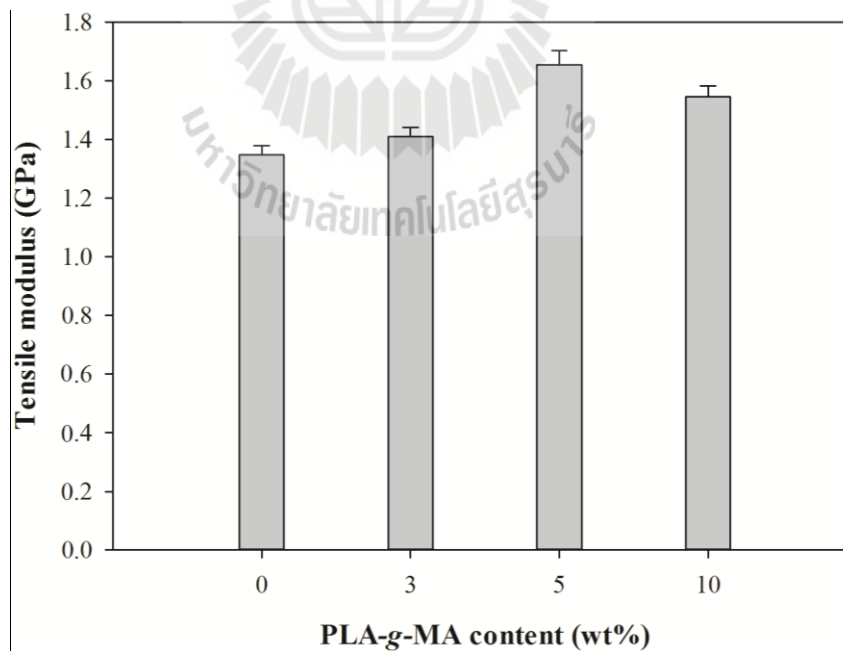


Figure 4.34 Tensile modulus of sawdust/PLA/PBAT composites with different PLA-g-MA contents.

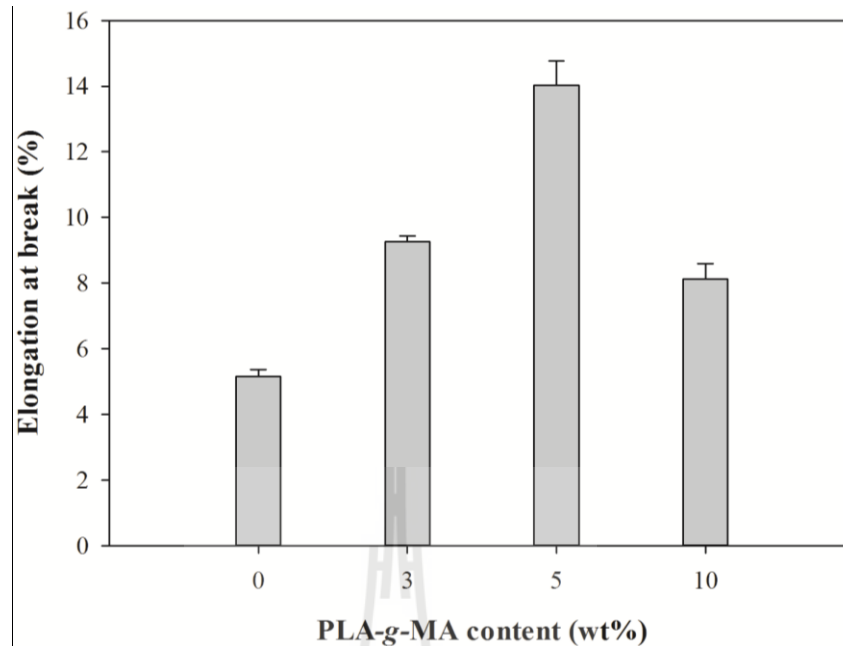


Figure 4.35 Elongation at break of sawdust/PLA/PBAT composites with different PLA-g-MA contents.

4.5.1.2 Flexural properties

Flexural properties of uncompatibilized sawdust/PLA/PBAT composite and compatibilized sawdust/PLA/PBAT composites with different PLA-g-MA contents are shown in Table 4.10. Flexural strength and flexural modulus also showed the similar trend as tensile strength and tensile modulus of the composites. Flexural strength and flexural modulus of compatibilized sawdust/PLA/PBAT composites were significantly increased with increasing PLA-g-MA content up to 5 wt% as seen in Figure 4.36 and 4.37, respectively. This was due to the enhancement of interfacial adhesion between PLA and PBAT through the intermolecular force between PLA-g-MA and polymer backbone (Lee, 2009; Yuan et al., 2009). When compared with the uncompatibilized composite, the compatibilized sawdust/PLA/PBAT composite with 5 wt% of PLA-g-MA exhibited 30 and 21% enhancement of flexural

strength and flexural modulus, respectively. Lee (2009) also found that flexural strength of bamboo flour/PLA/PBS composite was enhanced significantly with the incorporation of PLA-*g*-MA as a compatibilizer.

However, flexural strength and flexural modulus of the composites slightly decreased with increasing PLA-*g*-MA content up to 10 wt% as shown in Figure 4.36 and 4.37, respectively. This may be because higher PLA-*g*-MA content may induce chain scission of PLA resulting in a decrease of flexural properties of the compatibilized sawdust/PLA/PBAT composite. Sis et al. (2013) also reported that the addition of 2 wt% (3-aminopropyl)trimethoxysilane into kenaf/PLA/PBAT composite increased flexural strength up to 62.71%. This indicated that the compatibility between PLA and PBAT was improved when the compatibilizer was added into the composite system.

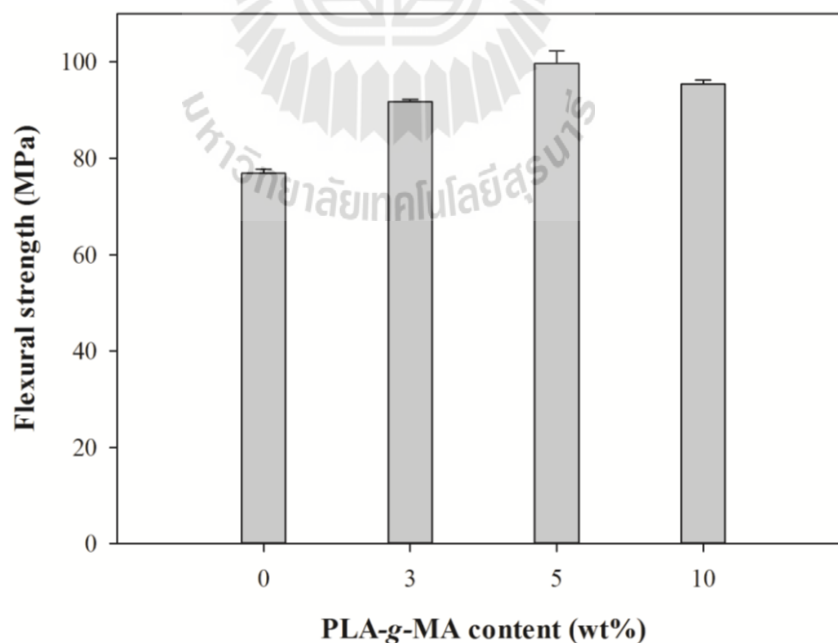


Figure 4.36 Flexural strength of sawdust/PLA/PBAT composites with different PLA-*g*-MA contents.

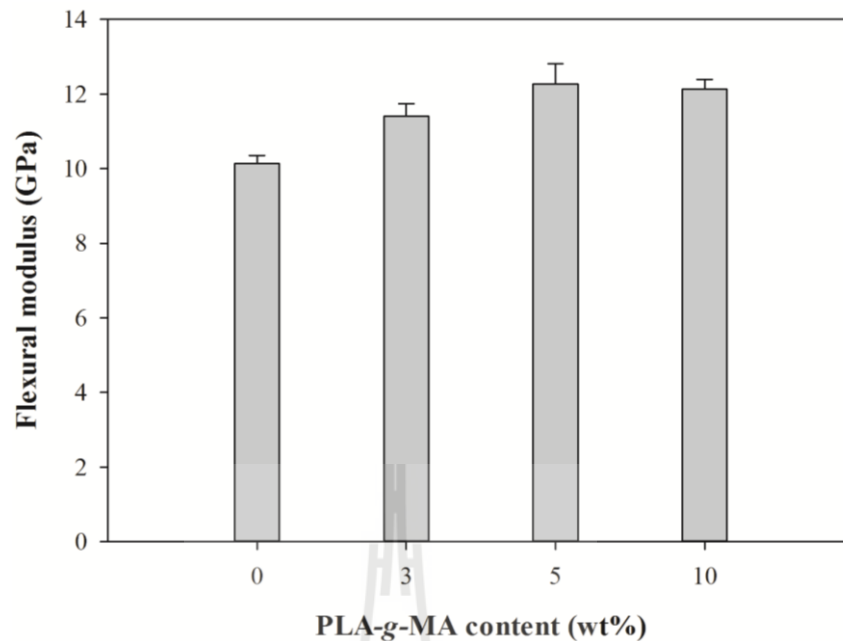


Figure 4.37 Flexural modulus of sawdust/PLA/PBAT composites with different PLA-g-MA contents.

4.5.1.3 Impact properties

Impact properties of uncompatibilized sawdust/PLA/PBAT composite and compatibilized sawdust/PLA/PBAT composites with different PLA-g-MA contents are shown in Table 4.10. With the addition of PLA-g-MA at 3 and 5 wt%, the impact strength of sawdust/PLA/PBAT composite increased up to 26 and 41%, respectively as shown in Figure 4.38. This implied that the incorporation of PLA-g-MA into the sawdust/PLA/PBAT composites improved the toughness of the composite due to the enhancement of compatibility between PLA and PBAT. When PLA-g-MA content was increased from 5 to 10 wt%, the impact strength of the composite was decreased due to chain scission by PLA-g-MA during melt mixing. Sis et al. (2013) also found that with the incorporation of 2 wt% (3-aminopropyl)-trimethoxysilane, impact strength of kenaf/PLA/PBAT composite increased up to 22%.

This was due to the improvement of interfacial adhesion between constituents of the composites by the compatibilizer. However, the impact strength of the composites started to decrease as content of APTMS was higher than 2 wt%.

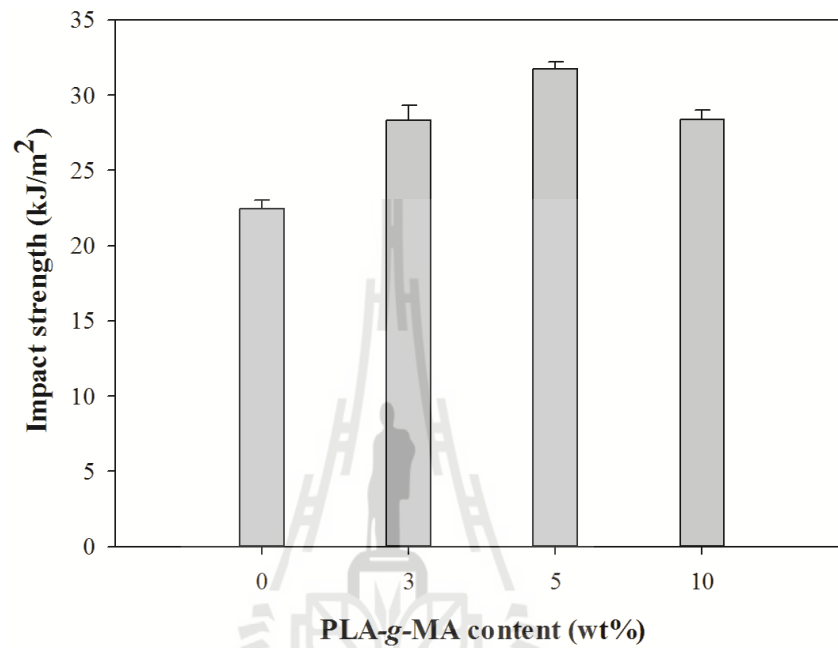
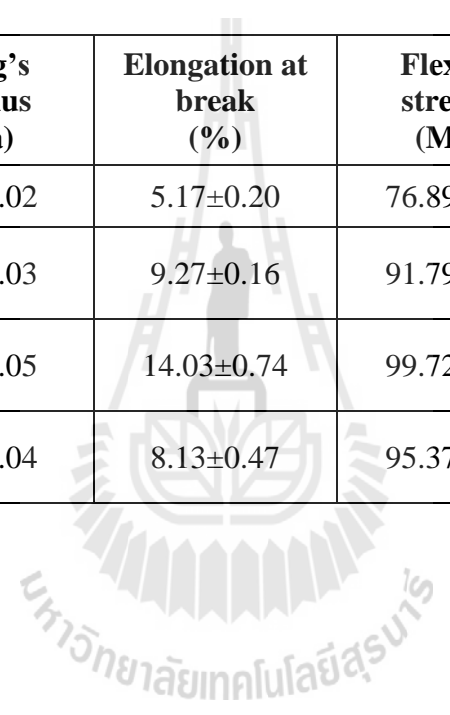


Figure 4.38 Impact strength of sawdust/PLA/PBAT composites with different PLA-g-MA contents.

Table 4.10 Mechanical properties of uncompatibilized sawdust/PLA/PBAT composite and compatibilized sawdust/PLA/PBAT composites with different PLA-g-MA contents.

Formulation	Tensile strength (MPa)	Young's modulus (GPa)	Elongation at break (%)	Flexural strength (MPa)	Flexural modulus (GPa)	Impact strength (kJ/m²)
PLA/AT30/PBAT20	37.05±0.21	1.35±0.02	5.17±0.20	76.89±0.83	10.13±0.22	22.47±0.54
PLA/AT30/PBAT20/ PLA-g-MA3	46.09±0.77	1.41±0.03	9.27±0.16	91.79±0.42	11.40±0.33	28.34±0.99
PLA/AT30/PBAT20/ PLA-g-MA5	50.09±1.34	1.65±0.05	14.03±0.74	99.72±0.42	12.27±0.53	31.75±0.47
PLA/AT30/PBAT20/ PLA-g-MA10	47.48±0.49	1.55±0.04	8.13±0.47	95.37±0.42	12.12±0.27	28.38±0.64



4.5.2 Thermal properties

TGA and DTA curves of uncompatibilized sawdust/PLA/PBAT composite and compatibilized sawdust/PLA/PBAT composites with different PLA-g-MA contents are shown in Figure 4.39 and 4.40, respectively. Thermal decomposition temperatures of uncompatibilized sawdust/PLA/PBAT composite and compatibilized sawdust/PLA/PBAT composites with different PLA-g-MA contents are shown in Table 4.11. From DTA curves in Figure 4.40, the uncompatibilized and the compatibilized sawdust/PLA/PBAT composites displayed two stages of the decomposition process with the first decomposition temperature ($T_{d,1}$) of sawdust and PLA at about 370°C and the second decomposition temperature of PBAT ($T_{d,2}$) at about 413°C. According to thermal decomposition temperatures in Table 4.11, T_5 , T_{50} , $T_{d,1}$, and $T_{d,2}$ of the uncompatibilized sawdust/PLA/PBAT composite were 314.18, 374.76, 372.00, and 413.83°C, respectively. Moreover, it could be seen that T_5 , T_{50} , and $T_{d,1}$ of the compatibilized sawdust/PLA/PBAT composites were higher than that of the uncompatibilized sawdust/PLA/PBAT composite. This indicated the thermal stability of the composite was improved with the presence of PLA-g-MA due to enhanced the compatibility between polymer constituents of the composites. Lee (2009) also observed that thermal degradation temperature of bamboo flour/PLA/PBS composite was improved with the addition of PLA-g-MA. This was attributed to the enhancement of interfacial adhesion between constituents of the composite.

However, T_5 , T_{50} , $T_{d,1}$, $T_{d,2}$, and char residue at 600°C did not change significantly with PLA-g-MA content. Yao (2008) also reported that compatibilizer content had no significant effect on thermal stability of rice straw fiber/high density polyethylene composite toughened with ethylene/propylene copolymer.

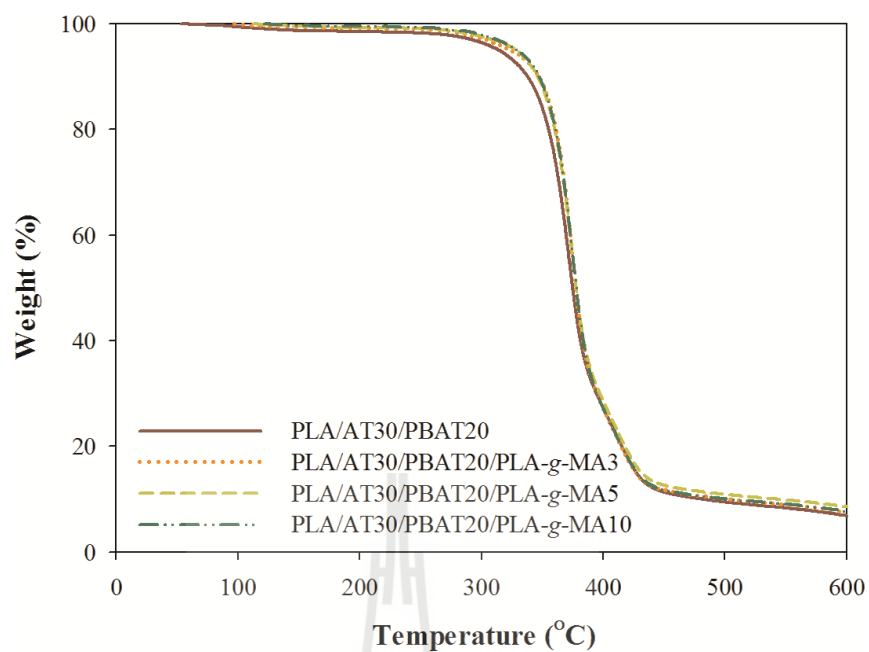


Figure 4.39 TGA curves of sawdust/PLA/PBAT composites with different PLA-g-MA contents.

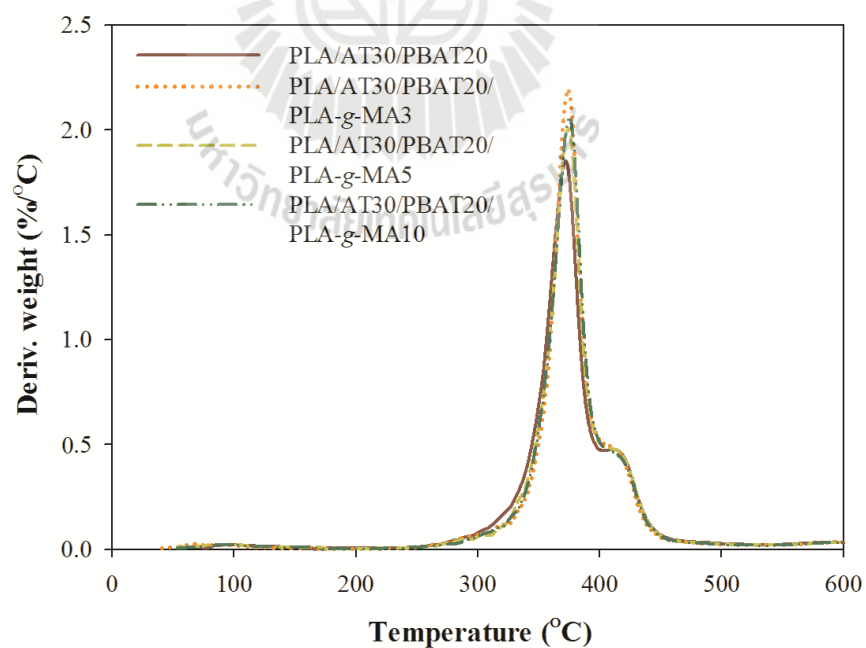


Figure 4.40 DTA curves of sawdust/PLA/PBAT composites with different PLA-g-MA contents.

Table 4.11 Thermal decomposition temperatures of uncompatibilized sawdust/PLA/PBAT composite and compatibilized sawdust/PLA/PBAT composites with different PLA-g-MA contents.

Formulation	T₅ (°C)	T₅₀ (°C)	T_{d,1} (°C)	T_{d,2} (°C)	Residue at 600°C (%)
PLA/AT30/PBAT20	314.18	374.76	372.00	413.82	7.35
PLA/AT30/PBAT20/ PLA-g-MA3	323.82	377.23	375.77	413.40	7.54
PLA/AT30/PBAT20/ PLA-g-MA5	328.54	377.68	376.45	413.56	8.52
PLA/AT30/PBAT20/ PLA-g-MA10	329.07	377.91	376.02	413.72	7.67

DSC curves of uncompatibilized sawdust/PLA/PBAT composite and compatibilized sawdust/PLA/PBAT composites with different PLA-g-MA contents are shown in Figure 4.41 and their thermal characteristics data are summarized in Table 4.12. The uncompatibilized sawdust/PLA/PBAT composite showed T_g , T_{cc} , T_{m1} , and T_{m2} at 53.9, 95.8, 142.4, and 153.5°C, respectively. With the addition of PLA-g-MA, T_g of PLA component in the composite decreased. As PLA-g-MA content was increased, T_g of PLA component in the composites decreased continuously. It was well known that compatibilization resulted in shifting of T_g values of components toward each other due to the formation of interaction between the compatibilizer and the polymer backbone at the interface (Karagoz and Ozkoc, 2013; Zhao et al., 2010). Thus, the decrease of T_g implied that PLA-g-MA enhanced the compatibility between polymer constituents of the composites. The incorporation of PLA-g-MA into the sawdust/PLA/PBAT composites decreased T_{m1} and T_{m2} of PLA component which was

probably due to formation of intermolecular interaction at the interface (Kumar et al., 2010). Additionally, T_{cc} of PLA in the composites was shifted to lower temperature with the incorporation of PLA-g-MA. With increasing PLA-g-MA content, T_{cc} of PLA in the composites decreased continuously. This suggested that adding PLA-g-MA had an influence on crystallizability of sawdust/PLA/PBAT composites. Moreover, with the addition of PLA-g-MA, χ_c of PLA component in the composites increased. This may be because the dispersed PBAT phase was reduced to smaller sizes when PLA-g-MA was added into sawdust/PLA/PBAT composites (Figure 4.42 (b)-(d)). Generally, a smaller dispersed phase size was believed to be a more effective nucleation agent compared to larger dispersed size (Shin, Jang, and Kim, 2011). This led to an increase of χ_c of PLA component in the compatibilized composites when PLA-g-MA was added. Lee (2009) also observed that with the addition of PLA-g-MA as a compatibilizer, T_g , T_{cc} , and T_m of PLA component in the bamboo flour/PLA/PBS composite decreased while χ_c increased. In addition, the compatibilized sawdust/PLA/PBAT composites had ΔH_c and ΔH_m lower than the uncompatibilized composite. These results also confirmed that the interfacial adhesion between PLA and PBAT was enhanced by PLA-g-MA (Kumar et al., 2010; Zhang, Wang, Ren, and Wang, 2009).

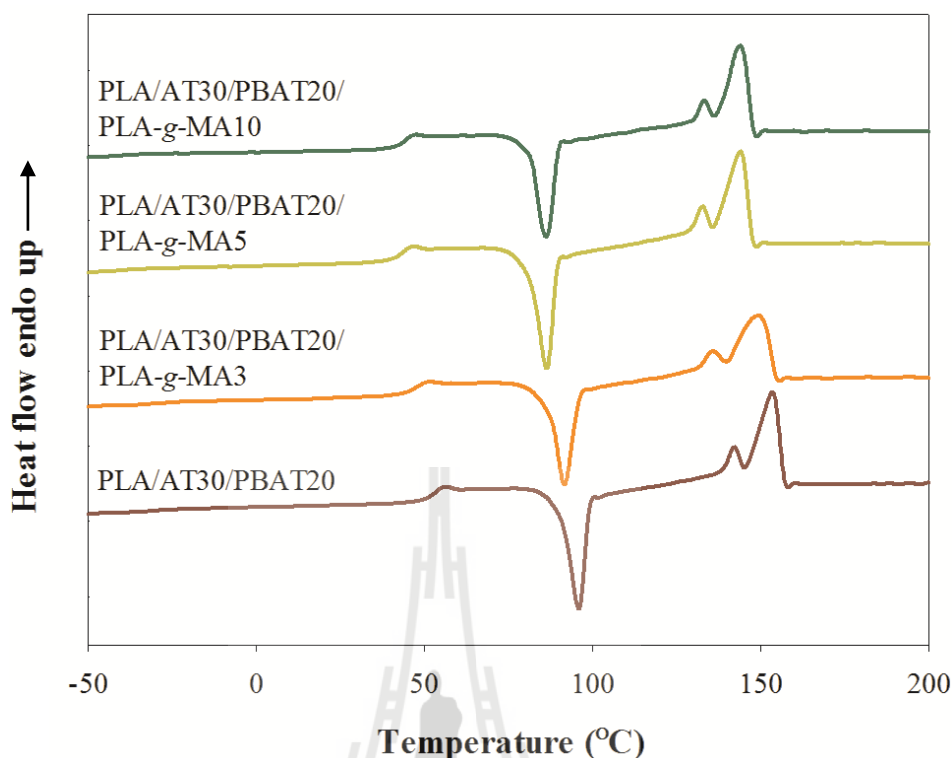


Figure 4.41 DSC thermograms of uncompatibilized sawdust/PLA/PBAT composite and compatibilized sawdust/PLA/PBAT composites with different PLA-g-MA contents (the second heating, heating rate 5°C/min).

Table 4.12 Thermal characteristics of uncompatibilized sawdust/PLA/PBAT composite and compatibilized sawdust/PLA/PBAT composites with different PLA-g-MA contents.

Formulation	T _g (°C)	T _{cc} (°C)	T _{m1} (°C)	T _{m2} (°C)	ΔH _c (J/g)	ΔH _m (J/g)	χ _c (%)
PLA/AT30/PBAT20	53.9	95.8	142.4	153.5	26.93	31.64	60.30
PLA/AT30/PBAT20/ PLA-g-MA3	48.0	92.0	138.9	149.9	24.56	31.50	62.26
PLA/AT30/PBAT20/ PLA-g-MA5	45.9	88.7	135.6	146.7	24.08	31.35	63.13
PLA/AT30/PBAT20/ PLA-g-MA10	45.2	88.3	135.4	146.5	23.53	29.84	63.69

4.5.3 Morphological properties

SEM micrographs of the impact fracture surface of uncompatibilized sawdust/PLA/PBAT composite and compatibilized sawdust/PLA/PBAT composites with different PLA-*g*-MA contents at 1500x magnification are shown in Figure 4.42. The uncompatibilized composite showed a coarse morphology with larger PBAT domain size in comparison to the compatibilized sawdust/PLA/PBAT composites. Moreover, it can be seen that the size of the dispersed PBAT phase significantly decreased with the addition of PLA-*g*-MA as shown in Figure 4.42 (b)-(d). This indicated that the compatibility between PLA and PBAT was improved (Jafari, Asadinezhad, Yavari, Khonakdar, and Böhme, 2005).

Furthermore, tensile fractured surface morphologies of compatibilized sawdust/PLA/PBAT composite with 5 wt% of PLA-*g*-MA at 200x and 1500x magnification are shown in Figure 4.43. The compatibilized sawdust/PLA/PBAT composite showed good interfacial adhesion between the constituents of the composite and also revealed ductile deformation which indicated by extensive elongated matrix on the fractured surface as shown in Figure 4.43 (a) and (b), respectively. This resulted in an improvement of overall mechanical properties including strength, stiffness, and toughness of the compatibilized sawdust/PLA/PBAT composites with PLA-*g*-MA.

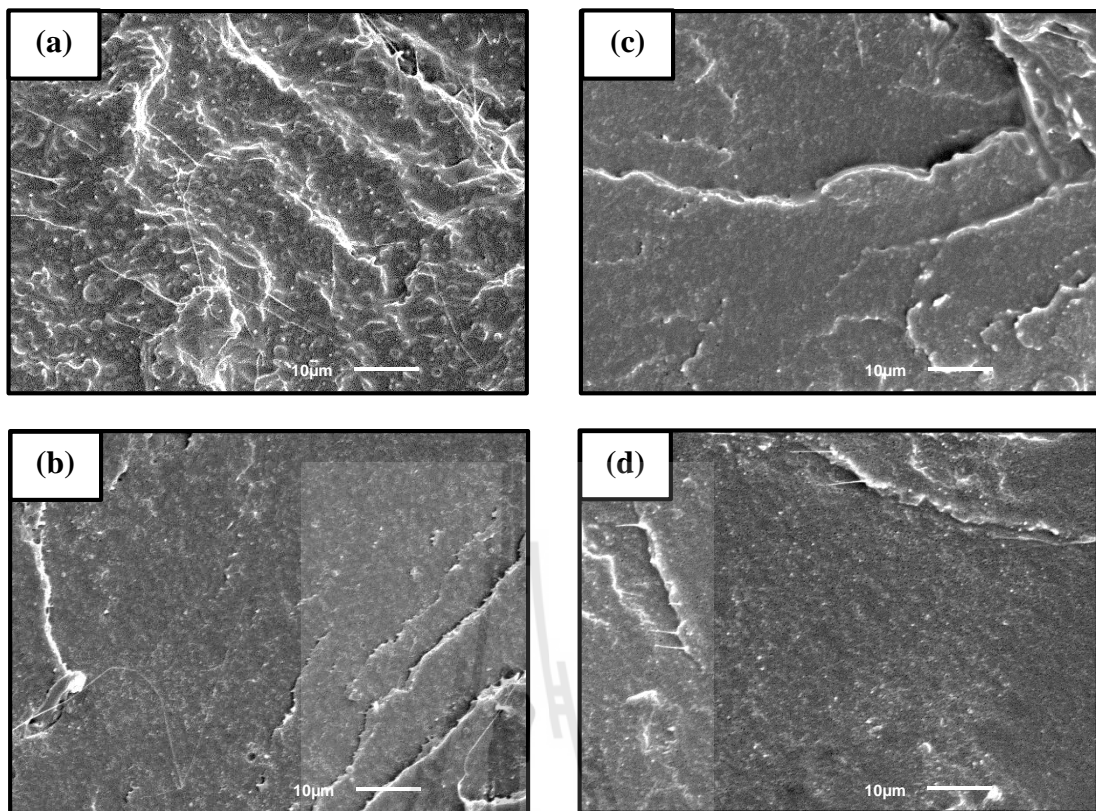


Figure 4.42 SEM micrographs of impact fractured surface at 1500x magnification of (a) PLA/AT30/PBAT20, (b) PLA/AT30/PBAT20/PLA-g-MA3, (c) PLA/AT30/PBAT20/PLA-g-MA5, and (d) PLA/AT30/PBAT20/PLA-g-MA10 composites.

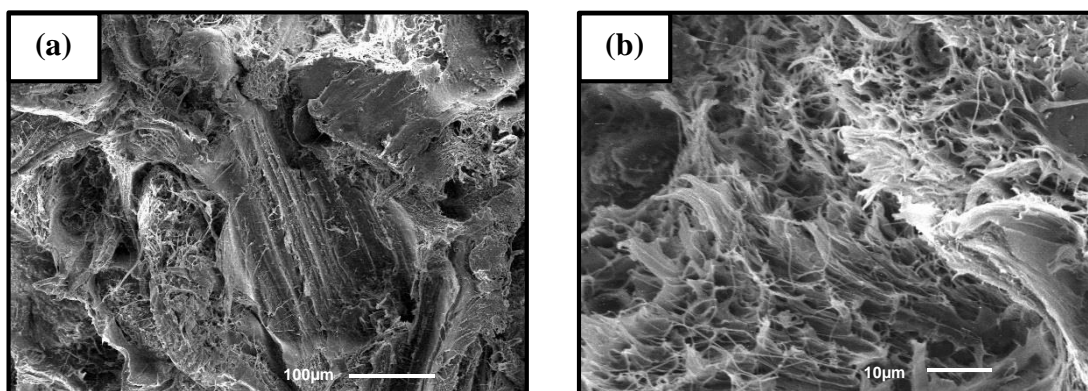


Figure 4.43 SEM micrographs of tensile fractured surface of PLA/AT30/PBAT20/PLA-g-MA5 composite (a) at 200x and (b) at 1500x magnification.



CHAPTER V

CONCLUSIONS

Effect of alkali treatment on physical properties of sawdust was investigated. After alkali treatment, hemicellulose and lignin contents of alkali treated sawdust (AT) significantly decreased whereas cellulose content increased. FTIR results exhibited a remarkable decrease of peak intensity at 3334, 2919, 2856, 1728, 1603, and 1508 cm^{-1} after alkali treatment due to the removal of hemicellulose and lignin. Moreover, TGA results showed a disappearance of low molecular weight compositions, hemicellulose, and lignin of AT leading to an improvement of thermal stability. SEM micrographs revealed that surface of AT was cleaner and rougher than untreated sawdust (UT). The optimum alkali treatment condition was 2% w/v NaOH for 30 min.

Effects of sawdust content and alkali treatment on mechanical, thermal, and morphological properties of sawdust/PLA composites were studied. Tensile modulus and flexural modulus of PLA composites increased continuously with increasing UT content while tensile strength, flexural strength, impact strength, and elongation at break of the composites decreased. Thermal stability of PLA composites was decreased with adding sawdust. Mechanical properties and thermal stability of AT/PLA composites were higher than those of UT/PLA composites at all sawdust contents due to a good dispersion of AT in PLA matrix and a good filler-matrix interfacial adhesion. Glass transition temperature and melting temperature of PLA insignificantly changed with increasing UT content. Crystallization temperature of PLA decreased with the addition of 20 wt% UT but tend to increase with increasing UT content due to the

restriction of chain mobility of PLA by the filler agglomeration. Degree of crystallization increased with the addition of UT and then decreased with increasing UT content. However, crystallization temperature of PLA in the AT/PLA composites decreased due to the nucleating ability of AT leading to an improvement of degree of crystallinity of PLA in the composites at all sawdust contents. SEM micrographs confirmed that alkali treatment resulted in good dispersion of AT in PLA matrix and improved interfacial adhesion between AT and PLA matrix.

With the incorporation of PBAT into PLA composites, elongation at break and impact strength increased whereas tensile strength, tensile modulus, flexural strength, and flexural modulus decreased due to the presence of soft elastomeric phase. Thermal stability of PLA composites improved with increasing PBAT content. In addition, PBAT exhibited insignificant effect on glass transition temperature and melting temperature but led to a decrease of crystallization temperature of PLA in the composites. An increase of degree of crystallinity was found when PBAT content was increased. SEM micrographs revealed some features of ductile fracture in the composites toughened with PBAT.

The addition of PLA-g-MA improved mechanical properties and thermal stability of the sawdust/PLA/PBAT composites due to enhanced interfacial adhesion between polymer constituents of the composites. The optimum content of PLA-g-MA for sawdust/PLA/PBAT composites was 5 wt%. Glass transition temperature, melting temperature, and crystallization temperature of PLA in the composite were decreased with increasing PLA-g-MA content while degree of crystallinity of PLA component was increased. SEM micrographs confirmed that PLA-g-MA improved the compatibility of the composites.

REFERENCES

- Afrifah, K. A., and Matuana, L. M. (2013). Fracture toughness of poly(lactic acid)/ethylene acrylate copolymer/wood-flour composite ternary blends. **Polym. Int.** 62 (7): 1053-1058.
- Arbelaiz, A., Fernández, B., Valea, A., and Mondragon, I. (2006). Mechanical properties of short flax fibre bundle/poly(ϵ -caprolactone) composites: Influence of matrix modification and fibre content. **Carbohydr. Polym.** 64 (2): 224-232.
- Arifuzzaman Khan, G. M., and Shamsul Alam, Md. (2012). Thermal characterization of chemically treated coconut husk fibre. **Indian J. Fibre Text.** 37 (1): 20-26.
- Avella, M., Gaceva, G. B., Buzđarovska, A., Errico, M. E., Gentile, G., and Grozdanov, A. (2007). Poly(3-hydroxybutyrate-co-3-hydroxyvalerate) based biocomposites reinforced with kenaf fibers. **J. Appl. Polym. Sci.** 104 (5): 3192-3200.
- Aydin, M., Tozlu, H., Kemaloglu, S., Aytac, A., and Ozkoc, G. (2011). Effects of alkali treatment on the properties of short flax fiber-poly(lactic acid) eco-composites. **J. Polym. Environ.** 19 (1): 11-17.
- Bachtiar, D., Sapuan, S. M., Zainudin, E. S., Khalina, A., and Dahlan, K. Z. H. M. (2013). Thermal properties of alkali-treated sugar palm fibre reinforced high impact polystyrene composites. **Pertanika J. Sci. Technol.** 21 (1): 141-150.
- Bettini, S. H. P., Bonse, B. C., Melo, E. A., and Muñoz, P. A. R. (2010). Effect of sawdust surface treatment and compatibilizer addition on mechanical behavior, morphology, and moisture uptake of polypropylene/sawdust composites. **Polym. Eng. Sci.** 50 (5): 978-985.

- Brígidaa, A. I. S., Caladob, V. M. A., Gonçalvesc, L. R. B., and Coelhoa, M. A. Z. (2010). Effect of chemical treatments on properties of green coconut fiber. **Carbohyd. Polym.** 79 (4): 832-838.
- Bwire, S. N., Christian, N., and Joseph, T. (2007). Chemical and thermal stability of rice husks against alkali treatment. **BioRes.** 3 (4): 1267-1277.
- Cai, G., Wang, J., Nie, Y., Tian, X., Zhu, X., and Zhou, X. (2011). Effects of toughening agents on the behaviors of bamboo plastic composites. **Polym. Compos.** 32 (12): 1945-1952.
- Cao, Y., Sakamoto, S., and Goda, K. (2007). Effects of heat and alkali treatments on mechanical properties of kenaf fibers. In **16th International Conference on Composite Materials (ICCM-16)**. Kyoto, Japan, July 8-13.
- Chattopadhyay, H., and Sarkar, P. B. (1946). A new method for the estimation of cellulose. In **Proceedings of the National Institute of Sciences of India.** 12: 23-46.
- Chen, F., Liu, L., Cooke, P. H., Hicks, K. B., and Zhang, J. (2008). Performance enhancement of poly(lactic acid) and sugar beet pulp composites by improving interfacial adhesion and penetration. **Ind. Eng. Chem. Res.** 47 (22): 8667-8675.
- Chun, K., Husseinsyah, S., and Osman, H. (2012). Mechanical and thermal properties of coconut shell powder filled polylactic acid biocomposites: Effects of the filler content and silane coupling agent. **J. Polym. Res.** 19 (5): 1-8.
- Chun, K. S., Husseinsyah, S., and Osman, H. (2013). Properties of coconut shell powder-filled polylactic acid ecomposites: Effect of maleic acid. **Polym. Eng. Sci.** 53 (5): 1109-1116.

- Das, M., and Chakraborty, D. (2006). Influence of alkali treatment on the fine structure and morphology of bamboo fibers. **J. Appl. Polym. Sci.** 102 (5): 5050-5056.
- De Rosa, I. M., Kenny, J. M., Puglia, D., Santulli, C., and Sarasini, F. (2010). Morphological, thermal and mechanical characterization of okra (*Abelmoschus esculentus*) fibres as potential reinforcement in polymer composites. **Compos. Sci. Technol.** 70 (1): 116-122.
- Demir, A., Seki, Y., Bozaci, E., Sarikanat, M., Erden, S., Sever, K., and Ozdogan, E. (2011). Effect of the atmospheric plasma treatment parameters on jute fabric: The effect on mechanical properties of jute fabric/polyester composites. **J. Appl. Polym. Sci.** 121 (2): 634-638.
- Derya, S. K., and Bilgin, G. (2008). The effect of heat treatment on physical properties and surface roughness of red-bud maple (*Acer trautvettevi* Medw.) wood. **Bioresour. Technol.** 99 (8): 2846-2851.
- Dimonie, M. and Rapa, M. (2010). Biodegradable blends based on PHB and wood fiber. **U.P.B. Sci. Bull.** 72 (3): 3-10.
- Dong, W., Zou, B., Yan, Y., Ma, P., and Chen, M. (2013). Effect of chain-extenders on the properties and hydrolytic degradation behavior of the poly(lactide)/poly(butylene adipate-*co*-terephthalate) blends. **Int. J. Mol. Sci.** 14 (10): 20189-20203.
- Edeerozey, A. M. M., Akil, H. M., Azhar, A. B., and Ariffin, M. I. Z. (2007). Chemical modification of kenaf fibers. **Mater. Lett.** 61 (10): 2023-2025.
- Frone, A. N., Berlioz, S., Chailan, J. F., Panaitescu, D. M., and Donescu, D. (2011). Cellulose fiber-reinforced polylactic acid. **Polym. Compos.** 32 (6): 976-985.

- Garlotta, D. (2001). A literature review of poly(lactic Acid). **J. Polym. Environ.** 9 (2): 63-84.
- Gassan, J., Gutowski, V. S., and Bledzki, A. K. (2000). About the surface characteristics of natural fibres. **Macromol. Mater. Eng.** 283 (1): 132-139.
- Gomes, A., Goda, K., and Ohgi, J. (2004). Effects of alkali treatment to reinforcement on tensile properties of curaua fiber green composites. **JSME Int. J. Ser. A.** 47 (4): 541-546.
- Goriparthi, B. K., Suman, K. N. S., and Nalluri, M. R. (2012). Processing and characterization of jute fiber reinforced hybrid biocomposites based on polylactide/polycaprolactone blends. **Polym. Compos.** 33 (2): 237-244.
- Gregorova, A., Sedlarik, V., Pastorek, M., Jachandra, H., and Stelzer, F. (2011). Effect of compatibilizing agent on the properties of highly crystalline composites based on poly(lactic acid) and wood flour and/or mica. **J. Polym. Environ.** 19 (2): 372-381.
- Haq, M., Burgueño, R., Mohanty, A. K., and Misra, M. (2008). Hybrid bio-based composites from blends of unsaturated polyester and soybean oil reinforced with nanoclay and natural fibers. **Compos. Sci. Technol.** 68 (15-16): 3344-3351.
- Hong, J. S., Namkung, H., Ahn, K. H., Lee, S. J., and Kim, C. (2006). The role of organically modified layered silicate in the breakup and coalescence of droplets in PBT/PE blends. **Polymer.** 47 (11): 3967-3975.
- Hu, R. and Lim, J. K. (2007). Fabrication and mechanical properties of completely biodegradable hemp fiber reinforced poly(lactic acid) composites. **J. Compos. Mater.** 41 (13): 1655-1669.

- Huda, M. S., Drzal, L. T., Misra, M., and Mohanty, A. K. (2006). Wood-fiber-reinforced poly(lactic acid) composites: evaluation of the physico-mechanical and morphological properties. **J. Appl. Polym. Sci.** 102 (5): 4856-4869.
- Islam, M. S., Pickering, K. L., and Foreman, N. J. (2010). Influence of alkali treatment on the interfacial and physico-mechanical properties of industrial hemp fibre reinforced polylactic acid composites. **Composite Part A.** 41 (5): 596-603.
- Jafari, S. H., Asadinezhad, A., Yavari, A., Khonakdar, H. A., Böhme, F. (2005). Compatibilizing effects on the phase morphology and thermal properties of polymer blends based on PTT and m-LLDPE. **Polym. Bull.** 54 (6): 417-426.
- Jandas, P. J., Mohanty, S., Nayak, S. K., and Srivastava, H. (2011). Effect of surface treatments of banana fiber on mechanical, thermal, and biodegradability properties of PLA/banana fiber biocomposites. **Polym. Compos.** 32 (11): 1689-1700.
- Jiang, F. and Qin, T. (2006). Toughening wood/polypropylene composites with polyethylene octene elastomer (POE). **J. For. Res.** 17 (4): 312-314.
- Jiang, L., Wolcott, M. P., and Zhang, J. (2006). Study of biodegradable poly(lactide)/poly(butylene adipate-co-terephthalate) blends. **Biomacromolecules.** 7 (1): 199-207.
- Joseph, P. V., Joseph, K., and Thomas, S. (1999). Effect of processing variables on the mechanical properties of sisal-fiber-reinforced polypropylene composites. **Compos. Sci. Technol.** 59 (11): 1625-1640.
- Kaewkuk, S., Sutapun, W., and Jarukumjorn, K. (2013). Effects of interfacial modification and fiber content on physical properties of sisal fiber/polypropylene composites. **Composites Part B.** 45 (1): 544-549.

- Karagoz, S., and Ozkoc, G. (2013). Effects of a diisocyanate compatibilizer on the properties of citric acid modified thermoplastic starch/poly(lactic acid) blends. **Polym. Eng. Sci.** 53 (10): 2183-2193.
- Kargarzadeh, H., Ahmad, I., Abdullah, I., Dufresne, A., Zainudin, S., and Sheltami, R. (2012). Effects of hydrolysis conditions on the morphology, crystallinity, and thermal stability of cellulose nanocrystals extracted from kenaf bast fibers. **Cellulose.** 19 (3): 855-866.
- Kfoury, G., Raquez, J. M., Hassouna, F., Odent, J., Toniazzo, V., Ruch, D., and Dubois, P. (2013). Recent advances in high performance poly(lactide): From “green” plasticization to super-tough materials via (reactive) compounding. **Front. Chem.** 1 (32): 1-46.
- Khammatova, V. V. (2005). Effect of high-frequency capacitive discharge plasma on the structure and properties of flax and lavsan materials. **Fibre Chem.** 37 (4): 293-296.
- Ko, S. W., Hong, M. K., Park, B. J., Gupta, R. K., Choi, H. J., and Bhattacharya, S. N. (2009). Morphological and rheological characterization of multi-walled carbon nanotube/PLA/PBAT blend nanocomposites. **Polym. Bull.** 63 (1): 125-134.
- Kumar, A., Negi, Y. S., Choudhary, V., Bhardwaj, N. K. (2014). Characterization of cellulose nanocrystals produced by acid-hydrolysis from sugarcane bagasse as agro-waste. **J. Mater. Phys. Chem.** 2 (1):1-8.
- Kumar, M., Mohanty, S., Nayak, S. K., and Rahail Parvaiz, M. (2010). Effect of glycidyl methacrylate (GMA) on the thermal, mechanical and morphological property of biodegradable PLA/PBAT blend and its nanocomposites. **Bioresour. Technol.** 101 (21): 8406-8415.

- Lee, S. (2009). **Evaluation on the high flexible polylactic acid and bamboo flour bio-composite by melting blend**. M. Eng. thesis, Seoul National University, South Korea.
- Lee, S. H. and Wang, S. (2006). Biodegradable polymers/bamboo fiber biocomposite with bio-based coupling agent. **Composites Part A**. 37 (1): 80-91.
- Lee, S. Y., Kang, I. A., Doh, G. H., Yoon, H. G., Park, B. D., and Wu, Q. (2008). Thermal and mechanical properties of wood flour/talc-filled polylactic acid composites: effect of filler content and coupling treatment. **J. Thermoplast. Compos. Mater.** 21 (3): 209-223.
- Li, Z., Zhou, X., and Pei, C. (2011). Effect of sisal fiber surface treatment on properties of sisal fiber reinforced polylactide composites. **Int. J. Polym. Sci.** 2011. doi:10.1155/2011/803428.
- Liu, H. and Zhang, J. (2011). Research progress in toughening modification of poly(lactic acid). **J. Polym. Sci., Part B: Polym. Phys.** 49 (15): 1051-1083.
- Liu, H., Wu, Q., Han, G., Yao, F., Kojima, Y., and Suzuki, S. (2008). Compatibilizing and toughening bamboo flour-filled HDPE composites: Mechanical properties and morphologies. **Composites Part A**. 39 (12): 1891-1900.
- Liu, L., Yu, J., Cheng, L., and Yang, X. (2009). Biodegradability of poly(butylene succinate) (PBS) composite reinforced with jute fibre. **Polym. Degrad. Stab.** 94 (1): 90-94.
- Liu, W., Mohanty, A. K., Askeland, P., Drzal, L. T., and Misra, M. (2004). Influence of fiber surface treatment on properties of Indian grass fiber reinforced soy protein based biocomposites. **Polymer**. 45 (22): 7589-7596.

- Liu, W., Mohanty, A. K., Drzal, L. T., Askel, P., and Misra, M. (2004). Effects of alkali treatment on the structure, morphology and thermal properties of native grass fibers as reinforcements for polymer matrix composites. **J. Mater. Sci.** 39 (3): 1051-1054.
- Lopattananon, N., Panawarangkul, K., Sahakaro, K., and Ellis, B. (2006). Performance of pineapple leaf fiber-natural rubber composites: The effect of fiber surface treatments. **J. Appl. Polym. Sci.** 102 (2): 1974-1984.
- Lu, N., and Oza, S. (2013). Thermal stability and thermo-mechanical properties of hemp-high density polyethylene composites: Effect of two different chemical modifications. **Composites Part B.** 44 (1): 484-490.
- Ma, P., Huang, J., Cao, G., and Xu, W. (2010). Influence of temperature on corona discharge treatment of cotton fibers. **Fiber Polym.** 11 (6): 941-945.
- Mani, R., Bhattacharya, M., and Tang, J. (1999). Functionalization of polyesters with maleic anhydride by reactive extrusion. **J. Polym. Sci., Part A: Polym. Chem** 37 (11): 1693-1702.
- Ming-Zhu, P., Chang-Tong, M., Xu-Bing, Z., and Yun-Lei, P. (2011). Effects of rice straw fiber morphology and content on the mechanical and thermal properties of rice straw fiber high density polyethylene composites. **J. Appl. Polym. Sci.** 121 (5): 2900-2907.
- Mofokeng, J. P. (2010). **Comparison of injection moulded, natural fibre reinforced composites with PP and PLA as matrices.** M. Eng. thesis, University of The Free State (Qwaqwa Campus).

- Mohamad Haafiz, M. K., Eichhorn, S. J., Hassan, A., and Jawaid, M. (2013). Isolation and characterization of microcrystalline cellulose from oil palm biomass residue. **Carbohydr. Polym.** 93 (2): 628-634.
- Mohan, D., Pittman, C. U., and Steele, P. H. (2006). Pyrolysis of wood/biomass for bio-oil: A critical review. **Energy Fuels.** 20 (3): 848-889.
- Obi Reddy, K., Shukla, M., Uma Maheswari, C., and Varada Rajulu, A. (2012). Mechanical and physical characterization of sodium hydroxide treated Borassus fruit fibers. **J. For. Res.** 23 (4): 667-674.
- Ochi, S. (2006). Development of high strength biodegradable composites using manila hemp fiber and starch-based biodegradable resin. **Composites Part A.** 37 (11): 1879-1883.
- Petinakis, E., Yu, L., Edward, G., Dean, K., Liu, H., and Scully, A. (2009). Effect of matrix-particle interfacial adhesion on the mechanical properties of poly(lactic acid)/wood-flour micro-composites. **J. Polym. Environ.** 17 (2): 83-94.
- Pilla, S., Gong, S., O'Neill, E., Rowell, R. M., and Krzysik, A. M. (2008). Polylactide-pine wood flour composites. **Polym. Eng. Sci.** 48 (3): 578-587.
- Qian, S., Mao, H., Sheng, K., Lu, J., Luo, Y., and Hou, C. (2013). Effect of low-concentration alkali solution pretreatment on the properties of bamboo particles reinforced poly(lactic acid) composites. **J. Appl. Polym. Sci.** 130 (3): 1667-1674.
- Qiang, T., Yu, D., and Gao, H. (2012). Wood flour/polylactide biocomposites toughened with polyhydroxyalkanoates. **J. Appl. Polym. Sci.** 124 (3): 1831-1839.

- Rachini, A., Le Troedec, M., Peyratout, C., and Smith, A. (2009). Comparison of the thermal degradation of natural, alkali-treated and silane-treated hemp fibers under air and an inert atmosphere. **J. Appl. Polym. Sci.** 112 (1): 226-234.
- Ragoubi, M., George, B., Molina, S., Bienaimé, D., Merlin, A., Hiver, J. M., and Dahoun, A. (2012). Effect of corona discharge treatment on mechanical and thermal properties of composites based on miscanthus fibres and polylactic acid or polypropylene matrix. **Composites Part A.** 43 (4): 675-685.
- Rahman, M. A., De Santis, D., Spagnoli, G., Ramorino, G., Penco, M., Phuong, V. T., and Lazzeri, A. (2013). Biocomposites based on lignin and plasticized poly(L-lactic acid). **J. Appl. Polym. Sci.** 129 (1): 202-214.
- Ray, D., Sarkar, B. K., Basak, R. K., and Rana, A. K. (2002). Study of the thermal behavior of alkali-treated jute fibers. **J. Appl. Polym. Sci.** 85 (12): 2594-2599.
- Reddy, K. O., Maheswari, C. U., Reddy, D. J. P., and Rajulu, A. V. (2009). Thermal properties of Napier grass fibers. **Mater. Lett.** 63 (27): 2390-2392.
- Rojo, E., Alonso, M. V., Domínguez, J. C., Saz-Orozco, B. D., Oliet, M., and Rodriguez, F. (2013). Alkali treatment of viscose cellulosic fibers from eucalyptus wood: Structural, morphological, and thermal analysis. **J. Appl. Polym. Sci.** 130 (3): 2198-2204.
- Rong, M. Z., Zhang, M. Q., Liu, Y., Yang, G. C., and Zeng, H. M. (2001). The effect of fiber treatment on the mechanical properties of unidirectional sisal-reinforced epoxy composites. **Compos. Sci. Technol.** 61 (10): 1437-1447.
- Rosa, M. F., Chiou, B., Medeiros, E. S., Wood, D. F., Williams, T. G., Mattoso, L. H. Orts, W. J., and Imam, S. H. (2009). Effect of fiber treatments on tensile and

- thermal properties of starch/ethylene vinyl alcohol copolymers/coir biocomposites. **Bioresour. Technol.** 100 (21): 5196-5202.
- Saheb, D. N., and Jog, J. P. (1999). Natural fiber polymer composites: A review. **Adv. Polym. Tech.** 18 (4): 351-363.
- Saikia, D. (2008). Investigations on structural characteristics, thermal stability, and hygroscopicity of sisal fibers at elevated temperatures. **Int. J. Thermophys.** 29 (6): 2215-2225.
- Sarasua, J. R., Prud'homme, R. E., Wisniewski, M., Le Borgne, A., and Spassky, N. (1998). Crystallization and melting behavior of polylactides. **Macromolecules.** 31 (12): 3895-3905.
- Sarkar, P. B., Mazumdar, A. K., and Pal, K. B. (1948). The hemicelluloses of jute fibre. **J. Text. Inst.** 39 (T44): 44-58.
- Satyanarayana, K. G., Arizaga, G. G. C., and Wypych, F. (2009). Biodegradable composites based on lignocellulosic fibers-An overview. **Prog. Polym. Sci.** 34 (9): 982-1021.
- Sawpan, M. A. (2009). **Mechanical performance of industrial hemp fibre reinforced polylactide and unsaturated polyester composites.** M. Eng. thesis, The University of Waikato, New Zealand.
- Sawpan, M. A., Pickering, K. L., and Fernyhough, A. (2011). Improvement of mechanical performance of industrial hemp fibre reinforced polylactide biocomposites. **Composites Part A.** 42 (3): 310-319.
- Schwanninger, M., Rodrigues, J. C., Pereira, H., and Hinterstoisser, B. (2004). Effects of short-time vibratory ball milling on the shape of FT-IR spectra of wood and cellulose. **Vib. Spectrosc.** 36 (1): 23-40.

- Seong, O. H., Mehdi, K., Sim, I. N., Bhuiyan, M. A., Jang, Y. H., Ghaffar, J., and Kalaitzidon, K. (2012). Understanding the reinforcing mechanisms in kenaf fiber/PLA and kenaf fiber/PP composites: A comparative study. **Int. J. Polym. Sci.** 2012: 1-8. doi:10.1155/2012/679252.
- Shakoor, A. (2013). **Development of novel bio-derived polymer composites reinforced with natural fibres and mineral fillers.** M. Eng. thesis, Loughborough University, United Kingdom.
- Shin, B. Y., Jang, S. H., and Kim, B. S. (2011). Thermal, morphological, and mechanical properties of biobased and biodegradable blends of poly(lactic acid) and chemically modified thermoplastic starch. **Polym. Eng. Sci.** 51 (5): 826-834.
- Sis, A., Ibrahim, N., and Yunus, W. (2013). Effect of (3-aminopropyl)trimethoxysilane on mechanical properties of PLA/PBAT blend reinforced kenaf fiber. **Iran. Polym. J.** 22 (2): 101-108.
- Sombatsompop, N., Yotinwattanakumtorn, C., and Thongpin, C. (2005). Influence of type and concentration of maleic anhydride grafted polypropylene and impact modifiers on mechanical properties of PP/wood sawdust composites. **J. Appl. Polym. Sci.** 97 (2): 475-484.
- Srisuwan, L. (2012). **Effect of rice husk fiber surface treatment on physical properties of rice husk fiber/natural rubber composites.** M. Eng. thesis, Suranaree University of Technology, Thailand.
- Srubar Iii, W. V., Pilla, S., Wright, Z. C., Ryan, C. A., Greene, J. P., Frank, C. W., and Billington, S. L. (2012). Mechanisms and impact of fiber-matrix compatibilization techniques on the material characterization of PHBV/oak

- wood flour engineered biobased composites. **Compos. Sci. Technol.** 72 (6): 708-715.
- Suardana, N. P. G., Abdalla, A., Kim, H. K., Choi, K. S., and Lim, J. K. (2011). Mechanical properties and biodegradability of green composites based on polylactic-acid polymer. In **18th International Conference on Composite Materials (ICCM-18)**. Jeju, Korea, August 21-26.
- Suardana, N. P. G., Lokantara, I. P., and Lim, J. K. (2011). Influence of water absorption on mechanical properties of coconut coir fiber/polylactic acid biocomposites. **Mater. Phys. Mech.** 12 (2): 113-125.
- Tawakkal, I. S. M. A., Talib, R. A., Abdan, K. and Ling, C. N. (2012). Mechanical and physical properties of kenaf derived cellulose (KDC)-filled polylactic acid (PLA) composites. **BioRes.** 7 (2): 1643-1655.
- Teamsinsungvon, A. (2010). **Physical properties of poly(lactic acid)/poly(butylene adipate-co-terephthalate) blends and their composites**. M. Eng. thesis, Suranaree University of Technology, Thailand.
- Teamsinsungvon, A., Ruksakulpiwat, Y., and Jarukumjorn, K. (2013). Preparation and Characterization of Poly(lactic acid)/Poly(butylene adipate-co-terephthalate) Blends and Their Composite. **Polym. Plast. Technol. Eng.** 52 (13): 1362-1367.
- Tran, H. N., Ogihara, S., and Kobayashi, S. (2011). Mechanical properties of short coir/PBS biodegradable composites: effect of alkali treatment and fiber content. In **18TH International Conference on Composite Materials (ICCM-18)**. Jeju, Korea, August 21-26.
- Tran, H. N., Ogihara, S., Nguyen, H. T., and Kobayashi, S. (2011). Effect of alkali treatment on interfacial and mechanical properties of coir fiber reinforced

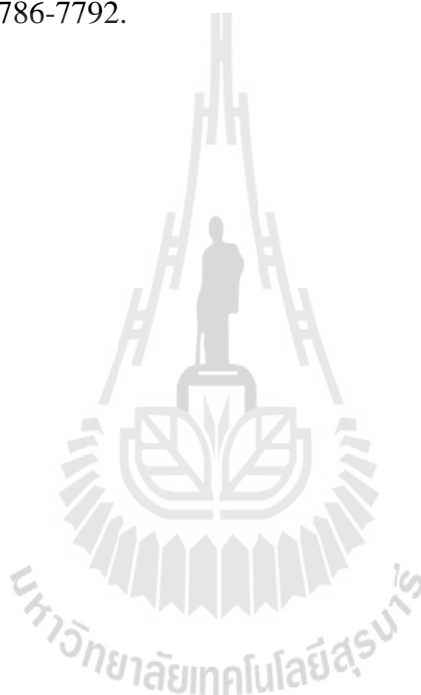
- poly(butylene succinate) biodegradable composites. **Composites Part B.** 42 (6): 1648-1656.
- Victor, H. O., Witold, B., Wunpen, C., and Betty, L. L. (2009). Preparation and characterization of poly(lactic acid)-g-maleic anhydride and starch blends. **Macromol. Symp.** 277 (1): 69-80.
- Wang, H. M., Chou, Y. T., Wu, C. S., and Yeh, J. T. (2012). Polyester/cellulose acetate composites: Preparation, characterization and biocompatible. **J. Appl. Polym. Sci.** 126 (S2): E242-E251.
- Way, C., Dean, K., Wu, D., and Palombo, E. (2011). Polylactic acid composites utilising sequential surface treatments of lignocellulose: chemistry, morphology and properties. **J. Polym. Environ.** 19 (4): 849-862.
- Wenjia, J., Kaushlendra, S., and John, Z. (2013). Pyrolysis kinetics of physical components of wood and wood-polymers using isoconversion method. **Agriculture.** 3 (1): 12-32.
- Williams, T., Hosur, M., Theodore, M., Netravali, A., Rangari, V., and Jeelani, S. (2011). Time effects on morphology and bonding ability in mercerized natural fibers for composite reinforcement. **Int. J. Polym. Sci.** 2011. doi: 10.1155/2011/192865.
- Wootthikanokkhan, J., Kasemwananimit, P., Sombatsompop, N., Kositchaiyong, A., Isarankura na Ayutthaya, S., and Kaabbuathong, N. (2012). Preparation of modified starch-grafted poly(lactic acid) and a study on compatibilizing efficacy of the copolymers in poly(lactic acid)/thermoplastic starch blends. **J. Appl. Polym. Sci.** 126 (S1): E389-E396.

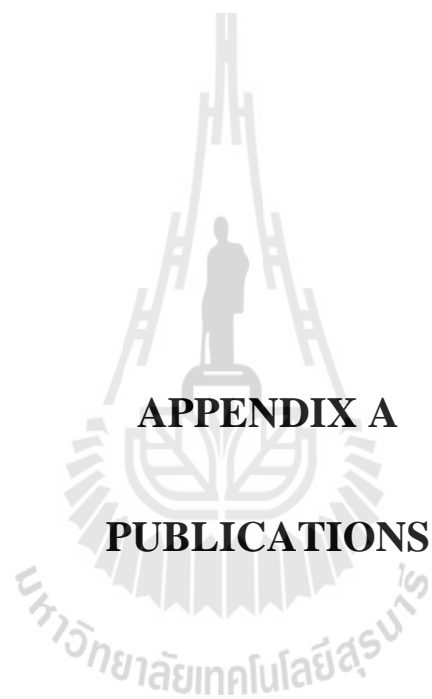
- Wu, C. S. (2003). Physical properties and biodegradability of maleated polycaprolactone/starch composite. **Polym. Degrad. Stab.** 80 (1): 127-134.
- Wu, C. S. (2011). Process, characterization and biodegradability of aliphatic aromatic polyester/sisal fiber composites. **J. Polym. Environ.** 19 (3): 706-713.
- Wu, C. S. (2012). Characterization and biodegradability of polyester bioplastic-based green renewable composites from agricultural residues. **Polym. Degrad. Stab.** 97 (1): 64-71.
- Wu, C. S. (2012). Preparation, characterization, and biodegradability of renewable resource-based composites from recycled polylactide bioplastic and sisal fibers. **J. Appl. Polym. Sci.** 123 (1): 347-355.
- Wu, C. S. and Liao, H. T. (2012). Polycaprolactone-based green renewable eco-composites made from rice straw fiber: characterization and assessment of mechanical and thermal properties. **Ind. Eng. Chem. Res.** 51 (8): 3329-3337.
- Wu, C. S., Yen, F. S., and Wang, C. Y. (2011). Polyester/natural fiber biocomposites: preparation, characterization, and biodegradability. **Polym. Bull.** 67 (8): 1605-1619.
- Xiao, H., Lu, W., and Yeh, J. T. (2009). Crystallization behavior of fully biodegradable poly(lactic acid)/poly(butylene adipate-co-terephthalate) blends. **J. Appl. Polym. Sci.** 112 (6): 3754-3763.
- Xu, X., Wang, Y., Zhang, X., Jing, G., Yu, D., and Wang, S. (2006). Effects on surface properties of natural bamboo fibers treated with atmospheric pressure argon plasma. **Surf. Interface Anal.** 38 (8): 1211-1217.
- Yao, F. (2008). **Rice straw fiber polymer composites: thermal and mechanical performance.** M. Eng. thesis, Louisiana State University, United States.

- Yao, F., Wu, Q., Liu, H., Lei, Y., and Zhou, D. (2011). Rice straw fiber reinforced high density polyethylene composite: Effect of coupled compatibilizing and toughening treatment. **J. Appl. Polym. Sci.** 119 (4): 2214-2222.
- Yi, C., Tian, L., Tong, Y., and Xu, W. (2008). Thermal stability of sisal fiber in cycle process. **J. Therm. Anal. Calorim.** 94 (1): 129-135.
- Yilmaz, N.D. (2013). Effect of chemical extraction parameters on corn husk fibres characteristics. **Indian J. Fibre Text.** 38 (1): 29-34.
- Yu, T., Ren, J., Li, S., Yuan, H., and Li, Y. (2010). Effect of fiber surface-treatments on the properties of poly(lactic acid)/ramie composites. **Composites Part A.** 41 (4): 499-505.
- Yuan, H., Liu, Z., and Ren, J. (2009). Preparation, characterization, and foaming behavior of poly(lactic acid)/poly(butylene adipate-co-butylene terephthalate) blend. **Polym. Eng. Sci.** 49 (5): 1004-1012.
- Zaini, L. H., Jonoobi, M., Tahir, P. Md., and Karimi, S. (2013). Isolation and characterization of cellulose whiskers from kenaf (*Hibiscus cannabinus* L.) bast fibers. **J. Biomater. Nanobiotechnol.** 4 (1): 37-44.
- Zhang, N., Wang, Q., Ren, J., and Wang, L. (2009). Preparation and properties of biodegradable poly(lactic acid)/poly(butylene adipate-co-terephthalate) blend with glycidyl methacrylate as reactive processing agent. **J. Mater. Sci.** 44 (1): 250-256.
- Zhao, P., Liu, W., Wu, Q., and Ren, J. (2010). Preparation, mechanical, and thermal properties of biodegradable polyesters/poly(lactic acid) blends. **J. Nanomater.** 2010 (4): 1-8.

Zhao, Y., Qiu, J., Feng, H., and Zhang, M. (2012). The interfacial modification of rice straw fiber reinforced poly(butylene succinate) composites: Effect of aminosilane with different alkoxy groups. **J. Appl. Polym. Sci.** 125 (4): 3211-3220.

Zhu, R., Liu, H., and Zhang, J. (2012). Compatibilizing effects of maleated poly(lactic acid) (PLA) on properties of PLA/soy protein composites. **Ind. Eng. Chem. Res.** 51 (22): 7786-7792.





APPENDIX A
PUBLICATIONS

List of Publications

- Nomai, J. and Jarukumjorn, K. (2013). Mechanical and morphological properties of sawdust/poly(lactic acid) composites: effects of alkali treatment and sawdust content. In **Proceeding of Pure and Applied Chemistry International Conference 2013 (PACCON2013)** (pp 669-672). Chonburi, Thailand.
- Nomai, J. and Jarukumjorn, K. (2013). Effects of alkali treatment and sawdust content on mechanical and morphological properties of sawdust/poly(lactic acid) composites. In **Abstract of The 4th Research Symposium on Petrochemical and Materials Technology and The 19th PPC Symposium on Petroleum, Petrochemicals, and Polymers** (pp 97). Bangkok, Thailand.
- Jarukumjorn, K. and Nomai, J. (2013). Toughness improvement of sawdust/poly(lactic acid) composites. In **Proceeding of The 4th International Conference on Biodegradable and Biobased Polymers (BIOPOL-2013)**. Rome, Italy.
- Nomai, J. and Jarukumjorn, K. (2013). Effect of maleic anhydride grafted poly(lactic acid) on properties of sawdust/poly(lactic acid) composites toughened with poly(butylene adipate-co-terephthalate). **Adv. Mater. Res.** 970: 74-78.

MECHANICAL AND MORPHOLOGICAL PROPERTIES OF SAWDUST/ POLY(LACTIC ACID) COMPOSITES: EFFECTS OF ALKALI TREATMENT AND SAWDUST CONTENT

Jiraporn Nomai^{1,2} and Kasama Jarukumjorn^{1,2*}

¹ School of Polymer Engineering, Institute of Engineering, Suranaree University of Technology, Nakhon Ratchasima 30000, Thailand

² Center of Excellence on Petrochemical and Materials Technology, Bangkok 10330, Thailand

* Author for correspondence; E-mail: kasama@sut.ac.th, Tel. +66 44224437, Fax. +66 44 224605

Abstract: Sawdust/poly(lactic acid) (PLA) composites were prepared using a twin screw extruder and test specimens were molded using an injection molding machine. Sawdust with particle size between 300 and 425 μm was used at contents of 20, 30, and 40 wt%. Mechanical and morphological properties of the composites were investigated. With increasing sawdust content, tensile modulus and flexural modulus of the PLA composites increased whereas tensile strength, flexural strength, impact strength, and elongation at break decreased. In addition, the effect of alkali treatment on the properties of sawdust/PLA composites was studied. Sawdust was treated with 2% w/v sodium hydroxide (NaOH) for 30 min at room temperature. Tensile, flexural, and impact properties of alkali treated sawdust/PLA composites were higher than those of untreated sawdust/PLA composites at all sawdust contents. The composites prepared from 40 wt% sawdust showed an improvement of tensile strength by 16.64%, tensile modulus by 7.90%, flexural strength by 28.95%, flexural modulus by 16.59%, and impact strength by 24.19% compared to those of untreated sawdust/PLA composites. SEM micrographs revealed that alkali treatment enhanced the interfacial adhesion between sawdust and PLA matrix.

1. Introduction

Increasing concerns about the environmental impact and sustainability of petrochemical polymer materials have motivated industries to develop biodegradable polymers from renewable resources. Among the biodegradable polymers, poly(lactic acid) (PLA) has attracted increasing interest in various industrial applications such as packaging, biomedical, and automotive, etc. PLA has a number of interesting properties including biodegradability, high strength, and high modulus [1]. However, its high brittleness and high cost limit its large scale commercial application [2]. One of the possible methods to minimize effective end product costs is to incorporate filler into biodegradable polymers [3]. Lignocellulosic fillers are widely used as reinforcing fillers in thermoplastic composites to provide positive environmental benefits with respect to ultimate disposability. The major advantages of these composite materials are low cost, light weight, high specific strength, and recyclability. In wood industries, sawdust is wood processing residue from consumer

good manufacture. Basically, sawdust is used as a fuel source or used to make others furniture product such as particle board. However, in many countries, sawdust is often disposed as landfill or incinerated causing environmental problems. Therefore, using sawdust as reinforcing fillers for polymers composites is an alternative way to add value to sawdust and also benefit the environment [4]. However, the main problem of using lignocellulosic filler to reinforce PLA is the incompatibility between lignocellulosic filler and PLA matrix, leading to poor mechanical properties of the composites. The interfacial adhesion between lignocellulosic filler and PLA can be improved by various methods such as matrix modification [5-6], addition of compatibilizer [7-9], and filler surface treatment [10-12]. Alkali treatment is found to be an effective way to improve interfacial adhesion of lignocellulosic filler/PLA composites. Alkali treatment can remove a certain amount of lignin, hemicellulose, and pectin covering the external surface of filler. The removal of surface impurities made the filler cleaner and rougher than untreated filler resulted in better mechanical interlocking with PLA matrix [10,13-14].

In this work, the effects of sawdust content and alkali treatment on mechanical and morphological properties of sawdust/PLA composites were investigated.

2. Materials and Methods

2.1 Materials

A commercial grade of PLA (PLA 3052D) was purchased from Natural Works LLC. Iron wood sawdust (*Hopea odorata* Roxb) with particle size between 300 and 425 μm was supplied by Piyarat sawmill, Nakhon Ratchasima, Thailand. Sodium hydroxide (RPE-ACS, Carlo Erba) was purchased from Italmar (Thailand) Co., Ltd. Tris(2,4-ditert-butylphenyl)phosphite antioxidant (Irgafos 168, Ciba) and pentaerythritol tetrakis(3-(3,5-di-tert-butyl-4-hydroxyphenyl)propionate) antioxidant (Irganox 1010, Ciba) were purchased from Merit Solution Co., Ltd.

2.2 Alkali treatment of sawdust

Sawdust was treated with 2% w/v sodium hydroxide solution (NaOH) with vigorous stirring for

30 min at room temperature. Then, sawdust was washed several times with water until pH7 was attained. Then sawdust was dried at 70 °C for 24 h.

2.3 Composites preparation

Designation and composition of the composites are shown in Table 1. Before mixing, PLA, untreated (UT) or alkali treated (AT) sawdust were dried at 70 °C in oven for 4 h. The compounds were mixed using a co-rotating intermeshing twin screw extruder (Brabender, DSE 35/17D) at the barrel temperature of 175/170/165/160/155 °C. The screw speed was 15 rpm. Then, test specimens were molded using an injection molding machine (Chuan Lih Fa model CLF 80P).

2.4 Composites characterization

Mechanical properties: Tensile properties were obtained according to ASTM D638 using an Universal testing machine (Instron, 5565) with a load cell of 5 kN and crosshead speed of 5 mm/min. Five samples were tested for each composition.

Flexural properties were obtained according to ASTM D790 using an Universal testing machine (Instron, 5565) with a load cell of 5 kN, span length of 53 mm, and crosshead speed of 1.4 mm/min. Five samples were evaluated for each composition.

Izod impact test was performed according to ASTM D256 using an Atlas testing machine (model BPI). Unnotched impact strength was tested at room temperature using the impact pendulum with impact energy of 2.7 J. Five samples were investigated for each composition.

Morphological properties: Morphology of the tensile fractured surface of sawdust/PLA composites was performed by a scanning electron microscope (JEOL, JSM5000). Acceleration voltage of 10 kV was used to collect SEM images of the samples. The fractured surface of specimens was coated with gold before analysis.

Table 1: Designation and composition of the composites

Designation	PLA wt%	Sawdust wt%		Irgafos 168 phr	Irganox 1010 phr
		UT	AT		
PLA	100	-	-	0.5	0.5
PLA/UT20	80	20	-	0.5	0.5
PLA/UT30	70	30	-	0.5	0.5
PLA/UT40	60	40	-	0.5	0.5
PLA/AT20	80	-	20	0.5	0.5
PLA/AT30	70	-	30	0.5	0.5
PLA/AT40	60	-	40	0.5	0.5

3. Results and Discussion

3.1 Mechanical properties

Tensile properties: Tensile strength, tensile modulus, and elongation at break of PLA, untreated and alkali treated sawdust/PLA composites with

different filler contents are shown in Figure 1 (a)-(c). It can be seen that modulus gradually increased with increasing sawdust content due to the reinforcement of sawdust in PLA matrix. However, with increasing sawdust content from 20 to 40 wt%, tensile strength of the composites slightly decreased due to a poor interfacial adhesion between sawdust and PLA matrix. Moreover, at high sawdust content, dispersion of sawdust was poor and sawdust was easy to agglomeration which resulted in a decrease in tensile strength of the composites [15]. Elongation at break of the composites decreased when the sawdust was added into the PLA matrix and decreased continuously with increasing sawdust content. This may be due to decreased deformability of a rigid interphase between the sawdust and the PLA matrix [15].

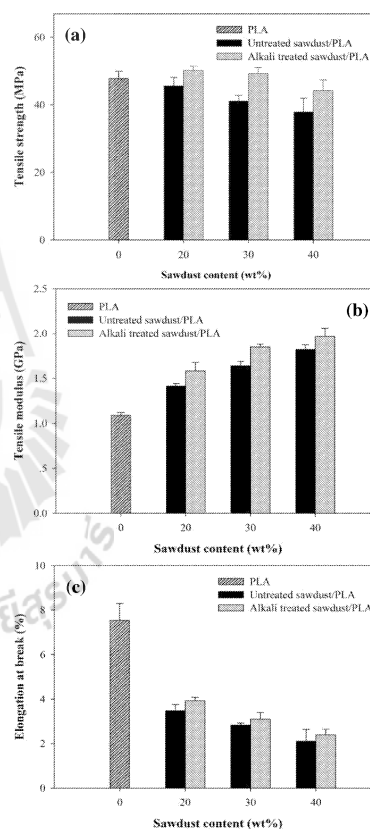


Figure 1. Tensile properties of PLA, untreated and alkali treated sawdust/PLA composites with different filler contents: (a) tensile strength, (b) tensile modulus, and (c) elongation at break

Tensile strength, tensile modulus, and elongation at break of alkali treated sawdust/PLA composites also showed the same trend as untreated sawdust/PLA composites. However, all of the composites filled with alkali treated sawdust exhibited higher tensile properties than the composites filled with untreated sawdust. This was because alkali treatment increased the filler surface roughness resulted in better mechanical interlocking with PLA matrix [16]. When compared with untreated sawdust/PLA composites, alkali treated sawdust/PLA composites at 20, 30, and 40 wt% sawdust content exhibited 10.08%, 19.96%, and 16.64% enhancement in tensile strength, 12.02%, 12.91%, and 7.90% enhancement in tensile modulus, and 12.90%, 9.63%, and 13.18% enhancement in elongation at break, respectively.

Flexural properties: Flexural strength and flexural modulus of PLA, untreated and alkali treated sawdust/PLA composites with different filler contents are shown in Figure 2 (a)-(b). Flexural properties also showed the same trend as tensile properties of sawdust/PLA composites. Flexural modulus increased with increasing sawdust content from 20 to 40 wt%. This was attributed to the addition of the rigid filler into the matrix. However, flexural strength of the composites decreased with increasing sawdust content. This was because a poor filler-matrix interfacial adhesion and filler agglomeration at high sawdust content resulted in difficult stress transfer from matrix to filler [15].

However, flexural strength and flexural modulus of alkali treated sawdust/PLA composites were significantly greater than those of untreated composites. This was due to the enhancement in the interfacial adhesion between sawdust and PLA matrix through mechanical interlocking. When compared with untreated sawdust/PLA composites, alkali treated sawdust/PLA composites at 20, 30, and 40 wt% sawdust content exhibited 27.02%, 29.69%, and 28.95% improvement in flexural strength and 15.38, 17.87%, and 16.59% improvement in flexural modulus, respectively.

Impact properties: Impact strength of PLA, untreated and alkali treated sawdust/PLA composites with different filler contents are shown in Figure 3. It was seen that as sawdust content was increased from 20 to 40 wt%, impact strength of the composites was reduced because the filler agglomeration increased, creating regions of stress concentration [15]. However, the improvement in impact strength was observed in the composites prepared from alkali treated sawdust. This was due to strong interfacial adhesion between the sawdust and the PLA matrix which allowed better matrix to fillers stress transfer during testing. The composites prepared from 20, 30, and 40 wt% alkali treated sawdust showed an improvement of impact strength by 20.02%, 31.02%, and 24.19% compared to those of untreated sawdust/PLA composites.

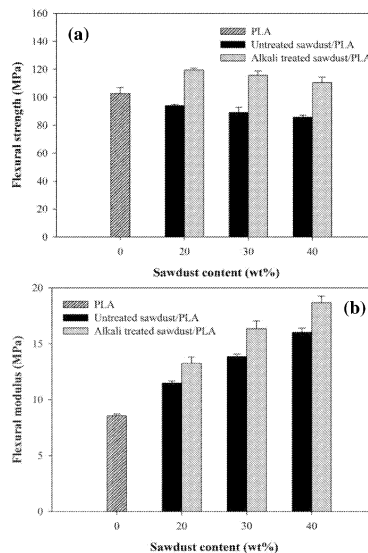


Figure 2. Flexural properties of PLA, untreated and alkali treated sawdust/PLA composites with different filler contents: (a) flexural strength and (b) flexural modulus

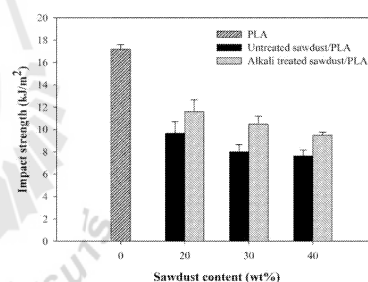


Figure 3. Impact strength of PLA, untreated and alkali treated sawdust/PLA composites with different filler contents

3.2 Morphological properties

Tensile fractured surface morphologies of untreated and alkali treated sawdust/PLA composites are shown in Figure 4 (a)-(f). Figure 4 (a)-(c) showed holes that left after untreated sawdust was pulled out from PLA matrix. Gaps between untreated sawdust and PLA matrix were observed. These characteristics indicated poor interfacial adhesion between the filler and the PLA matrix.

However, for all composites filled with alkali treated sawdust, sawdust was embedded in PLA matrix

without gap in the interfacial area indicating good interface adhesion between the filler and the matrix as shown in Figure 4 (d)-(f). These results suggested that alkali treatment provided good compatibility between sawdust and PLA matrix, resulting in significant improvement of mechanical properties of the composites.

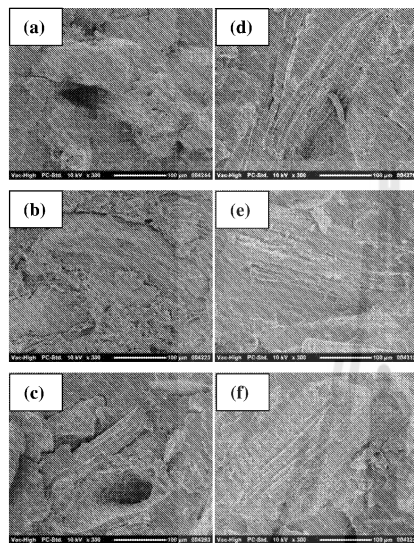


Figure 4. SEM micrographs at 300x magnification of (a) PLA/UT20, (b) PLA/UT30, (c) PLA/UT40, (d) PLA/AT20, (e) PLA/AT30, and (f) PLA/AT40 composites.

4. Conclusions

Tensile modulus and flexural modulus of PLA composites increased with increasing sawdust content whereas tensile strength, flexural strength, impact strength, and elongation at break decreased. Alkali treatment improved the interfacial adhesion between sawdust and PLA matrix leading to the enhancement in the mechanical properties of sawdust/PLA composites. SEM micrographs confirmed that alkali treatment enhanced the interfacial adhesion between sawdust and PLA matrix.

Acknowledgements

The authors would like to thank Suranaree University of Technology and Center of Excellence on Petrochemical and Material Technology for financial support, Piyarat sawmill for supplying iron wood sawdust.

References

- [1] H. Lui and J. Zhang, *J. Polym. Sci. Part B*, **49** (2011) 1051-1083.
- [2] T. Qiang, D. Yu and H. Gao, *J. Appl. Polym. Sci.* **124** (2012) 1831-1839.
- [3] M. Dimonie and M. Rapa, *U.P.B. Sci. Bull.* **72** (2010) 3-10.
- [4] S. H. P. Bettini, B. C. Bonse, E. A. Melo and P. A. R. Muñoz, *Polym. Eng. Sci.* **50** (2010) 978-985.
- [5] C. S. Wu, *Polym. Degrad. Stabil.* **97** (2012) 64-71.
- [6] A. Arbelaiz, B. Fernández, A. Valea and I. Mondragon, *Carbohydr. Polym.* **64** (2006) 224-232.
- [7] E. Petinakis, L. Yu, G. Edward, K. Dean, H. Liu and A. Scully, *J. Polym. Environ.* **17** (2009) 83-94.
- [8] F. Chen, L. Liu, P. H. Cooke, K. B. Hicks and J. Zhang, *Ind. Eng. Chem. Res.* **47** (2008) 8667-8675.
- [9] C. Nyambo, A. K. Mohanty and M. Misra, *Macromol. Mater. Eng.* **296** (2001) 710-718.
- [10] M. Aydin, H. Tozlu, S. Kemaloglu, A. Aytac and G. Ozkoc, *J. Polym. Environ.* **19** (2011) 11-17.
- [11] A. N. Frone, S. Berlioz, J. F. Chailan, D. M. Panaitescu and D. Donescu, *Polym. Compos.* **32** (2011) 976-985.
- [12] N. P. G. Suardana, I. P. Lokantara and J. K. Lim, *Mater. Phys. Mech.* **12** (2011) 113-125.
- [13] L. Liu, J. Yu, L. Cheng and X. Yang, *Polym. Degrad. Stab.* **94** (2009) 90-94.
- [14] A. S. Moyeenuddin, L. P. Kim and F. Alan, *Composites Part A* **42** (2011) 310-319.
- [15] P. Ming-Zhu, M. Chang-Tong, Z. Xu-Bing and P. Yun-Lei, *J. Appl. Polym. Sci.* **121** (2011) 2900-2907.
- [16] H. N. Tran, S. Ogihara, H. T. Nguyen and S. Kobayashi, *Composites Part B*, **42** (2011) 1648-1656.



The 4th Research Symposium on Petrochemical
and Materials Technology and
The 19th PPC Symposium on Petroleum,
Petrochemicals, and Polymers
April 23, 2013, Ballroom and Meeting 1-4, Queen
Sirikit National Convention Center, Bangkok, Thailand

Poster Sessions

PP-P-5 Effects of Alkali Treatment and Sawdust Content on Mechanical and Morphological Properties of Sawdust/Poly(lactic acid) Composites

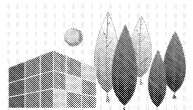
Jiraporn Noma^{a,b}, Kasama Jarukumjorn^{a,b}

^{a)}School of Polymer Engineering, Institute of Engineering, Suranaree University of Technology

^{b)}Center of Excellence on Petrochemical and Materials Technology

Sawdust/poly(lactic acid) (PLA) composites were prepared using a twin screw extruder and test specimens were molded using an injection molding machine. Sawdust contents were 20, 30 and 40 wt%. Sawdust was treated with 2% w/v sodium hydroxide (NaOH) for 30 min at room temperature. Mechanical and morphological properties of the composites were investigated. With increasing sawdust content, tensile modulus and flexural modulus of the PLA composites increased whereas tensile strength, flexural strength, impact strength and elongation at break decreased. Alkali treated sawdust/PLA composites exhibited higher tensile, flexural and impact properties than untreated sawdust/PLA composites at all sawdust contents due to improved adhesion between sawdust and PLA matrix. SEM micrographs revealed that alkali treatment enhanced the interfacial adhesion between sawdust and PLA matrix.





TOUGHNESS IMPROVEMENT OF SAWDUST/POLY(LACTIC ACID) COMPOSITES

Kasama Jarukumjorn and Jiraporn Nomai

School of Polymer Engineering, Institute of Engineering, Suranaree University of Technology,
Nakhon Ratchasima 30000, Thailand
E-mail: kasama@sut.ac.th

Introduction

Poly(lactic acid) (PLA) has attracted increasing interest in various industrial applications such as packaging, automotive, and biomedical applications. PLA has a number of interesting properties including biodegradability, high strength, and high modulus. However, its high brittleness and high cost limit its applications. One of the possible methods to effectively minimize end product costs is to incorporate lignocellulosic fillers into PLA (1). The major advantages of these composite materials are low cost, light weight, high specific strength, and recyclability. In wood industries, large amounts of sawdust are always found as waste. This sawdust is commonly little used and often disposed as landfill or incinerated. Therefore, using sawdust as reinforcing fillers for polymers composites is an alternative way to add value to sawdust and also benefit the environment (2). The main problem of using sawdust to reinforce PLA is the incompatibility between sawdust and PLA matrix, leading to poor mechanical properties of the composites. Alkali treatment is one of the most used chemical treatments to improve interfacial adhesion between lignocellulosic fillers and PLA matrix (3). However, one obstacle that restricts the application of PLA composites is owing to a remarkable decrease of toughness of the composites. In the recent year, many considerable interests have focused on toughening lignocellulosic filler/PLA composites with biodegradable polymers (4-5). In the view of high flexibility and biodegradability, PBAT is considered as a good choice for toughening PLA based lignocellulosic filler composites.

In this work, the effect of PBAT content on mechanical and morphological properties of sawdust/PLA composites was investigated.

Experimental

Poly(lactic acid), (PLA 3052D) was supplied from Natural Works LLC. Poly(butylene adipate-co-terephthalate) (PBAT, Ecoflex Mulch) was purchased from BASF Co., Ltd. Iron wood sawdust (*Hopea odorata* Roxb) with particle size between 300 and 425 μm was supplied by Piyarat sawmill, Nakhon Ratchasima, Thailand. Sodium hydroxide (NaOH, Carlo Erba) was purchased from Italmar (Thailand) Co., Ltd.

Sawdust was treated with 2% w/v NaOH for 30 min at room temperature. PLA/sawdust ratio was 70/30 wt%. PBAT contents were varied as 10, 20, and 30 wt%. The composites were prepared using a twin screw extruder (Brabender, DSE 35/17D) at a barrel temperature of 175/170/165/160/155 $^{\circ}\text{C}$. The screw speed was 15 rpm. Then, test specimens were molded using an injection molding machine (Chuan Lih Fa, CLF 80P).

Tensile properties were obtained according to ASTM D638 using a universal testing machine (Instron, 5565) with a load cell of 5 kN and crosshead speed of 5 mm/min. Unnotched izod impact test was performed according to ASTM D256 using an impact testing machine (Atlas, BPI). Morphology of the tensile fractured surface of sawdust/PLA composites was performed by a scanning electron microscope (JEOL, JSM6010). Acceleration voltage of 10 kV was used to collect SEM images of the samples. The fractured surface of specimens was coated with gold before analysis.

Results and Discussion

Tensile strength and tensile modulus of sawdust/PLA composites with different PBAT contents are shown in Figure 1. The addition of PBAT to sawdust/PLA composites reduced brittleness

characteristics of the composites. Tensile strength and tensile modulus of sawdust/PLA composites decreased with increasing PBAT content. This behavior was probably due to low stiffness of PBAT and incompatibility between constituents of the composites (5).

Elongation at break and impact strength of sawdust/PLA composites toughened with PBAT were higher than that of sawdust/PLA composite as shown in Figure 2. The addition of PBAT at content of 10, 20, and 30 wt% exhibited 37%, 67%, and 71% enhancement in elongation at break of the PLA composites, respectively. Moreover, impact strength of the PLA composites toughened with PBAT at 10, 20, and 30 wt% were 36%, 161%, and 181% higher than that of the composites without PBAT, respectively. The improvement of elongation at break and impact strength was attributed to the presence of soft elastomeric phase that exhibited high flexibility and toughness (4).

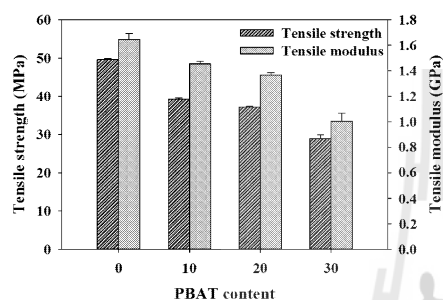


Figure 1 – Tensile strength and modulus of sawdust/PLA composites with different PBAT contents.

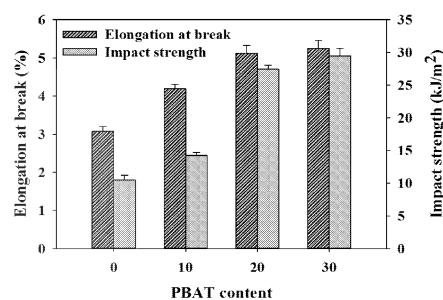


Figure 2 – Elongation at break and impact-strength of sawdust/PLA composites with different PBAT contents.

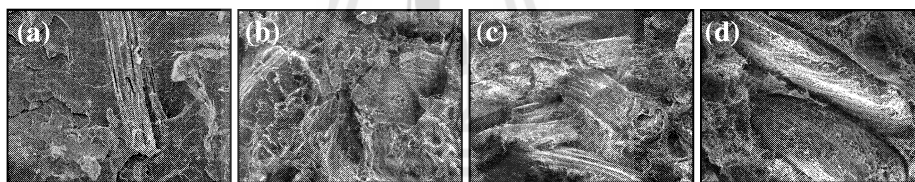


Figure 3 – SEM micrographs at 300x magnification of (a) sawdust/PLA, (b) sawdust/PLA/PBAT10, (c) sawdust/PLA/PBAT20, and (d) sawdust/PLA/PBAT30 composites.

Tensile fractured surface morphologies of sawdust/PLA composites are shown in Figure 3 (a)-(d). SEM micrographs of PLA composites without PBAT exhibited smooth fractured surfaces. This was attributed to brittle failure of the matrix system. The fractured surface morphologies of PLA composites toughened with PBAT showed some features of ductile fracture. This was evidence that the composites toughened with PBAT had rougher fractured surface as shown in Figure 3 (b)-(d). This indicated that the matrix of PLA composites toughened with PBAT were tougher than the composites without PBAT, resulting in the enhancement in elongation at break and impact strength of the composites (5).

Conclusion

Sawdust/PLA composites toughened with PBAT were prepared and their mechanical and morphological properties were studied. Elongation at break and impact strength of the PLA composites increased with increasing PBAT content while tensile strength and modulus decreased. SEM micrographs revealed some features of ductile fracture in the composites toughened with PBAT.

References

1. M. Dimonie; M. Rapa *U.P.B. Sci. Bull.* **2010**, *72*, 3-10.
2. S. H. P. Bettini; B. C. Bonse; E. A. Melo; P. A. R. Muñoz *Polym. Eng. Sci.* **2010**, *50*, 978-985.
3. L. Liu; J. Yu; L. Cheng; X. Yang *Polym. Degrad. Stab.* **2009**, *94*, 90-94.
4. T. Qiang; D. Yu; H. Gao *J. Appl. Polym. Sci.* **2012**, *124*, 1831-1839.
5. B. K. Goriparthi; K. N. S. Suman; M. R. Nalluri *Polym. Compos.* **2012**, *33*, 237-244.

Effect of Maleic Anhydride Grafted Poly(lactic acid) on Properties of Sawdust/Poly(lactic acid) Composites Toughened with Poly(butylene adipate-co-terephthalate)

Jiraporn Nomai^{1, a} and Kasama Jarukumjorn^{1, b*}

¹School of Polymer Engineering, Institute of Engineering, Suranaree University of Technology,
 Nakhon Ratchasima 30000, Thailand

^ajira_sut@hotmail.com, ^{b*}kasama@sut.ac.th

Keywords: Poly(lactic acid), Sawdust, Poly(butylene adipate-co-terephthalate), Maleic anhydride grafted poly(lactic acid), Mechanical properties, Thermal stability.

Abstract. Sawdust/poly(lactic acid) (PLA) composites toughened with poly(butylene adipate-co-terephthalate) (PBAT) were prepared using a melt blending process. Mechanical, thermal and morphological properties of the composites were investigated. With the addition of PBAT into the sawdust/PLA composite, elongation at break and impact strength increased whereas tensile strength and tensile modulus decreased. In addition, thermal stability of the PLA composite improved with the presence of PBAT. Maleic anhydride grafted poly(lactic acid) (PLA-g-MA) was used as a compatibilizer to improve the compatibility of sawdust/PLA/PBAT composites. The compatibilized composites showed higher mechanical properties and thermal decomposition temperatures than that of the uncompatibilized composite due to improved interfacial adhesion between constituents of the composites. The optimum content of PLA-g-MA for sawdust/PLA/PBAT composites was 5 wt%. SEM micrographs revealed some features of ductile fracture in the composites toughened with PBAT and confirmed that PLA-g-MA improved the compatibility of the composites.

Introduction

Poly(lactic acid) (PLA) has attracted increasing attention in various industrial applications. PLA has a number of interesting properties including biodegradability, high strength and high modulus. However, its high brittleness and high cost limit its applications. One of the possible methods to effectively minimize end product costs is to incorporate lignocellulosic fillers into PLA [1]. The major advantages of these composite materials are low cost, light weight, high specific strength and recyclability. In wood industries, large amounts of sawdust are always found as waste. This sawdust is commonly little used and often disposed as landfill or incinerated. Therefore, using sawdust as reinforcing filler for polymer composites is an alternative way to add value to sawdust and also benefit the environment. The main problem of using sawdust to reinforce PLA is the incompatibility between sawdust and PLA matrix, leading to poor mechanical properties of the composites. Alkali treatment is one of the most used chemical treatments to improve interfacial adhesion between lignocellulosic fillers and PLA matrix [2]. However, one obstacle that restricts the application of PLA based lignocellulosic filler composites is owing to a remarkable decrease of toughness of the composites. Therefore, the toughness of the PLA composites has to be improved to achieve balance overall properties. Recently, many considerable interests have focused on toughening lignocellulosic filler/PLA composite with biodegradable polymers due to their obvious environment friendly properties [3,4]. In the view of high flexibility and biodegradability, poly(butylene adipate-co-terephthalate) (PBAT) is considered as a good choice for toughening PLA based lignocellulosic filler composites. In fact, all of the investigated PLA/PBAT blends are immiscible or only partially miscible [5]. Therefore, interfacial adhesion between PBAT and PLA should be improved. Generally, maleic anhydride grafted poly(lactic acid) (PLA-g-MA) is considered to be an effective compatibilizer for improving the compatibility between PLA and PBAT [5]. Lignocellulosic filler/PLA composites gain more interest in the areas of interior automotive part such as indoor panel, seatback panels, armrest liner, console bins and trays. The

objective of this work is to investigate the effect of PLA-g-MA on mechanical, thermal and morphological properties of sawdust/PLA composites toughening with PBAT.

Experimental

Materials. Poly(lactic acid), (PLA, 3052D) was supplied from Natural Works LLC. Poly(butylene adipate-co-terephthalate) (PBAT, Ecoflex FBX 7011) was purchased from BASF Co., Ltd. Iron wood sawdust (*Hopea odorata* Roxb) with particle size between 300 and 425 μm was supplied by Piyarat sawmill, Nakhon Ratchasima, Thailand. Sodium hydroxide (NaOH, Carlo Erba) was purchased from Italmar (Thailand) Co., Ltd. Maleic anhydride (MA) and 2,5-bis(tert-butylproxy)-2,5 dimethylhexane (L101) were purchased from Sigma-Aldrich. PLA-g-MA prepared in-house was used as a compatibilizer [5].

Preparation of Composites. Sawdust was treated with 2% w/v NaOH for 30 min at room temperature. The designation and composition of the composites are shown in Table 1. PLA/sawdust ratio was 70/30 w/w and PBAT content was fixed at 20 wt%. The composites were prepared using a twin screw extruder (Brabender, DSE 35/17D) at a barrel temperature of 175/170/165/160/155 $^{\circ}\text{C}$. The screw speed was 15 rpm. Then, test specimens were molded using an injection molding machine (Chuan Lih Fa, CLF 80T).

Characterization of Composites.

Mechanical Properties. Tensile properties were obtained according to ASTM D638 using a universal testing machine (Instron, 5565) with a load cell of 5 kN and crosshead speed of 5 mm/min.

Unnotched izod impact test was performed according to ASTM D256 using an impact testing machine (Atlas, BPI).

Thermal Properties. Thermal stability of the composites was analyzed using a thermogravimetric analyzer (Perkin Elmer, SDT 2960). The specimens were heat from 30 $^{\circ}\text{C}$ to 600 $^{\circ}\text{C}$ with a heating rate of 10 $^{\circ}\text{C}/\text{min}$ under a nitrogen atmosphere.

Morphological Properties. Morphology of the tensile fractured surface of the composites was performed by a scanning electron microscope (JEOL, JSM6010). The fractured surface of specimens was coated with gold before analysis.

Table 1. Designation and composition of the composites

Designation	Sawdust/PLA [wt%]	PBAT [wt%]	PLA-g-MA [wt%]
Sawdust/PLA	100	-	-
nc-20PBAT	80	20	-
3c-20PBAT	77	20	3
5c-20PBAT	75	20	5
10c-20PBAT	70	20	10

Results and Discussion

Mechanical Properties. Tensile strength and tensile modulus of sawdust/PLA composite and sawdust/PLA/PBAT composites with different PLA-g-MA contents are shown in Fig. 1 (a). Tensile strength and tensile modulus of sawdust/PLA composite decreased with the addition of PBAT. This behavior was probably due to low stiffness of PBAT and incompatibility between constituents of the composite [4]. Elongation at break and impact strength of sawdust/PLA composite toughened with PBAT were higher than that of sawdust/PLA composite as shown in Fig. 1 (b). The addition of

PBAT exhibited 46% and 114% enhancement in elongation at break and impact strength of the PLA composite, respectively. The improvement of elongation at break and impact strength was attributed to the presence of soft elastomeric phase that exhibited high flexibility and toughness [3]. Moreover, adding PLA-g-MA enhanced mechanical properties of sawdust/PLA/PBAT composites. This may be due to improved interfacial adhesion between constituents of the composites [5]. As PLA-g-MA content increased from 3 to 5 wt%, tensile strength, elongation at break and impact strength significantly improved while tensile modulus relatively unchanged. When compared with the uncompatibilized sawdust/PLA/PBAT composite, the addition of 5 wt% PLA-g-MA improved tensile strength, elongation at break and impact strength of the composite up to 38%, 20% and 41%, respectively. However, tensile strength, tensile modulus, elongation at break and impact strength of the composites slightly decreased with further increasing PLA-g-MA content to 10 wt%. This may be due to the saturation of PLA-g-MA at the interface resulting in a decrease in mechanical properties of the compatibilized sawdust/PLA/PBAT composite [6].

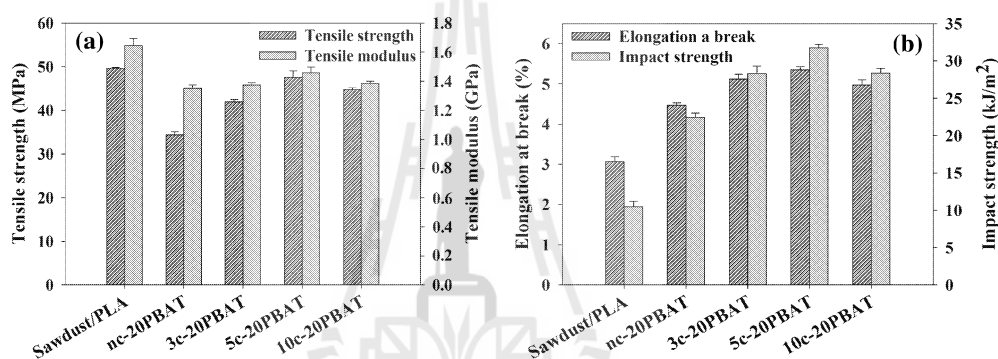


Figure 1. Mechanical properties of sawdust/PLA composite and sawdust/PLA/PBAT composites with different PLA-g-MA contents.

Thermal Properties. TGA curves of sawdust/PLA composite and sawdust/PLA/PBAT composites with different PLA-g-MA contents are shown in Fig. 2. Thermal decomposition temperature at 5% weight loss (T_5), thermal decomposition temperature at 50% weight loss (T_{50}) and thermal decomposition temperature (T_d) of the composites are summarized in Table 2. It could be seen that the decomposition of sawdust/PLA composite was in a single stage, as the decomposition stage of sawdust was overlapped with the decomposition stage of PLA [7]. T_5 , T_{50} and $T_{d,1}$ of the sawdust/PLA composite were 293.34, 352.70 and 354.20 °C, respectively. With the addition of PBAT into the sawdust/PLA composite, the composite exhibited two stages of the decomposition with the first decomposition temperature ($T_{d,1}$) of sawdust and PLA at 357.14 °C and the second decomposition temperature of PBAT ($T_{d,2}$) at 399.03 °C. Moreover, T_5 , T_{50} and $T_{d,1}$ of the sawdust/PLA/PBAT composite increased when compared to the sawdust/PLA composite, indicating the improvement of thermal stability of the composite [5]. The compatibilized sawdust/PLA/PBAT composites showed higher T_5 , T_{50} and $T_{d,1}$ than that of the sawdust/PLA/PBAT composite without PLA-g-MA. This was because PLA-g-MA enhanced the compatibility between constituents of the composites [5]. However, T_5 , T_{50} , $T_{d,1}$ and $T_{d,2}$ did not change significantly with PLA-g-MA content. Yao [8] also reported that compatibilizer content had no significant effect on thermal stability of rice straw fiber/high density polyethylene composite toughened with ethylene/propylene copolymer.

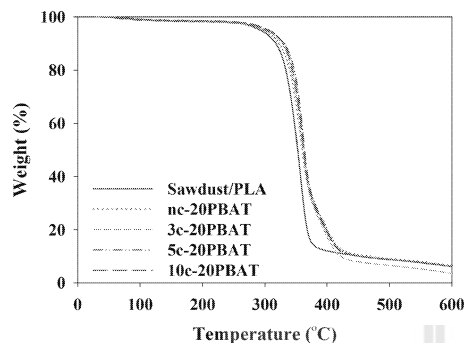


Table 2. Thermal decomposition temperatures of sawdust/PLA composite and sawdust/PLA/PBAT composites with different PLA-g-MA contents.

Designation	T ₅ [°C]	T ₅₀ [°C]	T _{d,1} [°C]	T _{d,2} [°C]
Sawdust/PLA	293.34	352.70	354.20	-
nc-20PBAT	297.35	357.92	357.14	399.03
3c-20PBAT	304.87	362.86	361.74	399.14
5c-20PBAT	306.36	364.02	362.15	399.18
10c-20PBAT	307.88	364.71	362.49	399.43

Figure 2. TGA curves of sawdust/PLA composite and sawdust/PLA/PBAT composites with different PLA-g-MA contents.

Morphological Properties. Tensile fractured surface morphologies of sawdust/PLA composite and sawdust/PLA/PBAT composites are shown in Fig. 3. Sawdust/PLA composite exhibited smooth fractured surfaces as shown in Fig. 3 (a) and (b). This was attributed to brittle failure of the matrix system. The fractured surface morphologies of the composites toughened with PBAT showed some features of ductile fracture. This was evidence from rougher fractured surface (at 300x) and longer fibrils pulled out during tensile testing at high magnification (1500x) as shown in Fig. 3 (c) and (d), respectively. This indicated that matrix of the sawdust/PLA/PBAT composite was tougher than that of the composite without PBAT, resulting in the enhancement in elongation at break and impact strength of the composites [4]. However, gaps between the sawdust and the matrix were observed as shown in Fig. 3 (c). These characteristics indicated poor interfacial adhesion between constituents of the composites. PLA-g-MA compatibilized sawdust/PLA/PBAT composites showed good interfacial adhesion between the sawdust and the matrix as shown in Fig. 3 (e). These results suggested that PLA-g-MA provided good compatibility between the constituents of the composites, resulting in the improvement of mechanical properties of the composites.

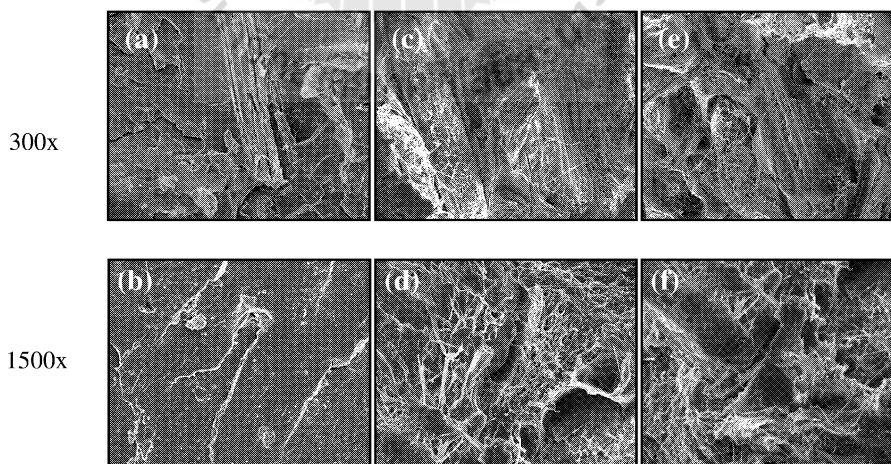


Figure 3. SEM micrographs of (a) sawdust/PLA (300x), (b) sawdust/PLA (1500x), (c) nc-20PBAT (300x), (d) nc-20PBAT (1500x), (e) 5c-20PBAT (300x), (f) 5c-20PBAT (1500x) composites.

Summary

Elongation at break and impact strength of the sawdust/PLA composites increased with the addition of PBAT while tensile strength and modulus decreased. Moreover, thermal stability of the composites was improved with the presence of PBAT. PLA-g-MA enhanced mechanical and thermal properties of the composites due to improved interfacial adhesion between the constituents of the composites. The optimum content of PLA-g-MA for sawdust/PLA/PBAT composites was 5 wt%. SEM micrographs revealed some features of ductile fracture in the composites toughened with PBAT and confirmed that PLA-g-MA enhanced the compatibility of the composites.

References

- [1] M. Dimonie, M. Rapa, U.P.B. Sci. Bull. 72 (2010) 3-10.
- [2] L. Liu, J. Yu, L. Cheng, X. Yang, Polym. Degrad. Stab. 94 (2009) 90-94.
- [3] T. Qiang, D. Yu, H. Gao, J. Appl. Polym. Sci. 124 (2012) 1831-1839.
- [4] B.K. Goriparthi, K.N.S. Suman, M.R. Nalluri, Polym. Compos. 33 (2012) 237-244.
- [5] A. Teamsinsungvon, Physical properties of poly(lactic acid)/poly(butylene adipate-co-terephthalate) blends and their composites, Master's Thesis. Suranaree University of Technology (2011).
- [6] P. Lomellini, M. Matos, B.D. Favis, Polymer. 37 (1996) 5689-5694.
- [7] K.S. Chun, S. Husseinsyah, H. Osman, Polym. Eng. Sci. 53 (2013) 1109-1116.
- [8] F. Yao, Rice straw fiber polymer composites: thermal and mechanical performance, Master's Thesis. Louisiana State University (2008).



BIOGRAPHY

Miss Jiraporn Nomai was born on January 19, 1989 in Nakhon Ratchasima, Thailand. She finished high school from Suranari Wittaya School in 2007. She earned her Bachelor's Degree in Polymer Engineering from Suranaree University of Technology (SUT) in 2011. After that, she then continued her Master's degree in Polymer Engineering at School of Polymer Engineering, Institute of Engineering, Suranaree University of Technology. During her master's degree study, she presented three posters and one oral presentations entitle: **“Mechanical and morphological properties of sawdust/poly(lactic acid) composites: effects of alkali treatment and sawdust content”** in the Pure and Applied Chemistry International Conference 2013 (PACCON2013) in Chonburi Province, Thailand, **“Effects of alkali treatment and sawdust content on mechanical and morphological properties of sawdust/poly(lactic acid) composites”** in The 4th Research Symposium on Petrochemical and Materials Technology and The 19th PPC Symposium on Petroleum, Petrochemicals, and Polymers, in Bangkok, Thailand, **“Toughness improvement of sawdust/poly(lactic acid) composites”** in 4th International Conference on Biodegradable and Biobased Polymers (BIOPOL-2013), in Rome, Italy. **“Effect of maleic anhydride grafted poly(lactic acid) on properties of sawdust/poly(lactic acid) composites toughened with poly(butylene adipate-co-terephthalate)”** in 1st International Conference on the Science and Engineering of Materials 2013 (ICoSEM2013), Kuala Lumpur, Malaysia.